Mapping molecular datasets back to the brain regions they are extracted from: Remembering the native countries of hypothalamic expatriates and refugees

Arshad M. Khan[1,3,4*+], Alice H. Grant[1–3], Anais Martinez[1–3], Gully A. P. C. Burns[5], Brendan S. Thatcher[6], Vishwanath T. Anekonda[6], Benjamin W. Thompson[6], Zachary S. Roberts[6], Daniel H. Moralejo[8], and James E. Blevins[6,7]

[1]UTEP Systems Neuroscience Laboratory, [2]Graduate Program in Pathobiology, [3]Department of Biological Sciences and [4]Border Biomedical Research Center, University of Texas at El Paso, El Paso, TX 79968, USA; [5]Information Sciences Institute, Viterbi School of Engineering, University of Southern California, Marina del Rey, CA 90292, USA; [6]VA Puget Sound Health Care System, Office of Research and Development Medical Research Service, Department of Veterans Affairs Medical Center, Seattle, WA 98108, USA; [7]Division of Metabolism, Endocrinology, and Nutrition, Department of Medicine, University of Washington School of Medicine, Seattle, WA 98195, USA; [8]Division of Neonatology, Department of Pediatrics, University of Washington School of Medicine, Seattle, WA, 98195, USA.

+ senior author

.

*** Address correspondence to:**

Arshad M. Khan, Ph.D.
Associate Professor
Department of Biological Sciences and Border Biomedical Research Center
Director, UTEP Systems Neuroscience Laboratory
University of Texas at El Paso
El Paso, TX 79968
Tel: +1 (915) 747-8436
E-mail: amkhan2@utep.edu

Abstract

This article, which includes novel unpublished data along with commentary and analysis, focuses on approaches to link transcriptomic, proteomic, and peptidomic datasets mined from brain tissue to the original locations within the brain that they are derived from using digital atlas mapping techniques. We use, as an example, the transcriptomic, proteomic and peptidomic analyses conducted in the mammalian hypothalamus. Following a brief historical overview, we highlight studies that have mined biochemical and molecular information from the hypothalamus and then lay out a strategy for how these data can be linked spatially to the mapped locations in a canonical brain atlas where the data come from, thereby allowing researchers to integrate these data with other datasets across multiple scales. A key methodology that enables atlas-based mapping of extracted datasets – laser capture microdissection – is discussed in detail, with a view of how this technology is a bridge between systems biology and systems neuroscience.

Table of Contents

1: Introduction **5**

1.1: Summary and rationale 5

1.2: Topic and organization 5

2: Why does location matter? **6**

3: Historical antecedents **6**

3.1: Heuristic entry points to relevant history 6

3.2: Sampling at the level of the single cell 7

3.3: Sampling at the level of isolated tissues 7

Figure 1: *Demonstrations of single-neuron isolation procedures* 8

4: Molecular mining of the hypothalamus **9**

4.1: Early studies 9

Figure 2: *Rat hypothalamic sub-regions microdissected for molecular analyses* 10

4.2: Studies of the hypothalamus using high throughout methods 11

Figure 3: *Transcriptomic, proteomic and peptidomic coverage of hypothalamus* 12

4.2.1: Whole brain extraction and multi-region comparison studies 13
4.2.2: Molecular extraction from whole hypothalamus 13
4.2.3: Molecular extraction from the hypothalamic circadian system 15
4.2.4: Molecular extraction from the hypothalamo-neurophypohysial system 15
4.2.5: Molecular extraction from the arcuate hypothalamic nucleus (ARH) 17
4.2.6: Molecular extraction from other hypothalamic sub-regions (LHA, VMH) 18

4.3: A note about "hypothalamic-derived" molecules 19

5: Laser-capture microdissection studies: Methodological considerations **19**

5.1: LCM for general sampling of brain regions 20

5.2: Immuno-LCM 21

Figure 4: *Fasting-elicited increases in ARH NPY and AgRP mRNA expression* 21

5.2.1: Advantages 21
5.2.2: Challenges and pitfalls 22

5.3: Use of LCM to target cells using fluorescent conjugates 22

5.3.1: Advantages 22
5.3.2: Challenges and pitfalls 23

5.4: RNA Integrity 23

6: Anchoring molecular information to their native regions using digital atlas maps 24

6.1: Documenting the native substrate before extraction 24

6.2: Mapping to standardized atlases 25

Figure 5: *Example of a plane-of-section analysis and Fos expression maps* 26

Figure 6: *Mapping LCM tissue samples: Steps and advantages* 27

7: The benefits of mapping native substrates and anchoring datasets 28

7.1: Data integration 29

7.2: Data migration 30

7.3: Data refinement 31

8: Concluding remarks and future directions 31

8.1: Future directions in data management 31

Figure 7: *Choropleth flatmaps of rat ARH afferent input densities* 32

8.2: Future directions in imaging 33

8.3: Future directions in molecular analysis 34

8.4: Future directions in mapping 35

8.5: Final remarks 35

Funding 36

Acknowledgements 37

Abbreviations used 38

References 41

Tables 1–3 76

1: Introduction

1.1: Summary and rationale. In this article, we envision ways in which molecular information extracted from the brain using methods such as transcriptomics, proteomics, and peptidomics can be anchored to locations in standardized atlas maps of the brain in order to preserve the provenance of the datasets and contextualize them with other datasets. We argue that whereas most researchers probe, dissect, mine, or interrogate the living brain and report back with valuable scientific information, such information would be worth more if it included *mapped locations* of where they traveled and what they found there. Mapping to a standardized reference allows current and future travelers to return to the same landscape with accuracy and precision, generate reproducible data from reproducible experiments, and allows them further to integrate and contextualize new data they gathered in that mapped location with other data gathered in the same space. By carefully documenting the locations, for example, of brain regions from which molecular information is extracted for large-scale analyses, scientists can contribute further to our collective history of the native landscape from which this expatriated molecular information originated.

1.2: Topic and organization. We have chosen to use the hypothalamus as an exemplar structure to illustrate the possibilities of such an effort, a choice that is predicated in part on our own experiences in mapping and modeling multi-scale data for this brain region (e.g., Khan et al., 2006; Khan, 2013; Zséli et al., 2016; Khan et al., 2017; 2018), and because a review of "-omics" work on the hypothalamus in the context of spatial mapping has not yet, to our knowledge, been attempted. So far, molecule extraction from hypothalamus has been focused primarily on mining either the whole hypothalamus or its well-defined sub-regions to the virtual exclusion of parts that are less well understood. If wider and more systematic sampling of areas within the hypothalamus were to be conducted, atlas mapping efforts will play an even greater role in helping us understand the organization of those areas that remain poorly defined. The additional benefit of mapping molecular data to a standardized atlas is that the data can be contextualized with multi-scale datasets mapped to the same reference map.

Below, following a brief exploration of the biological importance of location information in the brain (**Section 2**), we summarize the historical antecedents to current molecular extraction work done on the brain (**Section 3**) and the hypothalamus specifically (**Section 4.1**), focusing on those datasets that include spatial data about the regions extracted. We then survey studies that have examined the molecular landscape of the hypothalamus using transcriptomics, proteomics and peptidomics (**Section 4.2**). The rationale behind the separation of proteomics from its sub-domain, peptidomics, is based on the fact that the latter involves analytical procedures that are distinct from those in general proteomics, including more rigorous purification and more comprehensive identification procedures (Schrader et al., 2014). The differences are great enough in methodology and concept that a separate consideration of peptidomic studies is warranted. The narrative then shifts to specific strategies that we envision will be required, especially the technique of laser capture microdissection (LCM) (**Section 5**), to enable the accurate mapping of hypothalamic molecular datasets to a standardized atlas of the brain (**Section 6**), and the benefits of such mapping (**Section 7**). We conclude with a view to current and future directions for this research (**Section 8**).

2: Why does location matter?

The brain is a very heterogeneous organ that contains diverse, non-repeating, and non-redundant sub-regions. Studies in many animal model systems have now revealed that brain region is a major determinant of gene expression patterns. Therefore, the location of areas sampled using "-omics" technologies will determine critically the complement of molecules expressed. In songbirds, for example, clustering analyses performed on retrieved sets of genes demonstrate a strong association of gene expression with brain region (Replogle et al., 2008; Drnevich et al., 2012; Balakrishnan et al., 2014). This also holds true for mammalian brain. Even between strains of mice, one report has estimated a 1% difference in baseline expression patterns in at least one brain region, and that gene expression differences in response to a physiological perturbation (in this case, seizure) produce marked differences in gene expression patterns in brain regions between strains (Sandberg et al., 2000). A re-analysis of the datasets of Sandberg et al., (2000) by Pavlidis & Noble (2001) reveals even greater differences in regional variation among the genes between the strains. Robust strain differences have also been documented for transcripts enriched in the rat hypothalamic neurohypophysial system (Hindmarch et al., 2007). Moreover, Dong et al., (2009) show that specific patterns of gene expression are associated with specific domains where distinct neural projection patterns emerge within the hippocampus, and Wolf et al., (2011) show that there is a strong predictive association of neural connections and gene expression within specific brain regions (also see Sun et al., 2012). Thus, it is important to consider just what we as scientists lose if we endeavor to extract molecular information from the brain without attempting to preserve the provenance of where the extraction took place. Before addressing this issue more directly, it is useful to survey the history behind efforts to identify chemical and molecular information encoded in the brain.

3: Historical antecedents

3.1: Heuristic entry points to relevant history. Current "-omics" work has been informed by seminal works conducted during the last 150 years which we have categorized heuristically along major research themes: *composition*, *communication*, *reaction* and *localization*. First, regarding *composition*, our current effort to understand dynamic changes in the expression of genes and proteins in the nervous system is predated by work that first identified its fundamental chemical (elemental) constituents (e.g., Thudicum, 1884; Richter, 1957; McIlwain, 1959). Studies of the molecular constituents of neural machinery were motivated in part by contemporaneous questions concerning the ionic and chemical bases of muscle and nerve excitability (Helmholtz, 1850; Nernst, 1888; Overton, 1902a,b; Hill, 1932; Hodgkin & Huxley, 1939; 1945; 1952a–f; Hodgkin et al., 1952; Fatt & Katz, 1952; see various reviews by Boring, 1942; Kleinzeller, 1999; Häusser, 2000; Bennett, 2001; Huxley, 2002; De Palma & Pareti, 2011; Schwiening, 2012; also see Khan, 2009). Predating current work on proteomics and peptidomics, work on chemical composition was also marked by efforts in the 1980s by Tatemoto and colleagues to use chemical methods to isolate, identify and determine the sequence of neuropeptides such as galanin and neuropeptide Y (Tatemoto and Mutt, 1980; Tatemoto et al., 1982; 1983; see Schrader et al., 2014).

Second, concerning *communication*, the mining of molecules coding for neurotransmitter and neuropeptide machinery in the nervous system finds its antecedents in both Bayliss and Starling's discovery of peptide hormone secretion from the pancreas (Bayliss and Starling, 1902; also see Hirst, 2004; Schrader et al., 2014), and Loewi's discovery (1921) of cholinergic

neurotransmission in the peripheral nervous system. Ensuing efforts to gather evidence for a role for acetylcholine as a neurotransmitter in the central nervous system (e.g., Feldberg, 1952) were facilitated by histochemical methods (Koelle & Friedenwald, 1949; Anglade & Larabi–Godinot, 2010; but see Levey et al., 1983), which helped contribute to the maturation of chemical neuroanatomy as a sub-discipline of neuroanatomy. Importantly, histochemistry became useful to trace metabolic turnover in the brain, since it was performed on living tissue and was based on enzymatic activities catalyzing the conversion of substrates to detectable products.

This work complemented contemporaneous studies – grouped thematically under *reaction* – that concerned the metabolism of living neural tissue, pioneered by Warburg, McIlwain and others (e.g., see Warburg et al., 1924). Finally, a fourth long-standing body of work that informs "-omics" approaches concerns the historical quest to understand how various functions of the brain are derived from specific locations within its complex structure, the theme of *localization* (e.g., Flourens, 1822; Ferrier, 1873; Adrian, 1939; also see Swanson, 2007). This theme directly informs efforts to isolate portions of the nervous system for detailed study through careful extraction and sampling, a topic we delve into next.

3.2: Sampling at the level of the single cell. Early interests in sampling very small portions of the central nervous system prefigure current interests in developing "spatially resolved" approaches (e.g., Crosetto et al., 2015) for transcriptomics and proteomics of neural tissues. Otto Deiters (1865) famously provided the first anatomical descriptions distinguishing the axon from dendrites by studying motor neurons from the anterior horn of the spinal cord which he isolated individually by hand from chromic acid- or potassium bichromate-hardened (i.e., fixed) tissue (**Fig. 1A**). Several investigators such as Hans Held and others followed suit using a variety of fixed preparations to study neurons in greater detail (see introductory comments in Chu (1954) for an overview).

Deiters' manual single-cell microdissection technique anticipates, by almost a century, single cell isolation from *fresh* neural tissue preparations pioneered by Ezio Giacobini (1956) for frog, rat and cat spinal cord and peripheral ganglia; and Holger Hydén (1959) for the mammalian brain. Hydén, for example, used manual microdissection to isolate and chemically analyze (fittingly) the "giant neurons of Deiters" found in the lateral vestibular nucleus (**Fig. 1B**; Hydén, 1959; also see Hydén, 1967; Sotelo & Palay, 1968; Rose, 1999). Along with Giacobini's and Hydén's work using freshly microdissected neurons, related methods developed by Lowry (1953), Chu (1954), Roots & Johnston (1965), Johnston & Roots (1966) and others using fixed, freeze-dried, and reagent-impregnated tissues ushered in an era of "micro-chemical methods", in which a variety of *chemical assays* could be performed on single cells isolated from various regions of the central nervous system (cogently reviewed by Johnston & Roots, 1970; also see Roberts & Baxter, 1963; Osborne, 1974). More recently, single-cell isolation has now been conducted using laser-capture microdissection (LCM) methods (e.g., Williams et al., 2008; Blevins et al., 2009; Landmann et al., 2012) or cell sorting methods (e.g., Henry et al., 2015; Macosko et al., 2015; Chen et al., 2017; Mickelsen et al., 2017; Romanov et al., 2017; also see Okaty et al., 2011). Thus, single cell isolation methods first used for the purposes of morphological and structural investigation evolved for use in biochemical and functional analyses.

3.3: Sampling at the level of isolated tissues. Alongside single-cell isolation methods were those procedures driven by the need to examine metabolically active states of the nervous system

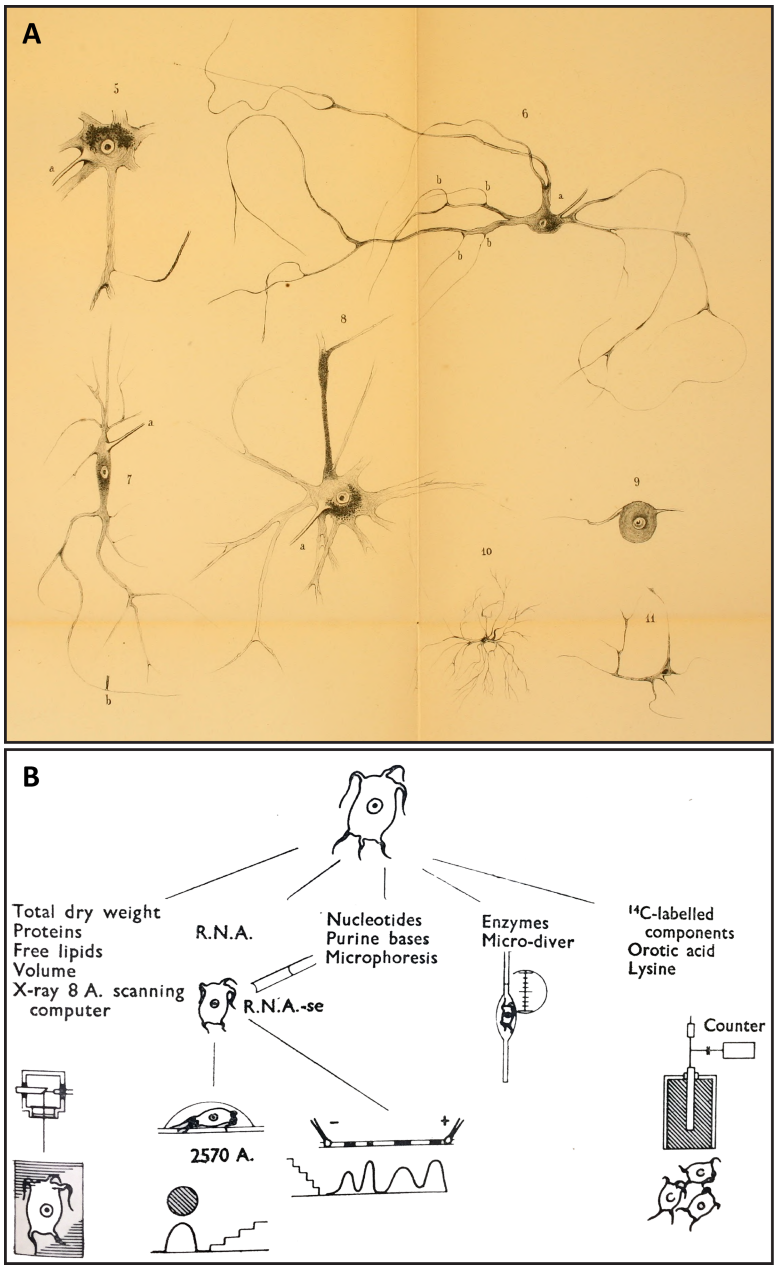

Fig. 1. Demonstrations of single-neuron isolation procedures, nearly a century apart, which anticipate isolation methods performed at present for studying single-cell transcriptomics, proteomics, and peptidomics. **(A).** *Figure 2* of Deiters (1865), showing the morphologies of neurons collected from the central nervous system by hand microdissection. Note the recovery of many fine processes extended from each perikaryon, including axons and dendrites. These drawings are in the public domain. **(B).** *Figure 2* of Hydén (1959) showing a workflow schematic of possible assays that can be performed on single neurons isolated from freshly prepared tissue of the lateral vestibular nucleus. Neurons in this region are named "giant cells of Deiters" in honor of Deiters's initial description of these cells (see Sotelo & Palay, 1968). Reproduced with permission from Nature Publishing Group.

in isolated tissue preparations where the local microenvironment of the cells was, to some extent, still maintained. Metabolic studies of living tissues maintained in isolation were pioneered by Otto Warburg's laboratory in the 1920s, including studies performed on the isolated retina (Warburg et al., 1924).

4: Molecular mining of the hypothalamus

4.1: Early studies. Prior to the advent of high throughput methods, several laboratories performed a variety of techniques to isolate and examine the molecular constituents of the hypothalamus, either using living samples or fixed samples *post mortem*. A number of such studies were conducted because investigators at the time were motivated to differentiate the functions of the pituitary gland from the overlying hypothalamus (e.g., see Lisser, 1927). Other investigators concerned themselves more with trying to understand, through histochemistry, the nature of chemical transmission in the hypothalamus (reviewed by Pilgrim, 1974), to validate, for example, the existence of cholinergic neurotransmission within hypothalamic regions (*see* **Section 2.1**). Feldberg & Vogt (1948) isolated the supraoptic hypothalamic nucleus in the dog to perform acetylcholinesterase (AchE) histochemistry, a method also performed in hypothalamus by Abrahams et al., (1957). Still others extended the tradition of Warburg and colleagues by examining the living hypothalamus for insights into metabolic processes occurring within this tissue, primarily through the use of radiolabeled phosphate incorporation. For example, Borell & Örström (1945) examined radiolabeled phosphate accumulation in the anterior and posterior portions of the hypothalamus, and Roberts & Keller (1953, 1955) studied glycolysis in hypothalamic tissue preparations. Bakay (1952) examined radiolabeled phosphate incorporation in the human hypothalamus *post mortem* following the deaths of terminally ill cancer patients who had received intravenous tracer to track their brain tumors.

In what is perhaps the earliest demonstration of chemical analysis performed on an explicitly defined microdissected sub-region of the hypothalamus, Forssburg & Larsson (1954) sampled a portion of the hypothalamus from male and female rats that were either food-deprived for 24 h or *ad libitum*-fed and that received radioactive (^{14}C; $Na_2H^{32}PO_4$) tracer injections to track their carbon and phosphate metabolism. Brains were rapidly dissected and frozen, and 20–50 µm-thick sections were obtained of the brain, and examined carefully for the incorporation of ^{14}C and ^{32}P in chemically extracted fractions of the microdissected tissue. Importantly, the authors included a schematic to outline the areas they micropunched (**Fig. 2A**), including areas they sampled outside of the hypothalamus that served as a control. Their careful documentation of the sampled area and use of a custom-made micropunch tool (which they also illustrated in their study) anticipates the later use of similar instruments as developed by Palkovits and colleagues to sample discrete parts of the brain (see Palkovits, 1973; 1975; 1986; 1989; Jacobowitz, 1974; also see Jacobowitz, 2006).

Using these micropunch methods, and leveraging refinements (O'Farrell, 1975) of the original two-dimensional gel electrophoresis method (Smithies and Poulik, 1956) that allowed proteins to be separated by their apparent molecular weights and isoelectric points (reviewed by Dunn, 1987), Jacobowitz and colleagues helped to pioneer the systematic study of proteins from discrete micropunched regions of the rat brain, including from within the hypothalamus (Heydorn et al., 1983). Importantly, their study included a schematic of atlas maps from the rat brain atlas of König and Klippel (1963) to identify the approximate locations and diameters of their tissue

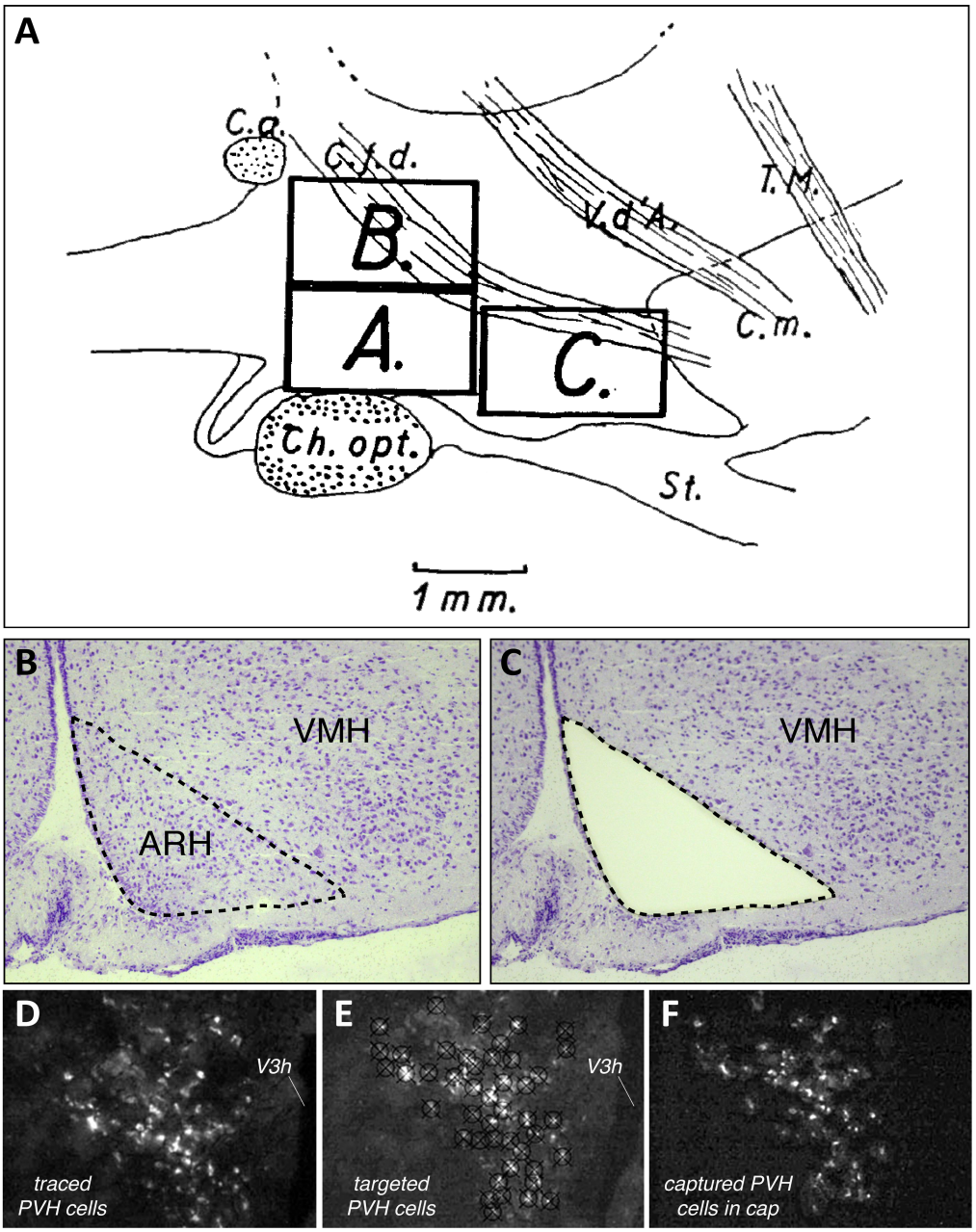

Fig. 2. Examples of documentation, past and more recent, of microdissected areas sampled from rat hypothalamus for chemical or molecular analyses – from gross micropunch (**A**), to region-level LCM **(B, C),** to single-cell LCM **(D–F)**. **(A).** *Figure 14* of Forssburg and Larsson (1954), showing a sagittal drawing of the hypothalamus, as defined by major fiber tract landmarks: Ch. Opt. = optic chiasm; C.a. = anterior commissure; C.f.d. = fornix; V.d'A. (*Tract of Vicq d'Azyr*) = mammillothalamic tract; T.M. (*Tractus Meynert*) = fasciculus retroflexus; St. = infundibular stalk. The boxes denoted by letters mark the regions micropunched from thin frozen sections at the locations indicated by the drawing, with A and B serving as control regions and C as the region of interest containing the lateral and ventromedial hypothalamus. Reproduced with permission from John Wiley & Sons, Ltd. **(B, C).** A Nissl-stained view of the arcuate hypothalamic nucleus (ARH) and ventromedial hypothalamic nucleus (VMH) in rat brain tissue sectioned in the coronal plane,

before **(B)** and after **(C)** the tissue was subjected to LCM. The dotted outline marks the region captured by the LCM instrument; note how the Nissl pattern helps to delineate the boundaries of the region to be sampled, and the remaining tissue after LCM can then be used to map the sampled region to a digital atlas. These images, generated from tissue sampled on 15 Sep 2016, are provided courtesy of Dr. Rebecca Hull and Nishi Gill (*see Acknowledgments*). **(D–F)**. Example of single-cell LCM capture of hypothalamic cells. These panels show photomicrographs adapted from *Figure 5* of Blevins et al., (2009), in which paraventricular hypothalamic (PVH) cells projecting to the hindbrain (as revealed in **(D)** by the presence of the retrograde tracer, cholera toxin subunit B (*white*), in PVH cells); have been targeted for LCM; see cross-patterns in **(E)**); and then have been collected into a microcentrifuge cap following LCM capture **(F)**.

---

micropunches. Among the many brain regions sampled were the anterior, paraventricular, ventromedial and dorsomedial hypothalamic nuclei. Although the authors were able to obtain apparent molecular weights, isoelectric points and relative amounts of proteins from their tissue punches (see also Heydorn et al., 1986), their study does not specifically identify the proteins themselves except in a few cases. Methods to do so, involving annotated databases, had not yet been developed. While micropunch methods continue to remain popular, finer-grained studies that require more precise sampling of brain regions utilize LCM (Emmert-Buck et al., 1996), which is described in greater detail in **Section 5**, and an example of which is shown in Panels B and C of **Figure 2**. This higher resolution sampling using LCM has now been performed at the level of single hypothalamic cells (*e.g.,* see **Figure 2D–F**).

4.2: Studies of the hypothalamus using high throughput methods. **Tables 1–3 (located after the References section)** summarize selected studies performed to extract molecular data from the hypothalamus using transcriptomics, proteomics, and peptidomics; respectively. A few of these studies are discussed below, beginning with studies which examined the hypothalamus as part of larger whole brain and/or multi-regional studies, and then on to studies in which the hypothalamus itself or its sub-regions were the main focus. Before these studies are examined in greater detail, it is useful to first consider the "state of the field" as a whole in terms of how much sampling of the hypothalamus and its various regions have been undertaken thus far. **Figure 3** is a snapshot of the level of coverage reported by the studies listed in **Tables 1–3**, organized by high throughput method and by spatial location within the hypothalamus. Specifically, a choropleth flatmap of the rodent brain, adapted from Swanson (2004), is utilized to highlight the degree to which either the whole hypothalamus (**Fig. 3A**), or individual sub-regions of the hypothalamus (**Fig. 3B–D**) have been sampled using transcriptomic, proteomic and peptidomic methods.

A number of observations can be made from an examination of the figure. First, of the total number of studies listed in **Tables 1–3**, 45–83% of them (depending on which molecular analysis was performed) provide no sub-regional specificity for their sampling but rather sample the whole hypothalamus (**Fig. 3A**). Second, of the studies performing high throughput extraction and molecular analysis of hypothalamic sub-regions, the greatest degree of coverage occurs for transcriptomic (**Fig. 3B**), followed by proteomic (**Fig. 3C**) and peptidomic (**Fig. 3D**) studies. Finally, across all methods, the overwhelming emphasis of sub-regional analyses of the

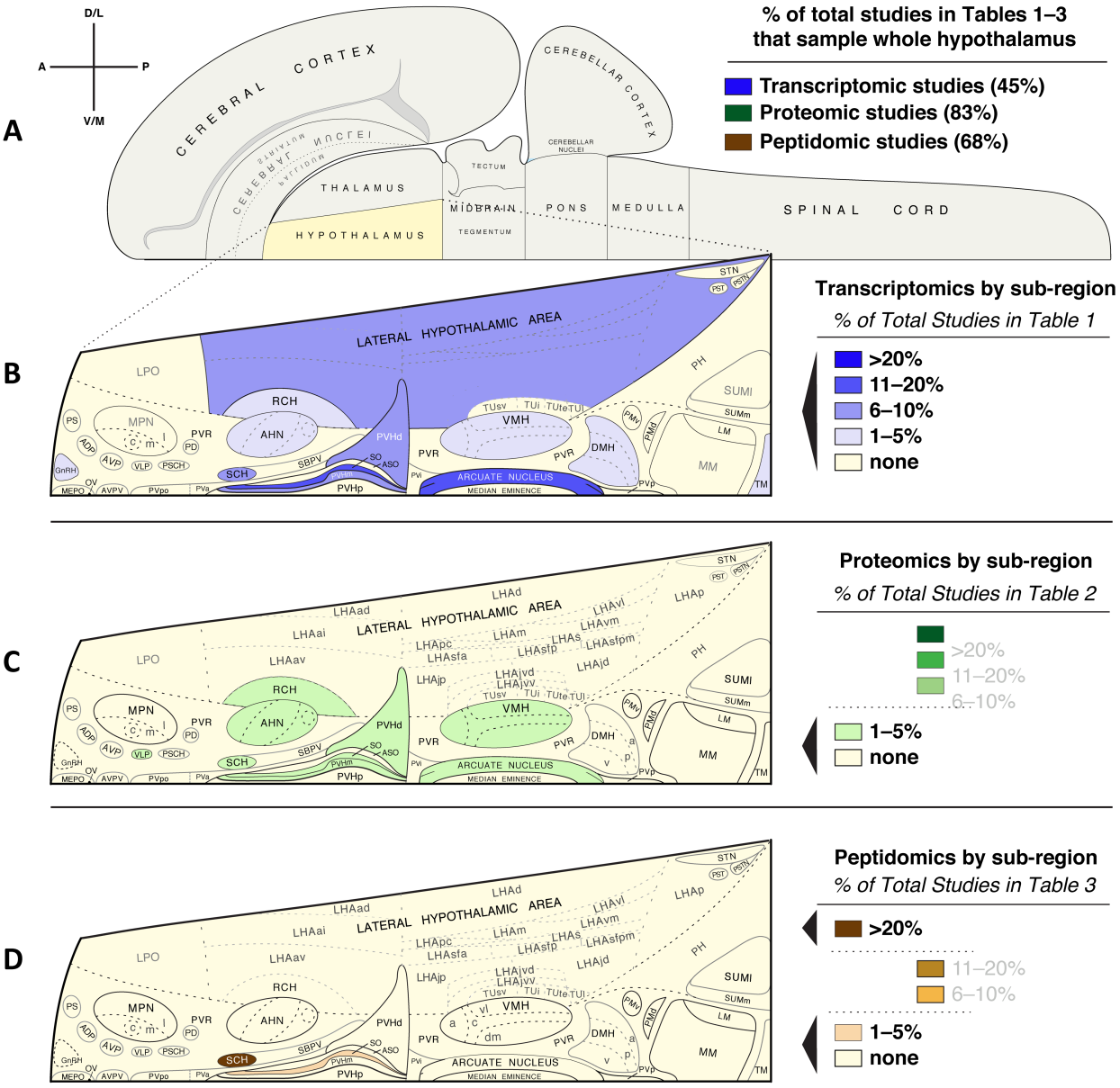

Fig. 3. Survey of coverage for the hypothalamus or its various regions by published transcriptomic, proteomic and peptidomic studies listed in **Tables 1–3**. **(A)** Choropleth flatmap of the rat central nervous system (CNS), modified from Swanson (2004), illustrating the various major CNS subdivisions, including the hypothalamus. Note the *legend* at the upper left, which indicates directions of orientation (A, anterior; P, posterior; D/L, dorsal/lateral; V/M, ventral/medial). The *chart* to the right of the flatmap in **(A)** lists the % of total studies reported in each of the tables in this review (**Tables 1–3**) that conducted transcriptomic, proteomic, or peptidomic studies of the *whole* hypothalamus. **(B–D)** A breakdown, by *hypothalamic region*, of the percentage of studies in which a particular region was sampled for analysis, with choropleth flatmaps in **B** showing all hypothalamic regions analyzed by transcriptomic analyses, in **C** showing all proteomic studies, and in **D** all peptidomic studies. The percentage ranges are coded by colors and reflect percentages of the total number of studies listed in each table. Note that although rat brain flatmaps are used

here, the studies are across many different taxonomic groups, including fish, chicken, goose, cow, pig, sheep, shrew, mouse and rat. Therefore, the maps are meant to be convenient vehicles to convey a sense of the amount of coverage in the literature for any particular region, differences in their neuroanatomy or cytoarchitectural boundaries notwithstanding. Note also that for many shaded regions, the smaller abbreviations have been removed for sub-regions within each region, to emphasize that studies did not sample at that level of resolution. Thus, the lateral hypothalamic area (LHA) may have been sampled, but the LHAjvv was not. Conversely, although large areas are shaded, in certain cases only a few cell types were specifically mined from the region rather than the region sampled as a whole, but this is not reflected in the diagrams. For explanation of all abbreviations, please see abbreviations list. The flatmaps from Swanson (2004) (and available at https://larrywswanson.com) are reproduced here under the conditions of a Creative Commons BY-NC 4.0 license (https://creativecommons.org/licenses/by-nc/4.0/legalcode

---

hypothalamus has been on medially located nuclei, with little to no examination of sub-regions within the larger lateral hypothalamic area (LHA). Even for transcriptomic studies (**Fig. 3B**), the greater majority of studies of the LHA have focused mainly on a few key peptidergic cell types and not the whole region *per se*. Below, after describing a few studies that have focused on the hypothalamus in the context of whole-brain or multiregional studies, we summarize a few key studies from among those listed in **Tables 1–3**.

4.2.1: Whole brain extraction and multi-region comparison studies. There are many excellent reasons investigators opt to extract molecular information from the whole brain or large subdivisions of the brain without attending to where exactly in the brain the molecules are located. Such reasons include the need for investigators to survey the effects of factors that produce global, whole-organism or whole-subdivision effects that are poorly understood at a regional or cellular level. These include environmental agents (Li et al., 2014), pharmacological interventions (Jin et al., 2016), ontogenic state (e.g., see introductory remarks in Balivada et al., 2017), or physiological processes. Miller et al., (2014) examined various hypothalamic sub-regions within the context of a hemispheric tissue analysis in prenatal human brain using high throughput transcriptomic methods. Zapala et al., (2005) contextualized regional specificity with embryonic development, taking care to provide supplementary information that includes photographic documentation of the tissue they dissected for their hypothalamic sample. In contrast, it is disappointing that in their "in-depth analysis of the mouse brain and its major regions and cell types" for the proteome, Sharma et al., (2015) neglected to sample the hypothalamus in what is otherwise a detailed and interesting study.

4.2.2: Molecular extraction from whole hypothalamus. In non-mammalian vertebrates, the hypothalamus has been studied for transcriptomics, proteomics, and peptidomics in fishes and birds; in some cases, in the context of animal husbandry. For example, hypothalamic and pituitary molecules associated with high egg production in chickens have been analyzed at the transcriptomic (Shiue et al., 2006; Chen L-R et al., 2007; **Table 1**) and proteomic (Kuo et al., 2005) levels. Egg-laying traits have also been compared alongside transcripts identified to be associated with high egg production (Chen C-F et al., 2007). The hypothalamic transcriptomes of the Huoyan goose (Luan et al., 2014) and the Sichuan white goose (Gao et al., 2015) have been profiled before, during, or after their egg laying periods in the interests of finding clues to improve

the reproductive performance of these economically valuable domestic animals. In the interests of optimizing feed intake in chickens or to understand how they cope with environmentally-induced pressures, many studies have also examined the role of body composition, fasting, diet, or heat stress on gene expression in chicken hypothalamus (e.g., Byerly et al., 2010; Fang et al., 2014; Sun et al., 2015; Tu et al., 2016; see also Kuenzel et al., 1999). Despite the intensive investigations of chicken hypothalamus for molecular mining and extraction, these studies have not contextualized sub-regional changes in expression for molecules in relation to published stereotaxic atlases of the chicken that include illustrations, maps and drawings of the hypothalamus with stereotaxic coordinates (van Tienhoven and Juhász, 1962; Yasuda & Lepkovsky, 1969; Feldman et al., 1973).

In mammals, whole hypothalamus has been mined for gene transcripts in mouse, rat, shrew pig, cow, sheep and dog **(Table 1)**. Gautvik et al., (1996) provided the first large-scale *in situ* hybridization-based study of hypothalamus-enriched transcripts in the rat by using directional tag PCR subtraction. Friedman and colleagues utilized a novel molecular technique that extends the principles underlying an earlier approach (Heiman et al., 2008), to isolate and extract activated transcriptional systems in the hypothalamus under conditions of salt-loading, fasting, light exposure, or various other stimulus paradigms (Knight et al., 2012). Specifically, they immunoprecipitated the phosphorylated form of the ribosomal protein, S6, to isolate and enrich mRNAs that are actively being translated (i.e., in transcriptionally activated neurons) in mouse hypothalamic samples. Using TaqMan® technology (Holland et al., 1991), RNA-Seq and microarrays, they isolated several mRNAs, many of which displayed expression in pS6-immunoreactive neurons in various sub-regions of the hypothalamus.

Using Drop-Seq, a method that allows for single-cell transcriptomics to be performed in a manner that preserves the cell provenance of the RNA that is extracted (Macosko et al., 2015), Chen and colleagues (2017) reported single-cell RNA sequencing results from the adult mouse hypothalamus. They used clustering analysis to identify 11 non-neuronal (including oligodendrocytes, astrocytes, ependymocytes, tanycytes, microglia, and macrophages) and 34 neuronal cell types (including 15 glutamatergic and 18 GABAergic clusters, and one histaminergic neuron cluster) from tissue dissociated from manually dissected hypothalamus, and confirmed some of their key findings by performing immunohistochemistry for neuropeptides or comparing their results with those found in the publicly available Allen Brain Atlas. Importantly, their workflow revealed the spatially restricted expression of novel molecules in the hypothalamus, including retinoic acid binding protein (*Crabp1*) in the ARH. They also found restricted expression of the neurodevelopmental factor, *Pax6*, in the zona incerta, which the authors assign as a hypothalamic structure but which is considered as a thalamic structure by others (e.g., see Swanson, 2018). Importantly, their datasets indicate that all hypothalamic peptidergic neurons can also be classified by the small neurotransmitter they synthesize (glutamate or GABA). Recently, Romanov et al., (2017) provided evidence of numerous novel neuronal phenotypes of hypothalamic cells using single cell RNA-Seq and DropSeq technologies, but the only provenance that could be attributed to these cells was from within the large heterogeneous group of hypothalamic sub-regions partially sampled within their microdissected tissue sample, which include large portions of the medial, but not lateral hypothalamus. In contrast, Yelin-Bekerman et al., (2015) sampled from the whole hypothalamus of zebrafish to identify transcripts specific to neurons – isolated by fluorescence-activated cell sorting (FACS) – that expressed the neuropeptide

hypocretin/orexin (H/O); these neurons are typically enriched in the lateral hypothalamus in most species (**Table 1**).

Very few studies have examined proteomic or peptidomic profiles of whole hypothalamic samples. Extending the protocol they developed for peptidomic analysis of small microdissected brain regions such as the motor cortex, thalamus and striatum (Sköld et al., 2002), the Andrén laboratory reported identifying novel peptides from hypothalamic extracts (Svensson et al., 2003; Sköld et al., 2007). Fälth et al., (2006) developed a database for endogenous peptides identified by mass spectrometry, into which they have incorporated their hypothalamic datasets.

4.2.3: Molecular extraction from the hypothalamic circadian system. The suprachiasmatic hypothalamic nucleus (SCH), a well-defined compact nucleus within the hypothalamus that is amenable to precise sampling or molecular studies (e.g., see Fig. 1 of Porterfield et al., 2007; Fig. 1 of Boone et al., 2013), is the primary neural substrate for the master circadian clock in the body, which receives signals that allow organisms to respond to shifts in light during the day-night cycle. Often, circadian rhythms are characterized by changes in gene expression within the SCH; studies using microarray analysis demonstrated, for example, that approximately 650 transcripts undergo cyclic changes in expression in the SCH and the liver of mice, with many of these specific to the SCH (Panda et al., 2002). After certain stimuli, immediate early genes in the SCH peak and return to baseline, while a few others maintain their expression levels to protect the nuclei from excitotoxicity (Porterfield et al., 2007; Porterfield & Mintz 2009). Similar to contrasts between light and dark cycles, the transcriptome of the SCH is also distinct during wake and sleep cycles (Winrow et al., 2009), and there is recent transcriptomic evidence that certain classes of genes in the SCH peak twice in their expression levels across the circadian cycle (Pembroke et al., 2015). Single-cell transcriptomic analyses of mouse SCH neurons isolated by LCM have also revealed novel transcripts expressed in correlation with phase shifts in the circadian cycle (Park et al., 2016).

During shifts in circadian time, gene expression is not the only mechanism affected, but protein levels as well. Certain studies have examined proteomic changes in the whole hypothalamus after experimental disruptions in circadian rhythms (Mishra et al., 2009). Moreover, analysis of the proteome has revealed that 13% of soluble proteins expressed in the SCH undergo circadian regulation (Deery et al., 2009), and that a "time of day proteome" exists in this structure, with several proteins exhibiting marked fluctuations specifically during the transitions from light to dark and vice versa (Chiang et al., 2014). Interestingly, the SCH has become something of a model system for peptidomic studies, in that most of the peptidomic studies to date for a hypothalamic sub-region have been focused mainly on this structure (**Fig. 3D**). Peptidomic studies have revealed differential peptide abundances that correlate with changes in the time of day, including vasoactive-intestinal polypeptide (VIP) and pituitary adenylate cyclase-activating polypeptide (PACAP) (Lee et al., 2010; Southey et al., 2014). However, peptidomic signatures of the SCH do not necessarily mark peptides designated for release, and an analysis of releasates has made it possible to detect peptides designated for cell-to-cell communication (Hatcher et al., 2008; see review by Mitchell et al., 2011). Future work along these lines could help to determine differential peptide release from SCH sub-regions (e.g., the core and shell), which are known to have distinct physiological characteristics (reviewed by Moore et al., 2002). For example, neurons have a firing rhythm that need to be reset after responding to stimuli and the dynamics in gene expression patterns associated with phase resetting are different between the core and shell (Zhu et al., 2012).

4.2.4: Molecular extraction from the hypothalamo-neurophypohysial system. The supraoptic nucleus of the hypothalamus (SO) is a well-studied structure known for its role in mediating fluid homeostasis and regulating parturition, and exhibits structural and functional plasticity in association with these physiological processes that signal underlying alterations in molecular expression. These hallmarks of plasticity include changes in nucleolar numbers (Hatton et al., 1972) that signify changes in ribosomal RNA synthesis; i.e., protein synthetic machinery levels (Pederson, 2011). Studies on the SO have been conducted to profile the transcriptome under normal, physiological conditions or after the effects of hypo-osmolality and/or dehydration. The main neuronal phenotypes of the SO are oxytocin (OT)- and vasopressin (VP)- expressing magnocellular neurons (MNs), which have been found to express 1,385 genes at levels that are more than twice those found in the rest of the hypothalamus, when sampled as a whole (Mutsuga et al., 2004). Taking advantage of the two types of MNs, Humerick and colleagues (2013) isolated SO MNs by their expression of OT or VP and found differential expression patterns; most notably in their transcription factors. However different these neuronal subtypes are, many studies have also examined global effects on MNs. For example, hypo-osmolality inhibits both OT and VP MNs and alters their transcriptome in comparison to the whole hypothalamus (Yue et al., 2006). Single MNs have also been isolated from rat SO and analyzed for neuropeptide phenotype markers (Xi et al., 1999; Glasgow et al., 1999; Yamashita et al., 2002; reviewed by Mutsuga & Gainer, 2006).

Together with the MNs of the paraventricular hypothalamic nucleus (PVH), the SO makes up the hypothalamo-neurohypophyseal system (HNS) that, along with several other functions, mediates fluid homeostasis. Dehydration/salt-loading can alter the HNS transcriptome, with certain genes enriched in the PVH and SO being especially sensitive to this physiological condition (Hindmarch et al., 2006; Qiu et al., 2011; Stewart et al., 2011; Qiu et al., 2014; Greenwood et al., 2015; see also Hindmarch et al., 2013). Similarly, the HNS proteome is also altered by dehydration, where 25 and 45 proteins have been reported to be affected in the SO and neurointermediate lobe (NIL), respectively (Gouraud et al., 2007). Johnson et al., (2015) have employed next generation sequencing technology (RNA-Seq) to examine the effects of salt loading on gene expression in the SO of rats, and found that nearly 6% of the genes alter their expression levels following this intervention. Given the roles of OT and VP in the HNS system, there is also a rich interest in other peptides MNs may express. For example, Bora et al., (2008) identified 85 peptides from isolated MNs of the SO. Moreover, Hazell and colleagues (2012) provide an overview of their studies concerning the presence of various G-protein coupled receptors in the PVH and SO using high-throughput methods, along with other techniques.

Along with MNs, the PVH also harbors distinct parvicellular neurons (PNs), although their similarity is highlighted by their comparable gene expression profiles (Bonaventure et al., 2002). Of the 2,145 profiled genes within these cell types, 65% were validated via *in situ* hybridization. The PNs of the PVH that express corticotropin-releasing hormone (CRH) are involved in the stress response as part of the hypothalamic–pituitary–adrenal (HPA) axis. Some studies on the PVH have been conducted to examine a handful of genes in PNs without technically resorting to "high-throughput methods", such as focused studies of certain genes using real-time PCR. For example, Wang et al., (2008) examined LCM-captured human hypothalamic tissue collected *post mortem*, and identified an up-regulation of corticotropin-releasing hormone (CRH) and other gene products in associated with patients who suffered from clinical depression. Other studies have used modern "-omics" technologies to either profile the transcriptome alone (Atkins et al., 2011) or to

investigate a mechanistic role for PVH genes within the HPA axis. For example, transcriptomic analysis, combined with morphometric and immunohistochemical evidence, demonstrated that select neurons, likely to be true PNs, express the gene encoding the molecule secretagogin, which is functionally linked to CRH release from these neurons (Romanov et al., 2014).

4.2.5: Molecular extraction from the arcuate hypothalamic nucleus (ARH). The arcuate hypothalamic nucleus (ARH) is a structure involved in the maintenance of energy homeostasis. Transcriptomic analyses have been conducted across multiple studies examining the effects of diet, peripheral signals, and environment on gene expression in ARH neurons. For example, the Paulsen et al., (2009) identified changes in neuropeptide Y (NPY) and pro-opiomelanocortin (POMC) mRNAs and an additional 3,480 transcripts in fasted, diet-induced obese rats. Similarly, Jovanovic et al., (2010) showed changes in hundreds of genes in the ARH after leptin treatment in 48-hr fasted animals. At a more detailed level, Landmann et al., (2012) used LCM to sample the ARH in fasted rats, fed rats, and rats refed with a glucose load and found an up-regulation of AgRP mRNA under fasted conditions that was greater in magnitude within single, LCM-captured neurons compared to what the authors term "ARH cell layers", which essentially meant a complete LCM of the full ARH expanse along its cytoarchitectonic boundaries in each sampled coronal section (note the investigators performed single-cell LCM on one hemisphere, and full ARH LCM on the opposite hemisphere). In response to the refed condition, AgRP was conversely found to be down-regulated and POMC mRNA up-regulated. Importantly, the authors specified a brain atlas they used and the specific atlas levels from which they sampled the ARH, setting this study apart from most others in its more careful delineation of anatomical boundaries.

Conducting cell type-specific transcriptomics, Henry and colleagues (2015) identified molecular pathways specific to AgRP neurons that were differentially affected in fed and food-deprived animals. Similarly, Campbell et al., (2017) found using Drop-Seq methodology (see **Section 4.2.2**) that thousands of genes coding for non-neuronal and neuronal cell types displayed altered expression in association with changes in feeding conditions and energy states. They found that the transcriptional response to fasting was generally stronger than that produced by a high-fat diet, with neuronal types responsive to fasting also responsive to high-fat feeding.

Transcriptomics has also addressed questions about the relationship between the ARH and the peripheral nervous system. For example, Adler et al., (2012) characterized the transcriptome of retrogradely-labeled neurons within the ARH projecting to white adipose tissue. Neurogenin 3, a transcription factor that helps differentiate pancreatic endocrine cells also comprised a portion of the transcriptomic profile of NPY neurons of the ARH (Arai et al., 2010). Other cell types in the ARH that have been targets of molecular profiling include cholinergic neurons, many of which were found to also express tyrosine hydroxylase and markers for GABAergic neurotransmission (Jeong et al., 2016).

Transcriptomic analyses have also been used to address how the environment can affect the ARH. For example, low protein diet during postnatal development reduces body fat, and increases leptin and melanocortin receptors (Stocker et al., 2012). The ARH also maintains stability in its expression patterns under certain changes within the internal environment, such as during pregnancy. Specifically, Phillipps and colleagues (2013) showed that despite higher shifts in plasma leptin and insulin and low blood glucose induced by pregnancy, there are no changes in the ARH transcriptome. These studies have provided understanding as to what extent the ARH transcriptome is affected by environment. Finally, transcriptomics traditionally provides

information about the expression levels of mRNA but can also provide valuable information expression concerning microRNA levels. A set of more than 210 microRNA genes was profiled in both the ARH and the PVH as potential regulators of mRNA (Amar et al., 2012).

In contrast to transcriptomics, only a few investigators have investigated the ARH proteome. For example, proteomic analysis of protein markers in the ARH after exposure of the organism to an inorganic compound demonstrated a few proteins that are altered in their levels of expression that are related to cell morphology, axonal growth and tissue remodeling (Amigó-Correig et al., 2012).

4.2.6: Molecular extraction from other hypothalamic sub-regions (LHA, VMH). A number of studies have performed molecular analyses of peptidergic neurons known to be enriched in the LHA For example, Volgin et al. (2004) reported isolating individual slices of brain containing portions of the LHA and creating suspensions of dissociated cells from that region. They then identified the peptidergic phenotype of the cells using antibodies raised against the precursor peptide encoding hypocretin/orexin (H/O). pre-pro-H/O; or melanin-concentrating hormone (MCH), and performed RT-PCR on each cell for the respective mRNAs for these neuropeptides, providing a proof of concept for their delicate methods. Harthoorn et al., (2005) reported using single-cell LCM to generate transcriptional profiles of neurons expressing MCH and H/O, and found that these neurons express transcripts for several other neuropeptides, such as dynorphin and cocaine- and amphetamine-related transcript (CART).

Using a translational profiling technique called TRAP (Translating Ribosome Affinity Purification; Doyle et al., 2008; Heiman et al., 2008; Dougherty et al., 2010), which involves affinity purification of polysomal mRNAs in defined cell populations, Dalal et al. (2013) generated mouse transgenic lines that expressed a fusion protein encoding enhanced green fluorescent protein and the large-subunit ribosomal protein L10a (eGFP-L10a) in hypothalamic neurons that express H/O. The expression of this fusion protein allows for the isolation of those mRNAs within H/O-expressing neurons that are undergoing translation at the site of polyribosomes, effectively allowing a translational profiling of a chemically identified neuron. Using this approach, the investigators identified >6,000 transcripts with signal above background levels; 188 of these were highly enriched in H/O neurons (Dalal et al., 2013). Fifteen of these transcripts were confirmed to be present within intact H/O neurons by dual-label *in situ* hybridization, including the transcription factor Lhx9, which the authors showed, using gene ablation experiments, that it contributes to maintaining wakefulness in mice. Using an extension of the TRAP approach on the same problem, which they dubbed "vTRAP" ("viral TRAP"), Nectow et al., (2017) engineered a Cre-dependent adeno-associated virus to harbor a construct encoding eGFP-L10a, to translationally profile specific a variety of cell types in layer 5 of the cerebral cortex, the dorsal thalamus, ventral tegmental area, dorsal raphe nucleus, and LHA. Within the latter region, they focused on targeting their viral construct to MCH-expressing neurons.

The Jackson laboratory has recently reported single-cell transcriptomic data obtained from LHA H/O-expressing neurons and MCH-expressing neurons in mouse transgenic lines (Mickelsen et al., 2017). Importantly, in their study, they show specific delineations of the regions they dissected using atlas-based coordinates and drawings of the estimated areas they micropunched. A surprising finding from their careful analyses was that virtually all MCH neurons and approximately half of H/O neurons express markers for glutamate release and GABA synthesis (but not GABA vesicular release), underscoring the importance of fast-acting, small

neurotransmitters within these peptidergic neurons and highlighting potentially interesting roles for GABA metabolism with glutamatergic neurons.

Studies have also been conducted to analyze the molecular expression patterns within the ventromedial hypothalamic nucleus (VMH). The Elmquist laboratory performed LCM to isolate and analyze the VMH from mice and used microarrays to detect genes enriched in this region of the hypothalamus (Segal et al., 2005). They compared the genes they obtained with those obtained from nearby regions (the ARH and dorsomedial hypothalamic nucleus; DMH). They used real-time PCR to validate nine of the twelve most robustly expressed genes, and went on to confirm the expression of three of these genes using *in situ* hybridization. Their work complements that conducted by the Ingraham laboratory, which furnished a transcriptome from manually microdissected tissue samples obtained from the developing mouse (Kurrasch et al., 2007), in which they identified and confirmed the expression of six different VMH-enriched markers from their initial screens.

4.3: A note about "hypothalamic-derived" molecules. Before moving on to discuss LCM, it is worth ending this portion of the narrative with a brief note regarding molecular provenance from the perspective of evolution. In this section, we have focused on molecular extraction of molecules from the hypothalamus, including, to name a few, neuropeptides of the hypothalamo-neurohypophysial system (OT and VP), the circadian system (VIP), and wakefulness and energy balance (H/O, MCH, AgRP). However, it is important to bear in mind that these "hypothalamic-derived" molecules are not strictly linked to the vertebrate hypothalamus *per se*, since large-scale molecular phylogenetic studies have identified precursors and analogs of these molecules in animal taxa that have evolved nervous systems lacking a hypothalamus (Jékely, 2013; Mirabeau and Joly, 2013). For example, Semmens et al., (2016) performed transcriptomic studies of the radial nerve cords of the European starfish, *Asterias rubens*, and identified >40 neuropeptide precursors in this echinoderm, many of which have homologs in the vertebrate hypothalamus. Indeed, precursors to neuropeptides found in the mammalian hypothalamus can be found in many phylogenetically ancient animal taxa (see Supplemental Data of Elphick et al., 2018). Thus, in our quest to preserve the provenance of molecular data from the hypothalamic regions from which they are extracted, we must bear in mind the ironic fact that many of the molecules, from an evolutionary standpoint, never "belonged" to the hypothalamus in the first place.

5: Laser-capture microdissection studies: Methodological considerations

In this section, we describe how laser microdissection or laser-capture microdissection (LCM) techniques are a useful step for precisely delineating regions of interest within the hypothalamus for subsequent high throughput molecular analyses. We describe a few approaches involving this technique and their advantages and disadvantages, followed in **Section 6** with how such samples can be traced back to their regions of extraction using digital atlas-based mapping techniques.

Since its development in the late 1990s (Emmert-Buck et al., 1996), LCM has been a useful procedure for obtaining RNA from single cells or whole regions of tissue (for selected reviews of techniques, see Espina et al., 2006; Baskin & Bastian, 2010; Datta et al., 2015). LCM has been widely used to collect individual cells (Backholer et al., 2010; Park et al., 2016) or groups of cells from tissue slices or cultured cells that have been identified using immunocytochemistry (termed

immuno-LCM; Baskin & Bastian, 2010) or specific fluorescent tags (*e.g.*, GFP) or fluorescent dyes such as Alexa Fluor™ 488). These approaches have enabled users to examine the expression of anywhere from a few genes of interest upwards to several hundred genes in specific cell types for various applications including genomics, transcriptomics (next-generation sequencing, microarrays; Paulsen et al., 2009), and proteomics (Moulédous et al., 2003; for a review of applications, see Datta et al., 2015). In this section, we describe findings and/or present data from our use of two different LCM systems: 1) the Arcturus AutoPix Fluorescent LCM System (Thermo Fisher Scientific, Waltham, MA) and 2) Leica LMD 7000 Microscope (Leica Microsystems Inc., Buffalo Grove, IL). In contrast to the Arcturus AutoPix LCM model in which the dissected tissue was collected onto a plastic cap (CapSure LCM Caps) *above the slide*, both dissected tissue and membrane surrounding the tissue was collected *below the slide* containing a UV-absorbing membrane (MembraneSlide) into a microcentrifuge tube cap using the Leica LMD7000 Microscope. Both LCM instruments have now been replaced by more recent models, including the ArcturusXT™ LCM System (now distributed through Thermo Fisher Scientific) and Leica LMD6/LMD7. Here we present ways in which LCM has been used to collect 1) regions of tissue from anatomically distinct areas of the brain (**Section 5.1**); and 2) targeted populations of cells that have been identified using immunocytochemistry (**Section 5.2**) or fluorescent conjugates (**Section 5.3**). We discuss advantages and pitfalls to using these approaches.

5.1: LCM for general sampling of brain regions. This is the most common application of LCM for collection of brain tissue involves collecting anatomically matched regions of tissue across several rostrocaudal levels of a particular brain site. We have used Arcturus AutoPix Fluorescent LCM System to confirm sufficient knockdown of oxytocin receptor mRNA following hindbrain nucleus of the solitary tract (NTS) injection of oxytocin-saporin toxin relative to control saporin toxin (Baskin et al., 2010). We collected bilateral samples of NTS tissue from slide-mounted cryostat sections (10 µm) at the level of the area postrema (AP) and rostral to the AP at 200 µm intervals (n=8 slides/brain). Following LCM collection, sections were dehydrated in ethanol and xylene, and then air-dried. We have found that this approach was suitable for measuring differences in NTS expression of oxytocin receptor mRNA. In addition, we have used the Arcturus AutoPix Fluorescent LCM System to confirm the "expected" reduction in cholecystokinin-1 receptor (CCK-1R) mRNA in both the ARH (–3.48 mm to –2.04 mm from Bregma; Paxinos & Watson, 2007) and dorsomedial hypothalamic nucleus (DMH) (–3.60 mm to –2.80 mm from Bregma; Paxinos & Watson, 2007) in rats that lack CCK-1Rs relative to wild-type rats (Blevins et al., 2012). As before, slide-mounted cryostat sections (10 µm) of ARH and DMH were selected at 200 µm intervals, dehydrated in ethanol and xylene, and then air-dried (n=6 slides/brain). Bilateral samples were collected from brain sites that normally express CCK-1R (i.e., ARH and DMH). Lastly, we have used the Arcturus AutoPix Fluorescent LCM System (**Figure 4A**) and Leica LMD 7000 Microscope (**Figure 4B**) to confirm the increase of neuropeptide Y (NPY)/agouti-related peptide (AgRP) in the ARH from 48-h fasted rats relative to *ad libitum* fed rats (Hahn et al., 1998; Mizuno and Mobbs, 1999; Korner et al., 2001; Swart et al., 2002; Bi et al., 2003). We collected bilateral samples of ARH (–3.48 mm to –2.04 mm from Bregma; Paxinos & Watson, 2007) from slide-mounted cryostat sections (10 µm) at 200 µm intervals (n=6 slides/brain). In all cases, sections from adjacent slides were stained with Cresyl violet (Blevins et al., 2000a,b; Baskin et al., 2010) to enable anatomical matching. As noted earlier, Panels B and C of **Figure 2** show an example of LCM capture of the ARH from Cresyl violet-stained tissue sections.

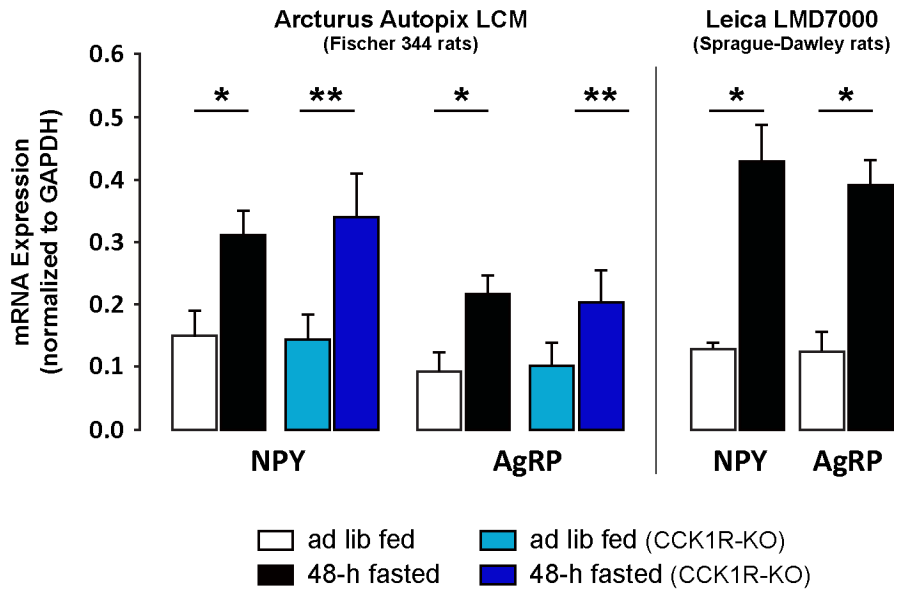

Fig. 4. Unpublished data furnished here to illustrate the efficacy of two LCM systems (Arcturus and Leica), along with qPCR, to confirm fasting-elicited increases in NPY and AgRP mRNA expression in the ARH in rats. Slide-mounted cryostat sections (10 µm-thick) were generated through the ARH from *ad libitum* fed or 48-h fasted wild-type or cholecystokinin-1 receptor (CCK1R) knockout (KO) Fischer 344 rats (**left panel**) or *ad libitum* fed or 48-h fasted wild-type Sprague-Dawley rats (**right panel**). Sections were thawed briefly prior to dehydration in ethanol and xylene and allowed to air dry as described previously (Blevins et al., 2000a; Baskin et al., 2010; Blevins et al., 2012). LCM was used to collect bilateral sections (10 µm-thick) from the ARH (200 µm intervals) from six anatomically matched levels and sections were mounted onto slides. All microdissected samples from a single brain were pooled for RNA extraction. NPY and AgRP mRNA expression were measured using qPCR. Data are expressed as mean ± SEM. *P<0.05 or **P=0.1 fed vs. fasted.

Landmann et al., (2012) have extended these findings by using LCM to demonstrate that fasting results in increased AgRP mRNA expression from the ARH (both when collected as a region or as single neuron pools consisting of 100 neurons). LCM has been used by other labs to profile the molecular composition of various hypothalamic regions (**Tables 1–3**). For example, to highlight a few studies by way of illustration, LCM has been used to confirm: 1) the effectiveness of adeno-associated viral knockdown of angiotensin II receptor subtype 1a in the subfornical organ (SFO) of rat brain (Walch et al., 2014); 2) reductions in gene expression in brains of steroidogenic factor 1 (SF-1) in the VMH of knock-out mice (Segal et al., 2005); and 3) fasting-elicited changes in gene expression in the PVH and the impact of leptin replacement on these genes (Tung et al., 2008).

5.2: Immuno-LCM

5.2.1: Advantages. Immuno-LCM (Fassunke et al., 2004; Fink et al., 2000; Waller et al., 2012) is the approach of using immunocytochemistry to identify cells to be collected by LCM. One of the primary advantages of immuno-LCM is that it enables the user to phenotype specific

cells of interest that could not be as easily identified using anatomical landmarks alone. This may be a particularly useful approach given that tissue sections collected by LCM cannot be coverslipped and, as a result, may not allow sufficient resolution to identify anatomical landmarks readily. One of our laboratories (JEB) has used this approach to identify (following a rapid immunostaining procedure for tyrosine hydroxylase (TH); a marker of catecholamine neurons) and collect catecholamine immunopositive neurons from the A2/C2 catecholamine cell groups in the hindbrain NTS. We used the Arcturus AutoPix to confirm the specificity of this approach by measuring TH mRNA from TH+ neurons relative to TH– neurons confirm TH mRNA for qPCR (Williams et al., 2008). There are a number of protocols for rapid immunostaining that have already been published (Fink et al., 2000; Uz et al., 2005; Williams et al., 2008; Baskin & Bastian, 2010; Park et al., 2016).

5.2.2: Challenges and Pitfalls. There are a number of challenges when using the rapid immunostaining approach that must be considered prior to incorporating immuno-LCM. For example, as reviewed by Baskin and Bastian (2010), the process of immunostaining can introduce the potential for RNA extraction and degradation. In an effort to minimize loss and degradation of RNA, common strategies are to implement rapid immunostaining protocols and the use of alcohol fixation (methanol or ethanol) in place of formaldehyde-based fixatives (which can result in much of the RNA being fragmented and degraded by formalin) (Gillespie et al., 2002; Soukup et al., 2003; Su et al., 2004; Hu et al., 2005; Baskin and Bastian, 2010; Park et al., 2016). We have previously shown that brief thawing (~30–60 sec) of cryostat-cut sections of frozen rat brain in combination with quick immunostaining after methanol fixation (~3 min) works well for immuno-LCM and qPCR for mRNA (Williams et al., 2008). Other challenges to the use of the rapid immunostaining approach include antibodies that require a low titer or are relatively nonspecific as well as antigens that are found in low-abundance (Baskin and Bastian, 2010). As Baskin and Bastian (2010) indicate, adjustments in staining times, incubation temperatures or more sensitive fluorochromes, may increase the specificity to acceptable levels. Rapid immunostaining approaches may be less suitable for targeting and collection of cells with low gene expression.

Another challenge when selecting specific cells is that contamination from neighboring cells may also be included in the sample. For example, Okaty et al., (2011) reported in their meta-analysis of various cell isolation methods conducted by certain laboratories that LCM produced higher contamination from spurious signals, as compared to other cell isolation methods, such as TRAP, FACS, immunopanning, and manual sorting of fluorescently labeled cells. Their analysis included an immuno-LCM study (Chung et al., 2005) and one in which LCM was performed on fresh-frozen brain tissue sections containing genetically labeled cells from transgenic mice (Rossner et al., 2006). One means to address this issue is to collect an equal number of neighboring cells outside of the intended region of analysis as negative controls to run alongside the positively labeled cells. We have found that selecting ~150-200 TH+ and adjacent non-catecholaminergic cells (TH–) cells from several adjacent sections was a suitable approach for measuring increases in TH mRNA from TH+ cells relative to TH– cells from the A2/C2 catecholamine cell groups in the hindbrain NTS (Williams et al., 2008).

5.3: Use of LCM to target cells using fluorescent conjugates.

5.3.1: Advantages. Similar to immuno-LCM, this approach enables the phenotyping of specific cells of interest that could not be as readily identified using anatomical landmarks. In contrast to immuno-LCM, there is no need for rapid immunostaining as the fluorescent tag is

already present. We have used this approach previously (Blevins et al., 2009; see **Figure 2D–F**) to identify those neurons in the PVH that project to the hindbrain NTS using Alexa Fluor™ 488-conjugated retrograde tracer, cholera toxin subunit B (CTB). We have found that brief thawing (~30–60 sec) of cryostat-cut sections of frozen rat brain, in combination with selecting ~250 CTB+ cells from three or four anatomically matched coronal sections from PVH, was a suitable approach for measuring OT, corticotropin-releasing hormone (CRH), and melanocortin-4 (MC4-R) receptor mRNAs (Blevins et al., 2009). We also collected the same number of neurons from the SCH as a negative control, as this site expresses relatively low levels of each of these transcripts (Mountjoy et al., 1994; Jing et al., 1998). In addition, unlabeled cells from the PVH were collected and screened for OT mRNA, CRH, and MC4-R mRNAs.

5.3.2: Challenges and Pitfalls. One potential limitation of using LCM to collect GFP-labeled cells is that free GFP is soluble and can leak out from cryostat-cut sections in the absence of fixation (Jockusch et al., 2003), thus necessitating perfusion and/or post-fixation of the tissue. Soluble eGFP is preserved in paraformaldehyde (PFA)-fixed tissues that are post-fixed in 50% ethanol and 100% *n*-butanol (Khodosevich et al., 2007). The authors noted that while PFA fixation of mouse tissue is sufficient in preserving the EGFP signal for up to 30–60 min, it was not sufficient in preserving EGFP signal for longer periods of time (Khodosevich et al., 2007). They also indicated that post-fixation in alcohol is "necessary not only to remove the water to prevent RNA degradation, but also to render the aldehyde-crosslinks more stable, thus preserving the fluorescence" (p. 2). They added that "alcohol fixation alone also was not sufficient to preserve fluorescence of the soluble EGFP and prevent it from leaching out and diffusing to neighboring tissue making it impossible to specifically identify green fluorescent cells" (p. 2). Although some groups have reported relative disadvantages of using formaldehyde-based fixatives to retrieve PCR product from LCM-sampled non-neural (Goldworthy et al., 1999) and neural tissues (Su et al., 2004), there are instances where LCM has been shown to work successfully on formaldehyde-fixed tissues (e.g., Kabra et al., 2016). Recent papers indicate that EGFP+ (or EYFP+) cells can also be harvested from fresh frozen mouse (Rossner et al., 2006; Liu et al., 2011) and rat brain tissue (Liberini et al., 2016), but the extent to which the fluorescent signal may have diffused or faded beyond 30–60 min were not addressed in these studies. It is worth noting that Leica has produced a protocol designed to optimize visualization of GFP from post-fixed tissue to be used for LCM.

5.4: RNA Integrity. The RNA Integrity Number (RIN) value is a tool developed by Agilent Technologies to assess RNA integrity using the Agilent 2100 Bioanalyzer and RNA LabChip® kits. The RNA integrity is based on the electrophoretic trace of the sample and allows the user to assess the amount of degradation products in the sample and to determine integrity of the sample. It is an important consideration when assessing gene expression data from samples generated by LCM. The RIN algorithm assesses RIN values that range from 1–10 with 1 representing completely degraded RNA, 5 representing partially degraded RNA, and 10 representing completely intact RNA. We have used the 2100 Electrophoresis Bioanalyzer (Agilent Technologies) to obtain RIN values from ARH tissue samples that had been stored for ~3 months at –80°C. We obtained RIN values ranging from 7.6–8.2 (7.92 ± 0.09). These RIN values are comparable to those we obtained from ARH tissue (7.8 and 8.5) that had been stored ~7–8 months at –80°C. While these values are in the higher range it does indicate some degree of degradation. These findings are also consistent to the RIN values (6.2) reported from tissue collected from patients with oral cancer that was stored for ~48 h at –80°C (Xu et al., 2008), as well as RIN values

(6–7) reported from pancreatic tissue collected from rats and humans (Butler et al., 2016). They are also consistent with RIN values (6.6–7.6) reported for hypothalamic tissue sampled using LCM from the supraoptic (SO) nucleus; the LCM was performed within one month following tissue sectioning and storage of the slide-mounted sections at –80°C (Johnson et al., 2015).

6: Anchoring molecular information to their native regions using digital atlas maps

Having reviewed in the preceding sections the importance of location information in the brain (**Section 2**), the historical antecedents of current high throughput work concerning molecular extraction of the brain (**Section 3**) and the hypothalamus (**Section 4**), and the methodology of LCM (**Section 5**); we now turn to the topic that constitutes the principal thesis of this review; namely, the mapping of datasets to standardized atlases of the brain. Using the backdrop of LCM procedures described in the preceding section, we discuss first how documenting the location of the native substrate from where tissue is extracted is critical for the subsequent mapping of that location, and then describe the mapping steps themselves.

6.1: Documenting the native substrate before extraction. Applying LCM to a tissue section to capture and sample a particular region of interest can be performed in a number of ways, a few of which were described in **Section 5**. Unstained tissue sections can be viewed under a dark field microscope to observe the region of interest in relation to white matter tracts that might be nearby. Such landmarks can aid greatly in the accurate and repeated sampling of a region, especially for large sub-regions of the hypothalamus, a part of the brain replete with white matter landmarks (e.g., anterior commissure, optic chiasm, optic tract, fornix, mammillothalamic tract). Indeed, what is perhaps the first documented sampling of the hypothalamus was reported diagrammatically in relation to many of these fiber systems (see **Fig. 2A**). Micropunch methods, first developed before the establishment of LCM, involve procedures where tissue punches are harvested from unstained frozen or fresh tissue sections; in such cases, white matter tracts also serve as important landmarks to orient the experimentalist as to where a particular region of interest was located and how much tissue to collect from that region (Palkovits, 1973; Jacobowitz, 1974).

Apart from unstained tissue, the most common method for identifying regions of interest in sectioned brain tissue is through the use of Nissl stains (stains that label basophilic substrates – 'Nissl substance' – in the cell, including rough endoplasmic reticulum and the nucleus, sites where nucleic acid molecules are concentrated). The use of such stains on brain tissue sections prior to LCM-based sampling from those sections is a common way of accurately delineating regions of interest for LCM-targeting (e.g., Boone et al., 2003; Ginsberg and Che, 2004). Nissl-based stains such as Cresyl violet (**Fig. 2B**), thionin, and hematoxylin have been used to guide sampling of hypothalamic sub-regions and cells, including the ARH (Segal et al., 2005; Jovanovic et al., 2010), SCH (Boone et al., 2003; Porterfield et al., 2007; Pembroke et al., 2015), SO (Xi et al., 1999; Glasgow et al., 1999; Yamashita et al., 2002; Wang et al., 2008), VMH (Segal et al., 2005; Kurrasch et al., 2007), DMH (Segal et al., 2005), and PVH (Wang et al., 2008; Blevins et al., 2009). Importantly, investigators have performed LCM on the Nissl-stained tissue itself (Boone et al., 2003; Segal et al., 2005; Porterfield et al., 2007; Jovanovic et al., 2010), but in principle, one can also use adjacent sections stained for Nissl substance to help delineate regions of interest on unstained companion sections sampled by LCM, as has been done for human tissue samples collected *post mortem* for the PVH and SO (Wang et al., 2008). In addition to using Nissl staining as a tool to help delineate LCM-captured tissue sample boundary conditions, other stains and labeling strategies have also been used in conjunction with LCM, including FluoroJade for

delimiting tissue pathology (Boone et al., 2013), NeuroTrace staining for visualizing fluorescent Nissl-like profiles (Benner et al., 2015), and *in situ* hybridization in human post-mortem tissue (Bernard et al. 2009). Finally, it is worth noting that although LCM procedures themselves do not appear to result in significant losses of protein as compared to manually dissected samples of comparably located regions, Nissl staining itself can be detrimental to the full retention of some proteins for subsequent proteomic analyses (Moulédous et al., 2002), and NeuroTrace staining can result in lower yields of transcripts from LCM-captured brain tissue (Benner et al., 2015).

6.2: Mapping to standardized atlases. Using aids such as the Nissl stain to identify a region of interest to be sampled by LCM not only helps ensure accurate sampling of that region, but also provides an opportunity to document the location of the excised tissue itself using standardized atlases of the brain. Such atlases have existed for several decades, and many have been created for a variety of animal models, including – to name but a few – toads (Hoffman et al., 1973), frogs (Wada et al., 1980), lizards (Greenberg, 1982), guinea pigs (Tindal, 1965), rabbits (Sawyer et al., 1954), mice (Dong, 2008; Paxinos and Franklin, 2012), and rats (Swanson, 2004; Paxinos and Watson, 2007) (for a detailed listing, see Ten Donkelaar and Nicholson, 1998). As detailed in Khan (2013), there are many advantages of using standardized atlases to map experimental data onto, not least of which is to be able to spatially align different datasets from diverse studies and contextualize them with some rigor and precision (also see Khan et al., 2018).

How is mapping experimental data to a reference atlas of the brain performed? Simmons and Swanson (2009) describe many aspects of how mapping experimental data to a standardized reference atlas is undertaken. A critical factor is reconciling the plane of section of the experimental tissue with the plane of the atlas map that will be used to contain the mapped dataset. Differences in plane of section, determined by the angle of cutting on the microtome or cryostat instrument used to section blocks of brain tissue, can potentially constitute a significant source of mapping errors, especially in the absence of any global (e.g., Nissl) stain to mark the cytoarchitecture of the tissue being sectioned. It is surprising to us how few investigators explicitly discuss how they have dealt with plane of section issues when analyzing the results of expression and distribution studies.

For example, many investigators have utilized immunohistochemistry of the transcription factor and immediate-early gene product, Fos, to identify regions of the brain *post mortem* that may be associated with patterns of activation or with particular behaviors that the organism was involved in during the life history immediately preceding death. However, to our knowledge, none of these studies presents a comparison of Fos expression patterns between groups of animals while providing an explicit discussion of how planes of section were taken into account in their determination of regional comparisons. Thus, as part of a collaborative study (Zséli et al., 2016), a few of us (AM, AMK) performed a plane of section analysis to map patterns of Fos expression in rats who had fasted for 40 h (but had ad libitum access to water) versus rats who fasted for 40 h but then were allowed to re-feed for 2 h.

Figure 5 shows a portion of these data. Compared to the plane of section of the Swanson (2004) reference atlas (**Fig. 5A**, *top panel*), the planes of section for the subjects examined for Fos expression were markedly different (**Fig. 5A**, *middle and bottom panels*), and any accurate comparison of the same regions at similar rostrocaudal levels between fasted and re-fed cohorts required reconciling the planes of section for tissues sectioned from both cohorts with the plane of section of the reference atlas. This was not only important for representing the patterns of

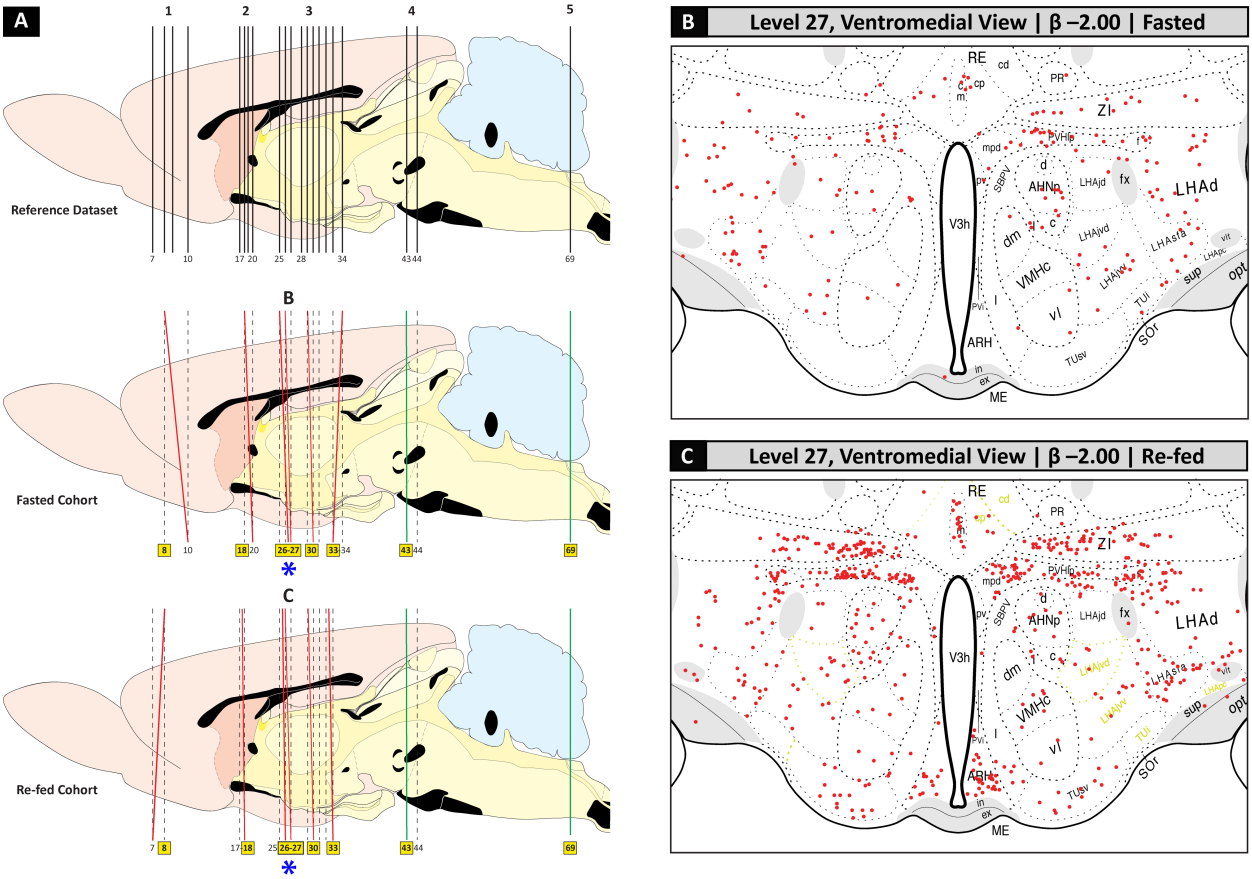

Fig. 5. Example of a plane-of-section analysis conducted on Fos transcription factor expression maps of hypothalamic tissue sections obtained from fasted *versus* refed adult male Wistar rats, conducted by the UTEP Systems Neuroscience Laboratory as part of a published collaborative study with the Hungarian Academy of Sciences and Tufts University (Zséli et al., 2016). **(A).** Sagittal views of the rat brain, modified from Swanson (2004), showing the plane of section of the Swanson atlas (*top panel*: 'Reference Dataset'), followed by the planes of section for a subject from the fasted cohort (*middle panel*) and the refed cohort (*bottom panel*). **(B, C).** Locations of Fos-immunoreactive neurons plotted onto coronal-plane maps from Swanson (2004) showing the ventromedial views of atlas level 27 for each cohort (which are denoted by *asterisks* in **A**). Reproduced from Zséli et al., (2016) and with permission from John Wiley & Sons, Ltd.

---

expression on the atlas, but also to ensure that we were not comparing levels of expression between regions that did not correspond with one another in terms of spatial positioning within the brain.

As detailed in our study (Zséli et al., 2016), we utilized the digital atlas maps for Swanson, (2004), which are now also available online (https://larrywswanson.com). These were manipulated in Adobe Illustrator (AI) software. Nissl counterstain in the Fos-immunoreacted tissue sections was used as a guide to identify cytoarchitectural boundaries for each section. The photomicrographs were imported into separate layers of AI, scaled, and compared to the atlas plates to determine whether there were differences in plane across the mediolateral and dorsoventral axes. In some cases, as delineated by Simmons and Swanson (2009), patterns on a

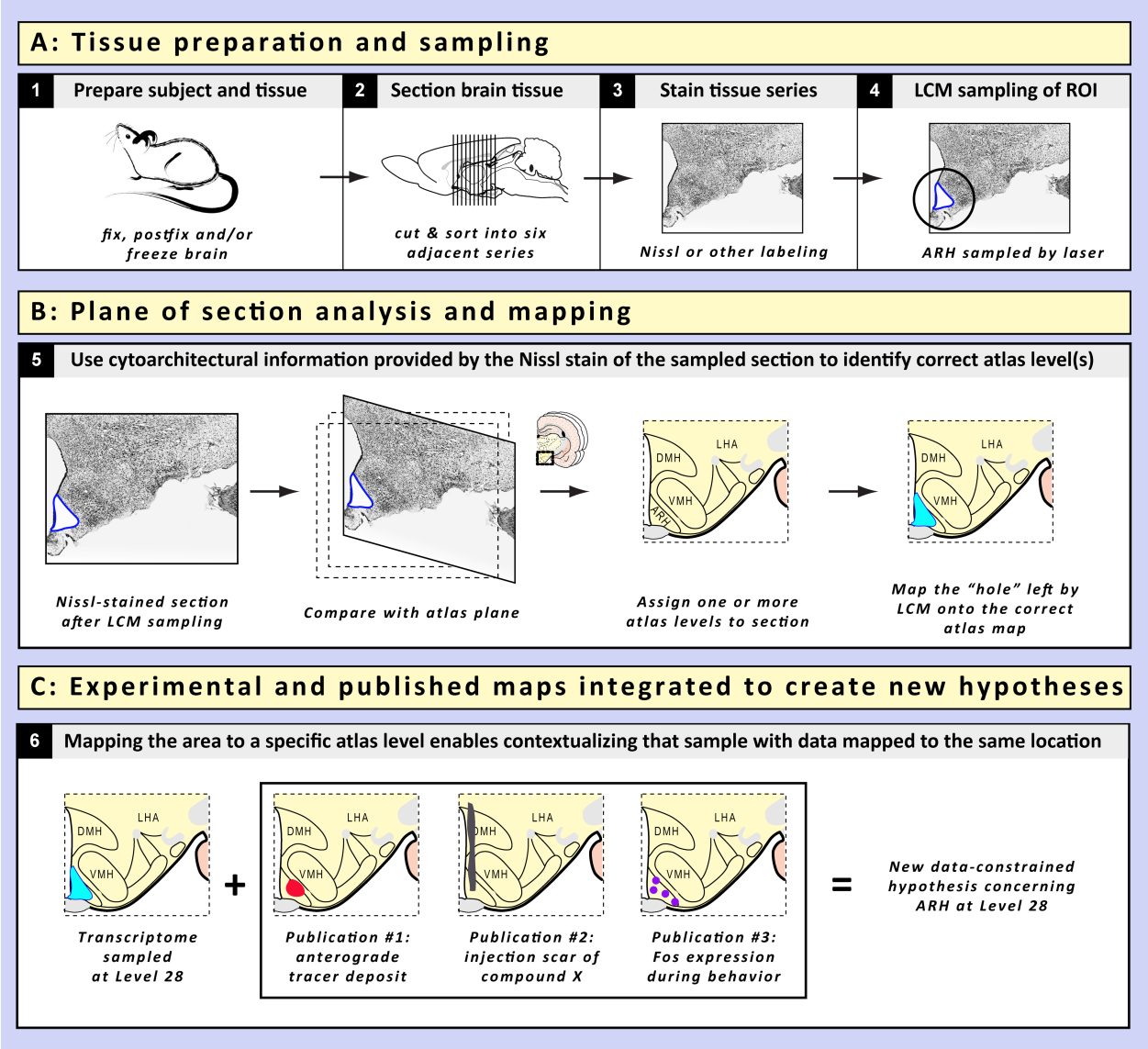

Fig. 6. Steps for mapping tissue samples collected using LCM, and the advantages of such mapping. Following steps to process brain tissue through the tissue fixation (**Panel A**, *Step 1*) and sectioning/staining/LCM-based sampling steps (**Panel A**, *Steps 2–4*), the remaining mounted and Nissl-stained tissue section from which the sample was excised can be mapped and analyzed for the location of the 'hole' left from sampling in relation to a standardized reference atlas of the brain (**Panel B**, *Step 5*). The hypothetical example shown here is for LCM-based capture of the arcuate hypothalamic nucleus (ARH) (**Panel A**, *Step 4*, *circled region* on the Nissl photomicrograph; the white region of interest (ROI) outlined in *dark blue* shows the region that was 'sampled'). **Panel C:** Once mapped, the location of the sampled tissue can be examined in relation to any other dataset that has been mapped to the same atlas level (*Step 6*). In this example, three hypothetical published datasets (a tract-tracing deposit, a drug injection site, and the distribution of activated immediate-early gene products) have all been mapped from different brains to the same reference location, thereby allowing a contextualization of the data in a spatially rigorous manner to generate new hypotheses concerning the ARH at that rostrocaudal level.

tissue section require mapping to more than one level of a reference atlas, and the differences in plane of section are often in more than one plane simultaneously, necessitating a segment-by-segment translation of the region of interest to the relevant location on a map or set of maps.

Another important point to note about deriving information for mapping on the basis of Nissl-stained tissues is that often Nissl stains do not fully reveal distinct patterns of cytoarchitecture within tissue; in such cases, it is at times difficult to discern a particular sub-region within a tissue section and determine precisely the boundaries of a region. In such cases, we have opted to report the uncertainty in our mapping that results from such ambiguous staining patterns, by noting within the reference atlas those portions of the map that are based on inferred positions of cytoarchitectonic boundaries as opposed to those that were directly observed (and distinct) within the stained tissue section. As shown in **Figure 5C**, we found certain sub-regions of the lateral hypothalamic area (LHA) to display Nissl patterns that were indistinct, which permitted us to only infer positions of the Fos-immunoreactive cells we were mapping. This uncertainty was represented in the form of a pale yellow color for the dotted line boundaries for those regions (**Figure 5C**).

For LCM-captured brain tissue, an outline of basic steps for mapping the sampled tissue to a reference atlas is shown in **Figure 6**. First, as described in **Section 5.2.2** and **Section 5.3.2**, investigators have to decide whether to employ fixatives such as methanol, alcohol or formaldehyde to preserve their tissues of interest before sectioning them, or instead opt to use freshly frozen, unfixed tissue sections (**Fig. 6A**, *Step 1*). Once sectioned and mounted onto slides (**Fig. 6A**, *Step 2*), a given tissue series can be Nissl-stained (**Fig. 6A**, *Step 3*), and then placed within an LCM instrument to excise a region of interest (ROI; **Fig. 6A**, *Step 4*). Apart from the sequestration and processing of the LCM-captured tissue of interest for further analyses using transcriptomics, proteomics, or peptidomics, etc., the remaining tissue section (i.e., the rest of the section that remains *after* the region of interest has been excised) can now be used as a key to unlock the precise location of the sampled area within a standardized reference space of the brain. Similar to the example of a plane-of-section analysis furnished in **Figure 5**, the section can be examined in relation to the Nissl-based landmarks of photographs within the reference atlas to be used, and the tissue's plane of section assigned to appropriate levels of the reference atlas (**Fig. 6B**, *Step 5*). The ROI within the tissue section can then be mapped using a digital atlas map of that reference level.

7: The benefits of mapping native substrates and anchoring datasets

7.1: Data integration. **Figure 6C** provides a view of the types of benefits that can be obtained by assiduously mapping a tissue sample obtained by LCM to a reference map of the brain. In addition to the data generated from the high throughput "-omics"-based extraction and analysis of the sample itself, the precise mapping of the sample in relation to its native landscape allows one to examine all previous studies that have been conducted on that sampled region that have been mapped within the same reference space. For example, for the Swanson (2004) reference atlas of the rat brain, several studies have utilized the digital maps of this work to map the datasets from their studies of the hypothalamus. Such studies include those involving central microinjections of molecules into the PVH (Khan et al., 2007; reviewed in Khan et al., 2017), protein expression in the LHA in response to water deprivation (Yao et al., 2005), transcription factor activation in several hypothalamic regions in response to fasting or re-feeding (Zséli et al., 2016), deposits of neuroanatomical tract tracer molecules into any of several hypothalamic regions

(e.g., Hahn and Swanson, 2010), and mapping of key neuropeptides within distinct subdivisions of the LHA (Swanson et al., 2005; Hahn, 2010).

In the hypothetical scenario furnished in **Figure 6C**, the location of the portion of the ARH sampled by LCM maps to Level 28 of Swanson (2004). Specifically, this region – at this same rostrocaudal level – could also have been the focus of investigations concerning anterograde tracing, central drug injection, and Fos transcription factor expression. Therefore, all of those published datasets could be considered in conjunction with the molecular analyses performed on the LCM-sampled ARH, and new hypotheses can be constructed that are constrained by the spatial patterns of data from these maps, when they are considered as a collective (**Figure 6C**). Together, therefore, the maps constitute a powerful way to help investigators see relationships among datasets, for the same region mapped in the same reference space, that they otherwise may not have seen or which they may have seen without any rigorous constraint placed upon such examination. The gene expression changes observed in molecular analyses of the sampled region, for example, may be occurring in neurons in that region for which anterograde tracing experiments have revealed prominent efferent connections. Thus, linking the molecular with neuroanatomical data would suggest new experiments that could test whether those genes play a role in shaping the function of those projection neurons. Setting aside hypothetical scenarios for a moment, we have recently reported the usefulness of this approach in a preliminary examination of published datasets for the LHA; specifically, those studies that have been performed that link LHA datasets mapped in Swanson reference space (Hernandez and Khan, 2016).

7.2: Data migration. A logical extension of contextualizing datasets mapped to the same reference space would be to migrate data from a different reference space to the reference space one has used to map the location of their LCM-sampled tissue. Thus, as in the example furnished earlier, if the ARH sample captured by LCM were mapped to Level 28 of Swanson, it would be interesting to determine whether data concerning this region, but which was mapped in a different atlas, could be "migrated" to this reference space and contextualized with the data obtained from the LCM sample at the same atlas level. This has been discussed in detail by one of us previously (Khan, 2013) and the details are not necessary to enumerate here again; suffice it to say that registration of data between atlas spaces – when performed under careful, lawful parameters – allows researchers to unlock the potential of data that may be residing, unattended, in a different reference space. This is important because many researchers use different atlases to map their datasets; this is true for the hypothalamus as much as any other brain region. For example, the locations of recording electrodes used to perform electrophysiological recordings of neurons in the PVH have been mapped to the atlas of Paxinos and Watson, along with inferred stereotaxic coordinates for the locations of the maps (Aramakis et al., 1996). The recordings are for responses these PVH neurons have to application of neuropeptide Y (NPY) or its receptor agonists, and understanding the locations of the neurons displaying these responses could be better contextualized in relation to other datasets mapped in Swanson reference space if the data were migrated to that space.

Fortunately, the alignment and registration between these atlas spaces appear to constitute a tractable problem (Wells and Khan, 2013; Khan, 2013; Hernandez and Khan, 2016; Perez et al., 2017), the mature, fully fledged solution for which may help to bring together datasets that would otherwise be separated in time and space. As a step towards such a solution, we have recently developed and implemented a computer vision algorithm that matches features detected in photomicrographs of the Nissl-stained sections of the Paxinos and Watson and Swanson reference

atlases to provide independent support of alignments we performed separately between the reference atlases based on craniometric measures in relation to the skull landmark, Bregma (Khan et al., 2018). The algorithm produces matches between atlas levels that are in close agreement with matches produced on the basis of craniometric alignments, providing support for the feasibility of data migration between the two reference spaces.

Other, older datasets could also be potentially migrated between atlas reference spaces, provided that the reference spaces can be aligned and registered in a fashion similar to that described above for the Paxinos and Watson / Swanson reference atlases. For example, Jacobowitz and colleagues combined micropunch methods with two-dimensional gel electrophoretic separation methods to generate protein profiles from discrete sub-regions of the hypothalamus and other brain regions (Heydorn et al., 1983), mapping their data using coordinates derived from the König and Klippel (1963) rat brain atlas. In principle, such data can be contextualized more broadly if they were migrated to other extant reference spaces.

7.3: Data refinement. Another benefit of mapping the location of LCM-captured brain tissue is the ability to improve our understanding of hypothalamic organization by refining the data generated from previously published studies. Prior to the advent of LCM (Emmert-Buck et al., 1996), the ability to sample brain tissue with high spatial resolution found perhaps its most precise expression in the micropunch methods mentioned above (reviewed by Palkovits, 1975; 1986; 1989). Notwithstanding notable examples using these and other methods (e.g., Heydorn et al., 1983), LCM offers investigators the ability for an even greater precision of sampling of brain tissue within a given region's 3-D expanse, thereby allowing more careful examination of sub-regions to detect possible differences in molecular expression patterns within a defined neural substrate.

This level of spatial resolution is important, as data has emerged that suggest heterogeneous neuronal constituents along the rostrocaudal extent of hypothalamic nuclei and areas. For example, within the ARH, data from the mouse model demonstrate a segregation of the effects of acutely administered leptin and insulin on populations of ARH POMC neurons (Williams et al., 2010). Specifically leptin-induced excitation was found in 35% of all POMC neurons throughout the rostrocaudal extent of the retrochiasmatic area (RCH) and ARH, but most of the POMC neuronal excitation was recorded from neurons in the lateral RCH and medial POMC group in the ARH. In contrast, insulin-induced hyperpolarization of POMC neurons was restricted to medial RCH and rostromedial ARH (Williams et al., 2010). More recently, Lam et al., (2017) used single-cell RNA sequencing to determine that the POMC neuronal population in the mouse ARH consists of heterogeneous populations that differ on the basis of their cell surface receptor expression. Clustering analysis resulted in the investigators identifying four different classes of POMC neuron. Similarly, an elegant study by Foster et al., (2016) has demonstrated the presence of distinct subsets of neurons in the VMH in the rat model that show a selective *absence* of Fos immunoreactivity in association with the hypoglycemia produced by systemic insulin injections. In particular, they found that the VMHdm (dorsomedial part of the VMH) and the smaller VMHc (central part) show marked reductions in Fos immunoreactive neurons from hypoglycemic animals as compared to their euglycemic controls, and that these reductions were proportional to the reductions in terminal plasma glucose concentrations. In contrast, sub-regions such as the VMHvl (ventrolateral part), which are believed to be involved mainly in social and reproductive behaviors, do not exhibit such reductions. Clearly, then, sampling from these smaller sub-regions of the ARH and VMH warrants careful documentation and mapping.

Our own preliminary data (Martinez et al., 2016) on ARH connectivity underscores this point as well. Specifically, initial experiments in which the retrogradely transportable tracers, Fluorogold or CTb, were injected into the rostral and caudal portions of the ARH have yielded results showing subtle differences in the distribution and density of retrogradely labeled neurons throughout the forebrain that project to these portions of the ARH. A summary of these unpublished data is furnished in **Figure 7**, simply to emphasize the point that it is no longer tenable to sample only one tissue section of a large expansive brain region such as the ARH, and make claims about its function as a whole without taking into consideration the possibility of heterogeneous properties for neurons along its full extent. A difference in afferent input implies different qualities for incoming signals to ARH neurons in the rostral end of the structure versus its caudal end; this in turn, implies that perhaps the neuronal populations receiving these differential signals may also be heterogeneous. Therefore, their molecular expression patterns, in terms of either phenotype or intrinsic state (or both) will likely also be non-uniform. Thus, the greater spatial resolution afforded by LCM sampling methods – together with careful digital atlas mapping of those locations of those samples – allows us as a community to continually refine our coarse datasets, rendering them sharper and more information-rich.

8: Concluding remarks and future directions

In this article, we have surveyed the historical antecedents of high throughput technologies to extract molecular information from the brain, focusing on studies of the hypothalamus. After surveying selected articles reporting high throughput transcriptomic, proteomic and peptidomic studies of the hypothalamus or its sub-regions, we discussed the importance of LCM and digital atlasing methods in facilitating the anchoring (mapping) of such information to a tractable spatial model of the brain. In doing so, we build upon earlier efforts to link molecular information with spatial locations in the brain in a large-scale manner, such as grid-based mapping based on voxelation methods (Chin et al., 2007; Petyuk et al., 2007) and analysis of gene expression patterns in the hypothalamus from the rich repository of *in situ* hybridization data within the Allen Brain Atlas (Olszewski et al., 2008).

8.1: Future directions in data management. We also apply the topics presented here to previous discussions we have raised concerning automated, informatics-based management of neuroscientific data; for example, using electronic laboratory notebooks to perform digital mapping and documentation of analyzed datasets (see Fig. 4 of Burns et al., 2003; Khan et al., 2006). As greater sophistication is brought to bear using methods that combine neuroanatomical tract tracing with molecular analysis of the traced projection neurons (e.g., see Pomeranz et al., 2017), both the mapping and management of data concerning such projection systems will become even more streamlined. An important aspect of developing informatics tools and methodologies is that much of the information used by expert biologists is technically specified, but informally defined. Naturally, expert neuroscientists are trained to understand the spatial structure of a published brain atlas, a flatmap, or a stained histological slide without requiring an explicitly defined logical representation. Informatics systems, however, must be grounded in a well-defined ontological model, which inevitably leads to some disagreement concerning the optimal design of such ontologies for neuroanatomical data. There are number of approaches put forward within the neuroinformatics community to represent mapped neuroanatomical data in ontologies. These include representations with a neuroimaging focus (Nichols et al., 2010); philosophically grounded approaches to neuroanatomy (Osumi-Sutherland et al., 2012); or comprehensive, cross-species

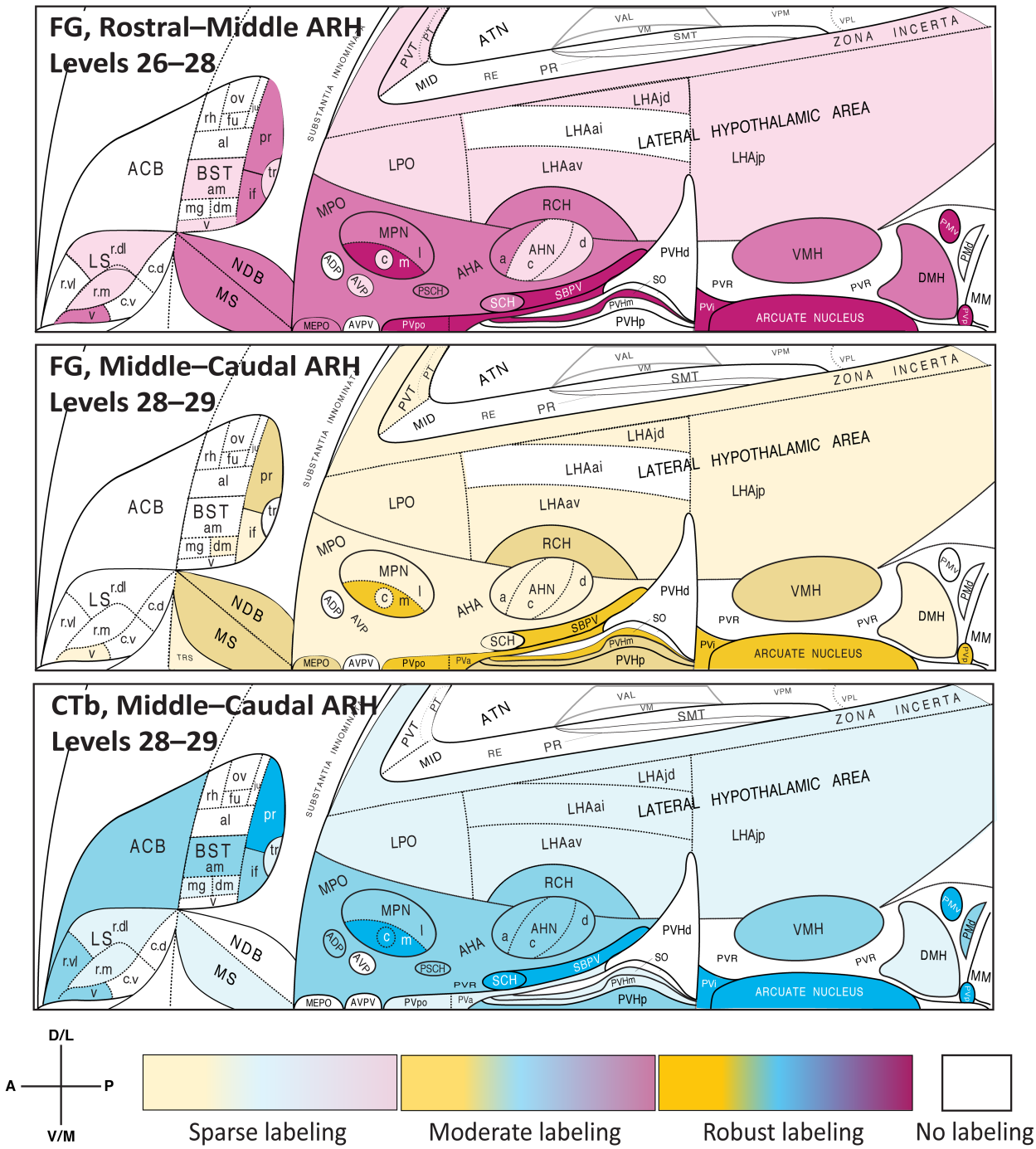

Fig. 7. Choropleth flatmaps of unpublished data (Martinez et al., 2016) are furnished here to illustrate differences in the distributions and densities of retrogradely labeled neurons traced from rostral versus caudal locations within the rat ARH using two different retrograde tracers across three test subjects (adult male Sprague-Dawley rats). The upper two panels show distributions and densities for neurons traced retrogradely from ARH injection sites containing deposits of the retrograde tracer, Fluorogold (FG). The bottom (*third from top*) panel is from a test subject receiving the retrogradely transportable tracer, cholera toxin subunit B (CtB). Note the locations

within the ARH of the deposits, which were mapped to specific atlas levels of Swanson (2004) that contain the ARH. The deposit in the case shown in the upper panel was localized to the anterior half (rostral–middle) of the ARH, whereas the lower two panels were from subjects receiving deposits mapped to the posterior third (middle–caudal) of the ARH. Note that at atlas level 28 there was overlap of injection deposits for all three cases. Light to heavy shading for each panel corresponds to sparse to robust numbers of retrogradely labeled cells for each sub-region, with no shading indicating an absence of cells in that region. While many regions show similar densities and distributions of afferent input as would be expected from an overlapping series of injection deposits, there are also clear significant differences in such input to the rostral versus caudal portions of the ARH; most notably, the dorsomedial subdivision of the bed nuclei of the stria terminalis (BSTdm), the central part of the medial preoptic nucleus (MPOc), the periventricular part of the paraventricular hypothalamic nucleus (PVHp), and the dorsal premammillary nucleus (PMd). These differences in afferent distribution and density suggest that ARH recipient neurons are heterogeneous in at least certain functions (and therefore may differ in cellular state or phenotype), underscoring the need for accurate ARH sampling along the rostrocaudal axis of the nucleus for transcriptomic, proteomic or peptidomic studies. The flatmaps from Swanson (2004) (and available at https://larrywswanson.com) are reproduced and modified here under the conditions of a Creative Commons BY-NC 4.0 license (https://creativecommons.org/licenses/by-nc/4.0/legalcode).

---

methods for neuroanatomical phenotype (Haendel et al., 2014; Mungall et al., 2017; also see Deans et al., 2015). It is important to note that selecting an appropriate formalization can have a deep impact on how a neuroinformatics system functions, and we feel that any formalization used to represent the data described in this chapter should reflect the expertise and practices of experimental scientists working in this field. Thus, we recommend lightweight, data-centric formalizations that mirror scientists' use of standard atlases, such as the Allen Brain Atlas portal (Sunkin et al., 2013). Neuroscientific knowledge carries a structured context that is inherited from the experimental design that ultimately generates the data. One methodology for representing this context in a general way is based on the relationships between independent and dependent variables within studies. This may serve as a convenient framework for describing neuroanatomically grounded data by treating the location of the phenomena of interest in the brain simply as one of several independent variables that describe the context of a particular datum (Russ et al., 2011; Tallis et al., 2011).

8.2: Future directions in imaging. Though it has not yet achieved the mesoscale resolution required to permit detailed mapping of most molecules, mass spectrometry imaging (MSI) – including imaging based on matrix assisted laser desorption technology (Karas et al., 1987), known as MALDI (Spengler et al., 1994; Caprioli et al., 1997) – will hopefully provide investigators the ability to rapidly sample the molecular landscape of the brain while simultaneously facilitating the preservation of the provenance of this molecular information at a resolution comparable to our proposed methods to map such information (for reviews on MALDI, see Cornett et al., 2007; Römpp et al., 2010; and Shariatgorji et al., 2014b). MALDI has now been performed for single neurons (Schwartz et al., 2003) and tissue sections (e.g., Heijs et al., 2015), including sections containing hypothalamus (Altelaar et al., 2006; Groseclose et al., 2007; Yao et al., 2008; Shariatgorji et al., 2014a) and pituitary (Altelaar et al., 2007). It is now being applied for metabolomics studies of the brain as well (Esteve et al., 2016). Modifications of the original

method, including MALDI Fourier Transform Ion Cyclotron Resonance (MALDI FTICR; Spraggins et al., 2016), offer greater mass resolution and accuracy. A promising future direction for MALDI with respect to mapping of molecular information to canonical atlases is the recently reported strategy of combining MALDI with LCM and LC-MS/MS on the same brain section (Dilillo et al., 2017), which would facilitate the retention of provenance information for the molecular datasets mined from the section. Similarly, image fusion strategies that create one image of a tissue section from two registerable source images produced by two separate imaging modalities (MALDI, optical microcopy) also hold great promise for mapping molecular information (van de Plas et al., 2015). Other modalities, such as Raman spectroscopic imaging (Manciu et al., 2013), may offer additional opportunities for high spatial resolution analysis of molecular datasets in the brain.

8.3: Future directions in molecular analysis. Alongside developments in imaging technologies are enhanced technologies that allow for spatially resolved molecular sampling of tissue (see Crosetto et al., (2015) for a review). For example, fluorescent *in situ* sequencing (FISSEQ) of RNA has been developed for intact tissue samples (Lee et al., 2014; 2015). Similarly, Ståhl et al., (2016) have reported the novel use of arrayed reverse transcription primers accompanied by unique positional barcodes, which can be used to generate RNA-sequencing data directly on tissue slides in a manner that preserves the location of the information (also see Navarro et al., 2017). Additionally, single-cell transcriptomic analysis can be performed on individual nuclei obtained from fixed tissue; these nuclei are sorted after tissue dissociation procedures via fluorescence-activated cell sorting (FACS) or nucleic acid barcoding. For example, Lake et al., (2016) characterized the single nuclear transcriptomes of cerebral cortical neurons from fixed *post mortem* human brain. Habib et al., (2017) used barcoded beads to sort individual nuclei taken from fresh or frozen brain samples from mouse and human, and developed a microfluidic device that enables the sorting process.

A key future direction would be to integrate spatially resolved transcriptomics procedures and single-cell sequencing efforts into a pipeline that allows for the retention and mapping of the locations from where the samples originate with respect to canonical brain atlases. Along these lines, the Retro-TRAP technology developed by Jeffrey Friedman and colleagues (Ekstrand et al., 2014; Nectow et al., 2015; Pomeranz et al., 2017; derived from the original TRAP technology to identify activated neurons: Knight et al., 2012) to retrogradely label neurons with GFP constructs and then capture translating mRNAs from these neurons using anti-GFP nanobodies (i.e., single-domain antibodies), could potentially allow for projections being mapped for neurons from which single-cell molecular information can also be harvested in a spatially documentable manner. A current limitation of the method for such purposes is that fresh not frozen tissue needs to be harvested to generate sufficient RNA yields, precluding the freezing of tissue sections in preparation for LCM.

8.4: Future directions in mapping. A larger issue concerning the mapping of molecular information is the need to change the scientific culture so that best practices of reporting molecular information in the brain include procedures to map the information to standardized atlases. At present, this is not a common practice by most investigators in neuroscience. Such changes in culture would greatly accelerate the integration of datasets among researchers, and the need to do so is now more critical than ever, given the deluge of spatial, molecular data that has already been shared in repositories such as the Allen Brain Atlas (http://www.brain-map.org) and the GENSAT Project (http://www.gensat.org).

8.5: Final remarks. For all of these and future advancements, it will remain critical to preserve information about the native lands from which so many molecules become expatriated, lest the information provided by these molecular datasets fails to link up with the larger neuronal information networks from which they came. Mapping the sampled tissue will provide the critical information that will bridge the gap between the systems biology of molecular information networks on the one hand, and the systems neuroscience of cellular information networks on the other. Without such a bridge, these domains of inquiry may never converge to form a unifying model of a dynamic brain, replete with diverse molecular citizens hailing from different but interconnecting cells, and communicating across local and regional boundaries to signal their neighbors, both near and far.

Funding

Work in the UTEP Systems Neuroscience Laboratory is supported by grants awarded to AMK from the National Institutes of Health (NIH; SC3GM109817), the Howard Hughes Medical Institute (UTEP PERSIST; PI: S. Aley), and the UTEP Office of Research and Sponsored Projects (Grand Challenges Award). This work is also supported by funds awarded to the Border Biomedical Research Center by the National Institute of Minority Health and Health Disparities of the NIH (5G12MD007592). AHG is supported by the Research Initiative for Scientific Enhancement (RISE) Graduate Fellowship program of the NIH (R25GM069621). AM has been supported by UTEP PERSIST funds and an NSF GK–12 fellowship. Some data in this study were also based upon work supported by the Office of Research and Development, Medical Research Service, Department of Veterans Affairs (VA); specifically, by Merit Review Awards 1l01BX001213-01A1 and BX004102-01 from the United States (U.S.) Department of Veterans Affairs Biomedical Laboratory Research and Development Service to JEB as well as NIH R01DK115976 to JEB. The contents do not represent the views of the U.S. Department of Veterans Affairs or the United States Government. This study was also supported by the University of Washington Diabetes Research Center Cellular and Molecular Imaging Core, which is supported by NIH grant P30DK017047. The contribution by GB to this work was funded by the Defense Advanced Research Projects Agency (DARPA) Big Mechanism program under Army Research Office (ARO) contract W911NF-1-0436 and by NIH grant R01LM012592.

Acknowledgments

We thank Dr. Sabiha Khan (UTEP) for thoughtful discussion on the organization of the manuscript. We also express our gratitude to Dr. Claude F. Baxter, Emeritus Professor of Psychiatry and Biobehavioral Sciences at the UCLA Brain Research Institute and past historian of the American Society for Neurochemistry, for providing AMK generous access to his personal library of seminal works in neurochemistry. We would also like to acknowledge the contributions of Dr. Rebecca Hull and Nishi Gill for the images provided in Figures 2B and 2C. Finally, we thank Dr. Alexander C. Jackson (University of Connecticut) for providing us with access to unpublished data from his single-cell transcriptomic studies of neuron populations in the mouse lateral hypothalamic area. This article is dedicated to the memory of Dr. John H. Ashe (University of California at Riverside), whose instruction and mentorship have deeply informed this narrative.

Abbreviations used

ACB	nucleus accumbens
AchE	acetylcholinesterase
ADP	anterodorsal preoptic nucleus
AgRP	Agouti-Related peptide
AHN	anterior hypothalamic nucleus
AHNa	anterior hypothalamic nucleus, anterior part
AHNc	anterior hypothalamic nucleus, central part
AHNd	anterior hypothalamic nucleus, dorsal part
AHNp	anterior hypothalamic nucleus, posterior part
AP	area postrema
ARH	arcuate hypothalamic nucleus
ATN	anterior nuclei, dorsal thalamus
AVP	anteroventral preoptic nucleus
AVPV	anteroventral periventricular nucleus hypothalamus
BST	bed nuclei of the stria terminalis
BSTal	bed nuclei of the stria terminalis, anterior division, anterolateral area
BSTam	bed nuclei of the stria terminalis, anterior division, anteromedial area
BSTdm	bed nuclei of the stria terminalis, anterior division, dorsomedial nucleus
BSTfu	bed nuclei of the stria terminalis, anterior division, fusiform nucleus
BSTif	bed nuclei of the stria terminalis, posterior division, interfascicular nucleus
BSTju	bed nuclei of the stria terminalis, anterior division, juxtacapsular nucleus
BSTmg	bed nuclei of the stria terminalis, anterior division, magnocellular nucleus
BSTov	bed nuclei of the stria terminalis, anterior division, oval nucleus
BSTpr	bed nuclei of the stria terminalis, posterior division, principal nucleus
BSTrh	bed nuclei of the stria terminalis, anterior division, rhomboid nucleus
BSTtr	bed nuclei of the stria terminalis, posterior division, transverse nucleus
BSTv	bed nuclei of the stria terminalis, anterior division, ventral nucleus
C.a.	anterior commissure
CCK1R	cholecystokinin 1 receptor
C.f.d.	fornix
Ch. Opt.	optic chiasm
CRH	corticotropin releasing hormone
CTB	cholera toxin subunit b
DMH	dorsomedial hypothalamic nucleus
EGFP	enhanced green fluorescent protein
FG	Fluorogold
fx	fornix
GFP	green fluorescent protein
HNS	hypothalamo-neurophypohysial system
I	internuclear area, hypothalamic periventricular region
KO	knockout
LCM	laser capture microdissection
LHA	lateral hypothalamic area
LHAai	lateral hypothalamic area, anterior region, intermediate zone
LHAav	lateral hypothalamic area, anterior region, ventral zone

LHAd	lateral hypothalamic area
LHAjd	lateral hypothalamic area, juxtadorsomedial region
LHAjp	lateral hypothalamic area, juxtaparaventricular region
LHAjvd	lateral hypothalamic area, juxtaventromedial region, dorsal zone
LHAjvv	lateral hypothalamic area, juxtaventromedial region, ventral zone
LHApc	lateral hypothalamic area, parvicellular region
LHAsfa	lateral hypothalamic area, subfornical region, anterior zone
LPO	lateral preoptic area
LS	lateral septal nucleus [Cajal]
LSc.d	lateral septal nucleus, caudal part, dorsal zone
LSc.v	lateral septal nucleus, caudal part, ventral zone
LSr.dl	lateral septal nucleus, rostral part, dorsolateral zone
LSr.m	lateral septal nucleus, caudal part, medial zone
LSr.vl	lateral septal nucleus, rostral part, ventrolateral zone
LSv	lateral septal nucleus, ventral part [Risold-Swanson]
MC4-R	melanocortin 4 receptor
ME	median eminence
MEex	median eminence, external lamina
MEin	median eminence, internal lamina
MEPO	median preoptic nucleus
MID	midline nuclei, dorsal thalamus
MM	medial mammillary nucleus, body
MNs	magnocellular neurons
MPN	medial preoptic nucleus
MPNc	medial preoptic nucleus, central part
MPNl	medial preoptic nucleus, lateral part
MPNm	medial preoptic nucleus, medial part
MPO	medial preoptic area
MS	medial septal nucleus [Cajal]
μ-array	microarray
NDB	diagonal band nucleus [Broca]
NPY	neuropeptide Y
NTS	nucleus of the solitary tract
opt	optic tract
OT	oxytocin
PCR	polymerase chain reaction
PFA	paraformaldehyde
PMd	dorsal premammillary nucleus
PMv	ventral premammillary nucleus
POMC	pro-opiomelanocortin
PR	perireuniens nucleus
PSCH	suprachiasmatic preoptic nucleus
PT	paratenial nucleus
PVH	paraventricular hypothalamic nucleus
PVHd	paraventricular hypothalamic nucleus, descending division
PVHf	paraventricular hypothalamic nucleus, descending division, forniceal part

PVHm	paraventricular hypothalamic nucleus, magnocellular division
PVHmpd	paraventricular hypothalamic nucleus, medial parvicellular part, dorsal zone
PVHp	paraventricular hypothalamic nucleus, parvicellular division
PVHpv	paraventricular hypothalamic nucleus, periventricular part
PVi	periventricular hypothalamic nucleus, intermediate part
PVp	periventricular hypothalamic nucleus, posterior part
PVpo	preoptic periventricular nucleus
PVT	paraventricular thalamic nucleus
PVR	hypothalamic periventricular region
qPCR	quantitative polymerase chain reaction
RCH	retrochiasmatic area, lateral hypothalamic area
RE	nucleus reuniens [Malone]
REcd	nucleus reuniens, caudal division, dorsal part
REcm	nucleus reuniens, caudal division, medial part [Gurdjian]
REcp	nucleus reuniens, caudal division, posterior part
RIN	RNA integrity number
SBPV	subparaventricular zone hypothalamus
SCH	suprachiasmatic nucleus [Spiegel-Zwieg]
SFO	subfornical organ
SMT	submedial nucleus thalamus
SO	supraoptic hypothalamic nucleus
SOr	supraoptic nucleus, retrochiasmatic part
S.t.	infundibular stalk
sup	supraoptic commissures
TH	tyrosine hydroxylase
T.M.	tractus Meynert (fasciculus retroflexus)
TUi	tuberal nucleus, intermediate part
TUsv	tuberal nucleus, subventricular part
V3h	third ventricle, hypothalamic part
V.d'A.	tract of Vicq D'Azyr (mammillothalamic tract)
vlt	ventrolateral hypothalamic tract
VMH	ventromedial hypothalamic nucleus
VMHa	ventromedial hypothalamic nucleus, anterior part
VMHc	ventromedial hypothalamic nucleus, central part
VMHdm	ventromedial hypothalamic nucleus, dorsomedial part
VMHvl	ventromedial hypothalamic nucleus, ventrolateral part
VP	vasopressin
VPL	ventral posterolateral nucleus thalamus, principal part
VPM	ventral posteromedial nucleus thalamus, principal part

References

Abrahams VC, Koelle GB, Smart P (1957) Histochemical demonstration of cholinesterases in the hypothalamus of the dog. J Physiol (London) 139:137–144.

Adler ES, Hollis JH, Clarke IJ, Grattan DR, Oldfield BJ (2012) Neurochemical characterization and sexual dimorphism of projections from the brain to abdominal and subcutaneous white adipose tissue in the rat. J Neurosci 32(45):15913–15921. DOI 10.1523/JNEUROSCI.2591-12.2012.

Adrian ED (1939) Ferrier Lecture: The localization of activity in the brain. Proc R Soc London B: Biol Sci 126:433–449. DOI 10.1098/rspb.1939.0001.

Akhtar RA, Reddy AB, Maywood ES, Clayton JD, King VM, *et al*. (2002) Circadian cycling of the mouse liver transcriptome, as revealed by cDNA microarray, is driven by the suprachiasmatic nucleus. Curr Biol 12:540–550. DOI 10.1016/S0960-9822(02)00759-5.

Ahmed SH, Lutjens R, van der Stap LD, Lekic D, Romano-Spica V, Morales M, *et al*. (2005) Gene expression evidence for remodeling of lateral hypothalamic circuitry in cocaine addiction. Proc Natl Acad Sci USA 102(32):11533–11538. DOI 10.1073/pnas.0504438102.

Alexandre-Gouabau M-C F, Bailly E, Moyon TL, Grit IC, Coupé B, *et al*. (2012) Postnatal growth velocity modulates alterations of proteins involved in metabolism and neuronal plasticity in neonatal hypothalamus in rats born with intrauterine growth restriction. J Nutr Biochem 23:140–152. DOI 10.1016/j.jnutbio.2010.11.008.

Altelaar AFM, Klinkert I, Jalink K, de Lange RPJ, Adan RAH, Heeren RMA, Piersma SR (2006) Gold-enhanced biomolecular surface imaging of cells and tissue by SIMS and MALDI mass spectrometry. Anal Chem 78:734–742. DOI 10.1021/ac0513111.

Altelaar AFM, Taban IM, McDonnell LA, Verhaert PDEM, de Lange RPJ, Adan RAH, *et al*. (2007) High-resolution MALDI imaging mass spectrometry allows localization of peptide distributions at cellular length scales in pituitary tissue sections. Int J Mass Spectr 260:203–211. DOI 10.1016/j.ijms.2006.09.028.

Alzate O (ed) (2010) Neuroproteomics. CRC Press/Taylor & Francis, Boca Raton. Available online at: https://www.ncbi.nlm.nih.gov/books/NBK56022/.

Amar L, Benoit C, Beaumont G, Vacher CM, Crepin D, Taouis M, *et al*. (2012) MicroRNA expression profiling of hypothalamic arcuate and paraventricular nuclei from single rats using Illumina sequencing technology. J Neurosci Meth 209(1):134–143. DOI 10.1016/j.jneumeth.2012.05.033.

Amigó-Correig M, Barceló-Batllori S, Soria G, Krezymon A, Benani A, Pénicaud L, *et al*. (2012) Anti-obesity sodium tungstate treatment triggers axonal and glial plasticity in hypothalamic feeding centers. PLoS One 7(7):e39087. DOI 10.1371/journal.pone.0039087.

Anglade P, Larabi-Godinot Y (2010) Historical landmarks in the histochemistry of the cholinergic synapse: Perspectives for future researches. Biomed Res 31:1–12. DOI 10.2220/biomedres.31.1.

Arai Y, Gradwohl G, Kameda Y (2010) Expression of neuropeptide Y and agouti-related peptide in the hypothalamic arcuate nucleus of newborn *neurogenin3* null mutant mice. Cell Tissue Res 340:137–145. DOI 10.1007/s00441-009-0925-4.

Aramakis VB, Stanley BG, Ashe JH (1996) Neuropeptide Y receptor agonists: multiple effects on spontaneous activity in the paraventricular hypothalamus. Peptides 17:1349–1357. DOI 10.1016/S0196-9781(96)00222-7.

Argüelles S, Cano M, Machado A, Ayala A (2011) Effect of aging and oxidative stress on elongation factor-2 in hypothalamus and hypophysis. Mech Ageing Dev 132:55–64. DOI 10.1016/j.mad.2010.12.002.

Atkins N, Miller CM, Owens JR, Turek FW (2011) Non-laser capture microscopy approach for the microdissection of discrete mouse brain regions for total RNA isolation and downstream next-generation sequencing and gene expression profiling. J Vis Exp 57:e3125. DOI 10.3791/3125.

Azzam S, Schlatzer D, Nethery D, Saleh D, Li X, Akladious A, *et al*. (2017) Proteomic profiling of the hypothalamus in two mouse models of narcolepsy. Proteomics 17 (13–14) 1600478. DOI 10.1002/pmic.201600478.

Backholer K, Smith JT, Rao A, Pereira A, Iqbal J, Ogawa S, *et al*. (2010) Kisspeptin cells in the ewe brain respond to leptin and communicate with neuropeptide Y and proopiomelanocortin cells. Endocrinol 151: 2233–2243. DOI 10.1210/en.2009-1190.

Bakay L (1952) Studies on blood-brain barrier with radioactive phosphorus: II. Hypophysis and hypothalamus in man. AMA Arch Neurol Psychiatr 68(5):629–640.

Balakrishnan CN, Mukai M, Gonser RA, Wingfield JC, London SE, Tuttle EM, Clayton DF (2014) Brain transcriptome sequencing and assembly of three songbird model systems for the study of social behavior. PeerJ 2:e396. DOI 10.7717/peerj.396.

Balázs R, Patel AJ, Richter D (1972) Metabolic compartments in the brain: Their properties and relation to morphological structures. In: *Metabolic compartmentation in the brain* (R Balázs, JE Cremer, eds.), pp. 167–184. New York: John Wiley & Sons.

Balivada S, Ganta CK, Zhang Y, Pawar HN, Ortiz RJ, Khan AM, Kenney MJ (2017) Microarray analysis of aging-associated immune system alterations in the rostral ventrolateral medulla of F344 rats. Physiol Genomics, [Epub ahead of print: 16 Jun 2017]. DOI 10.1152/physiolgenomics.00131.2016.

Baskin DG, Bastian LS (2010) Immuno-laser capture microdissection of rat brain neurons for real time quantitative PCR. Methods Mol Biol 588:219–230. DOI 10.1007/978-1-59745-324-0_23.

Baskin DG, Kim F, Gelling RW, Russell BJ, Schwartz MW, Morton GJ, *et al*. (2010) A new oxytocin-saporin cytotoxin for lesioning oxytocin-receptive neurons in the rat hindbrain. Endocrinol 151(9):4207–4213. DOI 10.1210/en.2010-0295.

Bayliss WM, Starling EH (1902) The mechanism of pancreatic secretion. J Physiol (London) 28(5):325–353. DOI 10.1113/jphysiol.1902.sp000920.

Benner S, Kakeyama M, Endo T, Yoshioka W, Tohyama C (2015) Application of NeuroTrace staining in the fresh frozen brain samples to laser microdissection combined with quantitative RT-PCR analysis. BMC Res Notes 8:252. DOI 10.1186/s13104-015-1222-9.

Bennett MR (2001) History of the synapse. Harwood Academic Press, Amsterdam.

Bernard R, Kerman IA, Meng F, Evans SJ, Amrein I, Jones EG, *et al*. (2009) Gene expression profiling of neurochemically defined regions of the human brain by *in situ* hybridization-guided laser capture microdissection. J Neurosci Meth 178(1):46–54. DOI 10.1016/j.jneumeth.2008.11.012.

Bi S, Robinson BM, Moran TH (2003) Acute food deprivation and chronic food restriction differentially affect hypothalamic NPY mRNA expression. Am J Physiol Regul Integr Comp Physiol 285:R1030–R1036. DOI 10.1152/ajpregu.00734.2002.

Blevins JE, Hamel FG, Fairbairn E, Stanley BG, Reidelberger RD (2000a) Effects of paraventricular nucleus injection of CCK-8 on plasma CCK-8 levels in rats. Brain Res 860:11–20. DOI 10.1016/S0006-8993(99)02478-6.

Blevins JE, Moralejo DH, Wolden-Hanson TH, Thatcher BS, Ho JM, Kaiyala KJ, *et al*. (2012) Alterations in activity and expenditure contribute to lean phenotype in Fischer 344 rats lacking the cholecystokinin-1 receptor gene. Am J Physiol Regul Integr Comp Physiol 303:R1231–R1240. DOI 10.1152/ajpregu.00393.2012.

Blevins JE, Morton GJ, Williams DL, Caldwell DW, Bastian LS, Wisse BE, *et al*. (2009) Forebrain melanocortin signaling enhances the hindbrain satiety response to CCK-8. Am J Physiol Regul Integr Comp Physiol 296:R476–R484. DOI 10.1152/ajpregu.90544.2008.

Blevins JE, Stanley BG, & Reidelberger RD (2000b) Brain regions where cholecystokinin suppresses feeding in rats. Brain Res 860:1–10. DOI 10.1016/S0006-8993(99)02477-4.

Bonaventure P, Guo H, Tian B, Liu X, Bittner A, Roland B, *et al*. (2002) Nuclei and subnuclei gene expression profiling in mammalian brain. Brain Res 943:38–47. DOI 10.1016/S0006-8993(02)02504-0.

Bonnavion P, Mickelsen LE, Fujita A, de Lecea L, Jackson AC (2016) Hubs and spokes of the lateral hypothalamus: cell types, circuits and behaviour. J Physiol 594(22):6443–6462. DOI 10.1113/JP271946.

Boone DR, Sell SL, Micci M-A, Crookshanks JM, Parsley M, Uchida T, *et al*. (2012) Traumatic brain injury-induced dysregulation of the circadian clock. PLoS One 7(10):e46204. DOI:10.1371/journal.pone.0046204.

Boone DR, Sell SL, Hellmich HL (2013) Laser capture microdissection of enriched populations of neurons or single neurons for gene expression analysis after traumatic brain injury. J Vis Exp 74:e50308. DOI:10.3791/50308.

Bora A, Annangudi SP, Millet LJ, Rubakhin SS, Forbes AJ, Kelleher NL, *et al.* (2008) Neuropeptidomics of the supraoptic rat nucleus. J Proteome Res 7(11):4992–5003. DOI 10.1021/pr800394e.

Borell U, Örström Å (1945) Metabolism in different parts of the brain, especially in the epiphysis, measured with radioactive phosphorus. Acta Physiol Scand 10(3–4):231–242.

Boring EG (1942) Sensation and Perception in the History of Experimental Psychology. Appleton Century Crofts, New York.

Brahic M, Haase AT (1978) Detection of viral sequences of low reiteration frequency by *in situ* hybridization. Proc Natl Acad Sci USA 75(12):6125–6129.

Bures EJ, Courchesne PL, Douglass J, Chen K, Davis MT, Jones MD, et al. (2001) Identification of incompletely processed potential Carboxypeptidase E substrates from CpE^{fat}/CpE^{fat} mice. Proteomics 1:79–92. DOI 10.1002/1615-9861(200101)1:1<79::AID-PROT79>3.0.CO;2-8.

Burns GAPC, Khan AM, Ghandeharizadeh S, O'Neill MA, Chen Y-S (2003) Tools and approaches for the construction of knowledge models from the neuroscientific literature. Neuroinformatics 1(1):81–109.

Butler AE, Matveyenko AV, Kirakossian D, Park J, Gurlo T, Butler PC (2016) Recovery of high-quality RNA from laser capture microdissected human and rodent pancreas. J Histotechnol 39:59–65. DOI 0.1080/01478885.2015.1106073.

Byerly MS, Simon J, Cogburn LA, Le Bihan-Duval E, Duclos MJ, Aggrey SE, *et al.* (2010) Transcriptional profiling of hypothalamus during development of adiposity in genetically selected fat and lean chickens. Physiol Genomics 42:157–167. DOI 10.1152/physiolgenomics.00029.2010.

Cai X, Wang C, Xu J, Xue X, Zhang X, et al. (2011) Application of matrix solid-phase dispersion methodology to the extraction of endogenous peptides from porcine hypothalamus samples for MS and LC-MS analysis. J Chromatogr B 879:657–661. DOI 10.1016/j.jchromb.2011.01.038.

Campbell JN, Macosko EZ, Fenselau H, Pers TH, Lyubetskaya A, Tenen D, *et al*. (2017) A molecular census of arcuate hypothalamus and median eminence cell types. Nat Neurosci 20(3):484–496. DOI 10.1038/nn.4495.

Caprioli RM, Farmer TB, Gile J (1997) Molecular imaging of biological samples: Localization of peptides and proteins using MALDI-TOF MS. Anal Chem 69:4751–4760. DOI 10.1021/ac970888i.

Carreño FR, Walch JD, Dutta M, Nedungadi TP, Cunningham JT (2011) Brain-derived neurotrophic factor-tyrosine kinase B pathway mediates NMDA receptor NR2B phosphorylation in the supraoptic nuclei following progressive dehydration. J Neuroendocrinol 23:894–905. DOI 10.1111/j.1365-2826.2011.02209.x.

Chadwick W, Martin B, Chapter MC, Park S-S, Wang L, Daimon CM, *et al*. (2012) GIT2 acts as a potential keystone protein in functional hypothalamic networks associated with age-related phenotypic changes in rats. PLoS ONE 7(5):e36975. DOI 10.1371/journal.pone.0036975.

Chao C-M, Cheng B-C, Chen C-Y, Lin M-T, Chang C-P, Yang S-T (2015) Proteomic analysis of hypothalamic injury in heatstroke rats. Proteomics 15:1921–1934. DOI 10.1002/pmic.201400492.

Che F-Y, Yuan Q, Kalinina E, Fricker LD (2005) Peptidomics of $Cpe^{fat/fat}$ mouse hypothalamus. J Biol Chem 280:4451–4461. DOI 10.1074/jbc.M411178200.

Che F-Y, Zhang X, Berezniuk I, Callaway M, Lim J, Fricker LD (2007) Optimization of neuropeptide extraction from the mouse hypothalamus. J Proteome Res 6:4667–4676. DOI 10.1021/pr060690r.

Chen C-F, Shiue Y-L, Yen C-J, Tang P-C, Chang H-C, Lee Y-P (2007) Laying traits and underlying transcripts, expressed in the hypothalamus and pituitary gland, that were associated with egg production variability in chickens. Theriogenol 68:1305–1315. DOI 10.1016/j.theriogenology.2007.08.32.

Chen J, Repunte-Canonigo V, Kawamura T, Lefebvre C, Shin W, Howell LL, *et al*. (2013) Hypothalamic proteoglycan syndecan-3 is a novel cocaine addiction resilience factor. Nat Commun 4:1955. DOI 10.1038/ncomms2955.

Chen L-R, Chao C-H, Chen C-F, Lee Y-P, Chen Y-L, Shiue Y-L (2007) Expression of 25 high egg production related transcripts that identified from hypothalamus and pituitary gland in red-feather Taiwan country chickens. Animal Reprod Sci 100:172–185. DOI 10.1016/j.anireprosci.2006.07.005.

Chen R, Wu X, Jiang L, Zhang Y (2017) Single-cell RNA-Seq reveals hypothalamic cell diversity. Cell Rep 18:3227–3241. DOI 10.1016/j.celrep.2017.03.004.

Chiang C-K, Mehta N, Patel A, Zhang P, Ning Z, Mayne J, *et al*., (2014) The proteomic landscape of the suprachiasmatic nucleus clock reveals large-scale coordination of key biological processes. PLoS Genet 10(10):e1004695. DOI 10.1371/journal.pgen.1004695.

Chin MH, Geng AB, Khan AH, Qian W-J, Petyuk VA, Boline J, *et al*. (2007) A genome-scale map of expression for a mouse brain section obtained using voxelation. Physiol Genomics 30:313–321. DOI 10.1152/physiolgenomics.00287.2006.

Chu L-Y (1954) A cytological study of anterior horn cells isolated from human spinal cord. J Comp Neurol 100(2):381–413.

Chung C-Y, Seo H, Sonntag KC, Brooks A, Lin L, Isacson O (2005) Cell type-specific gene expression of midbrain dopaminergic neurons reveals molecules involved in their vulnerability and protection. Hum Mol Genet 14:1709–1725. DOI: 10.1093/hmg/ddi178.

Colgrave ML, Xi L, Lehnert SA, Flatscher-Bader T, Wadensten H, *et al.* (2011) Neuropeptide profiling of the bovine hypothalamus: Thermal stabilization is an effective tool in inhibiting post-mortem degradation. Proteomics 11:1264–1276. DOI 10.1002/pmic.201000423.

Conti B, Maier R, Barr AM, Morale MC, Lu X, Sanna PP, *et al*. (2007) Region-specific transcriptional changes following the three antidepressant treatments electro convulsive therapy, sleep deprivation and fluoxetine. Mol Psychiatr 12:167–189. DOI 10.1038/sj.mp.4001897.

Cornett DS, Reyzer ML, Chaurand P, Caprioli RM (2007) MALDI imaging mass spectrometry: Molecular snapshots of biochemical systems. Nat Meth 4:828–833. DOI 10.1038/NMETH1094.

Crosetto N, Bienko M, van Oudenaarden A (2015) Spatially resolved transcriptomics and beyond. Nat Rev Genet 16:57–66. DOI 10.1038/nrg3832.

Dalal J, Roh JH, Maloney SE, Akuffo A, Shah S, Yuan H, *et al*. (2013) Translational profiling of hypocretin neurons identifies candidate molecules for sleep regulation. Genes Dev 27:565–578. DOI 10.1101/gad207654.112.

Datta S, Malhotra L, Dickerson R, Chaffee S, Sen CK, Roy S (2015) Laser capture microdissection: Big data from small samples. Histol Histopathol 30:1255–1269. DOI 10.14670/HH-11-622.

Deans AR, Lewis SE, Huala E, Anzaldo SS, Ashburner M, Balhoff JP, *et al.* (2015) Finding our way through phenotypes. PLoS Biol 13, e1002033. DOI 10.1371/journal.pbio.1002033.

Deiters O (1865) Untersuchungen über Gehirn und Rückenmark des Menschen und der Säugethiere. Von Friedrich & Son, Brunswick.

Del Pino Sans J, Krishnan S, Aggison LK, Adams HL, Shrikant MM, Lopez-Giraldez F, Petersen SL (2015) Microarray analysis of neonatal rat anteroventral periventricular transcriptomes identifies the proapoptotic *Cugbp2* gene as sex-specific and regulated by estradiol. Neurosci 303:312–322. DOI 10.1016/j.neuroscience.2015.07.008.

De Palma A, Pareti G (2011) Bernstein's long path to membrane theory: Radical change and conservation in nineteenth-century German electrophysiology. J Hist Neurosci 20(4):306–337. DOI 10.1080/0964704X.2010.532024.

Dilillo M, Pellegrini D, Ait-Belkacem R, de Graaf EL, Caleo M, McDonnell LA (2017) Mass spectrometry imaging, laser capture microdissection, and LC-MS/MS of the same tissue section. J Prot Res 16(8):2993–3001. DOI 10.1021/acs.jproteome.7b00284.

Ding F, Li HH, Li J, Myers RM, Francke U (2010) Neonatal maternal deprivation response and developmental changes in gene expression revealed by hypothalamic gene expression profiling in mice. PLoS One 5(2):e9402. DOI 10.1371/journal.pone.0009402.

Dong HW (2008) The Allen Reference Atlas: A Digital Color Brain Atlas of the C57BL/6J Male Mouse. New York, Wiley.

Dong H-W, Swanson LW, Chen L, Fanselow MS, Toga AW (2009) Genomic-anatomic evidence for distinct functional domains in hippocampal field CA1. Proc Natl Acad Sci USA 106(28):11794–11799. DOI 10.1073/pnas.0812608106.

Doubi-Kadmiri S, Benoit C, Benigni X, Beaumont G, Vacher C-M, Taouis M, *et al*. (2016) Substantial and robust changes in microRNA transcriptome support postnatal development of the hypothalamus in rat. Sci Rep 6:24896. DOI 10.1038/srep24896.

Dougherty JD, Schmidt EF, Nakajima M, Heintz N (2010) Analytical approaches to RNA profiling data for the identification of genes enriched in specific cells. Nucleic Acids Res 38:4218–4230. DOI 10.1101/gad.207654.112.

Doyle JP, Dougherty JD, Heiman M, Schmidt EF, Stevens TR, Ma G, *et al*. (2008) Application of a translational profiling approach for the comparative analysis of CNS cell types. Cell 135(4):749–762. DOI 10.1016/j.cell.2008.10.029.

Drnevich J, Replogle KL, Lovell P, Hahn TP, Johnson F, Mast TG, *et al*. (2012) Impact of experience-dependent and –independent factors on gene expression in songbird brain. Proc Natl Acad Sci USA 109 (Suppl 2):17245–17252. DOI 10.1073/pnas.1200655109.

Dunn MJ (1987) Two-dimensional gel electrophoresis of proteins. J Chromatogr B: Biomed Sci Appl 418:145–185.

Eberwine J, Yeh H, Miyashiro K, Cao Y, Nair S, Finnell R, *et al*. (1992) Analysis of gene expression in single live neurons. Proc Natl Acad Sci USA 89:3010–3014.

Eberwine J, Bartfai T (2011) Single cell transcriptomics of hypothalamic warm sensitive neurons that control core body temperature and fever response. Signaling asymmetry and an extension of chemical neuroanatomy. Pharmacol Therap 129(3):241–259. DOI 10.1016/j.pharmthera.2010.09.010.

Ekstrand MI, Nectow AR, Knight ZA, Latcha KN, Pomeranz LE, Friedman JM (2014) Molecular profiling of neurons based on connectivity. Cell 157(5):1230–1242. DOI 10.1016/j.cell.2014.03.059.

Elphick MR, Mirabeau O, Larhammar D (2018) Evolution of neuropeptide signaling systems. J Exp Biol 221(Pt. 3):jeb151092. DOI 10.1242/jeb.151092.

Emmert-Buck MR, Bonner RF, Smith PD, Chuaqui RH, Zhengping Z, Goldstein SR, *et al*. (1996) Laser capture microdissection. Science 274:998–1001.

Espina V, Wulfkuhle JD, Calvert VS, VanMeter A, Zhou W, Coukos G, *et al*. (2006) Laser-capture microdissection. Nat Protoc 1:586–603. DOI 10.1038/nprot.2006.85.

Esteve C, Tolner EA, Shyti R, van den Maagdenberg AMJM, McDonnell LA (2016) Mass spectrometry imaging of amino neurotransmitters: A comparison of derivatization methods and application in mouse brain tissue. Metabolomics 12:30. DOI 10.1007/s11306-015-0926-0.

Fälth M, Sköld K, Norrman M, Svensson M, Fenyö D, Andren PE (2006) SwePep, a database designed for endogenous peptides and mass spectrometry. Mol Cell Proteomics 5:998–1005. DOI: 10.1074/mcp.M500401-MCP200.

Fang X-L, Zhu X-T, Chen S-F, Zhang Z-Q, Zeng Q-J, Deng L, *et al*. (2014) Differential gene expression pattern in hypothalamus of chickens during fasting-induced metabolic reprogramming: Functions of glucose and lipid metabolism in the feed intake of chickens. Poultry Sci 93:2841–2854. DOI 10.3382/ps.2014-04047.

Farajzadeh L, Hornshøj H, Momeni J, Thomsen B, Larsen K, *et al*. (2013) Pairwise comparisons of ten porcine tissues identify differential transcriptional regulation at the gene, isoform, promoter and transcription start site level. Biochem Biophys Res Commun 438:346–352. DOI 10.1016/j.bbrc.2013.07.074.

Fassunke J, Majores M, Ullmann C, Elger CE, Schramm J, Wiestler OD, *et al*. (2004) In situ-RT and immunolaser microdissection for mRNA analysis of individual cells isolated from epilepsy-associated glioneuronal tumors. Lab Invest 84:1520–1525. DOI 10.1038/labinvest.3700165.

Fatt P, Katz B (1952) The electrical activity of the motor end-plate. Proc R Soc Lond B Biol Sci 140:183–186. Available online: http://0-www.jstor.org.lib.utep.edu/stable/82687.

Feldberg W (1952) Central excitation and inhibition from the view point of chemical transmission. Proc R Soc Lond B Biol Sci 140:199–202. Available online: http://0-www.jstor.org.lib.utep.edu/stable/82690.

Feldberg W, Vogt M (1948) Acetylcholine synthesis in different regions of the central nervous system. J Physiol 107:372–381.

Feldman SE, Snapir N, Yasuda M, Treuting F, Lepkovsky S (1973) Physiological and nutritional consequences of brain lesions: A functional atlas of the chicken hypothalamus. Hilgardia 41(19):605–630.

Ferrier D (1873) Experimental researches in cerebral physiology and pathology. The West Riding Lunatic Asylum Medical Reports 3:30–96.

Fink L, Kinfe T, Stein MM, Ermert L, Hanze J, Kummer W, *et al*. (2000) Immunostaining and laser-assisted cell picking for mRNA analysis. Lab Invest 80:327–333.

Flourens P (1824) Recherches expérimentales sur les propriétés et les fonctions du système nerveux, dans les animaux vertébrés. Chez Crevot, Paris.

Fodor SPA, Read JL, Pirrung MC, Stryer L, Lu AT, Solas D (1991) Light-directed, spatially addressable parallel chemical synthesis. Science 251(4995):767-773. DOI 10.1126/science.1990438.

Foster NN, Azam S, Watts AG (2016) Rapid-onset hypoglycemia suppresses Fos expression in discrete parts of the ventromedial nucleus of the hypothalamus. Am J Physiol Regul Integr Comp Physiol 310:R1177–R1185. DOI 10.1152/ajpregu.00042.2016.

Forssburg A, Larsson S (1954) Studies of isotope distribution and chemical composition in the hypothalamic region of hungry and fed rats. Published as Part II (pp. 41–63) of: Larsson S. 1954. On the hypothalamic organisation of the nervous mechanism regulating food intake. Acta Physiologica Scandinavica Supplementum 32(115):7–63.

Fortes MRS, Nguyen LT, Weller MMDCA, Cánovas A, Islas-Trejo A, Porto-Neto LR, *et al.*, (2016) Transcriptome analyses identify five transcription factors differentially expressed in the hypothalamus of post- versus prepubertal Brahman heifers. J Anim Sci 94:3693–3702. DOI 10.2527/jas2016-0471.

Fortes MRS, Snelling WM, Reverter A, Nagaraj SH, Lehnert SA, Hawken RJ, *et al*. (2015) Gene network analysis of first service conception in Brangus heifers: Use of genome and trait associations, hypothalamic-transcriptome information, and transcription factors. J Anim Sci 2012.90:2894–2906. DOI 10.2527/jas2011-4601.

Fouillen L, Petruzziello F, Veit J, Bhattacharyya A, Kretz R, Rainer G, *et al*. (2013) Neuropeptide alterations in the tree shrew hypothalamus during volatile anesthesia. J Proteomics 80:311–319. DOI 10.1016/j/jprot.2012.11.002.

Frese CK, Boender AJ, Mohammed S, Heck AJR, Adan RAH, Altelaar AFM (2013) Profiling of diet-induced neuropeptide changes in rat brain by quantitative mass spectrometry. Anal Chem 85:4594–4604. DOI 10.1021/ac400232y.

Friede RL (1966) Topographic brain chemistry. Academic Press, New York.

Gao G, Li Q, Zhao X, Ding N, Han Q, Su J, Wang Q (2015) Transcriptome profiling of the hypothalamus during prelaying and laying periods in Sichuan white geese (*Anser cygnoides*). Anim Sci J 86(8):800–805. DOI 10.1111/asj.12356.

Gao Y, Chen S, Xu Q, Yu K, Wang J, Qiao L, *et al*. (2013) Proteomic analysis of differential proteins related to anti-nociceptive effect of electroacupuncture in the hypothalamus following neuropathic pain in rats. Neurochem Res 38:1467–1478. DOI 10.1007/s11064-013-1047-7.

Gasperini L, Piubelli C, Carboni L (2012) Proteomics of rat hypothalamus, hippocampus and pre-frontal/frontal cortex after central administration of the neuropeptide PACAP. Mol Biol Rep 30:2921–2935. DOI 10.1007/s11033-011-1054-1.

Gautvik KM, de Lecea L, Gautvik VT, Danielson PE, Tranque P, Dopazo A, *et al*., (1996) Overview of the most prevalent hypothalamus-specific mRNAs, as identified by directional tag PCR subtraction. Proc Natl Acad Sci USA 93(16):8733–8738. DOI 10.1073/pnas.93.16.8733.

Gee CE, Chen CL, Roberts JL, Thompson R, Watson SJ (1983) Identification of proopiomelanocortin neurons in rat hypothalamus by *in situ* cDNA-mRNA hybridization. Nature 306(5941):374–376.

Giacobini E (1956) Histochemical demonstration of AChE activity in isolated nerve cells. Acta Physiol Scand 36(3):276–290.

Giardino WJ, de Lecea L (2015) Resting easy with a sleep regulator. Elife 4:e12093. DOI 10.7554/eLife.12093.

Gillespie JW, Best CJ, Bichsel VE, Cole KA, Greenhut SF, Hewitt SM, *et al*. (2002) Evaluation of non-formalin tissue fixation for molecular profiling studies. Am J Pathol 160:449–457. DOI 10.1016/S0002-9440(10)64864-X.

Ginsberg SD, Che S (2004) Combined histochemical staining, RNA amplification, regional and single-cell cDNA analysis within the hippocampus. Lab Invest 84:952–962. DOI 10.1038/labinvest.3700110.

Glasgow E, Kusano K, Chin H, Mezey E, Young WS III, Gainer H (1999) Single-cell reverse transcription-polymerase chain reaction analysis of rat supraoptic magnocellular neurons: Neuropeptide phenotypes and high voltage-gated calcium channel subtypes. Endocrinol 140:5391–5401. DOI 10.1210/endo.140.11.7136.

Goldsworthy SM, Stockton PS, Trempus CS, Foley JF, Maronpot RR (1999) Effects of fixation on RNA extraction and amplification from laser capture microdissected tissue. Mol Carcinogen 25:86–91.

González CR, Martínez de Morentin PB, Martínez-Sánchez N, Gómez-Díaz C, Lage R, Varela L, *et al*. (2012) Hyperthyroidism differentially regulates neuropeptide S system in the rat brain. Brain Res 1450:40–48. DOI 10.1016/j.brainres.2012.02.24.

Goraud SS, Yao ST, Heesom KJ, Paton JFR, Murphy D (2007) 14-3-3 proteins within the hypothalamic-neurohypophyseal system of the osmotically stressed rat: Transcriptomic and proteomic studies. J Neuroendocrinol 19:913–922. DOI 10.1111/j.1365-2826.2007.01604.x.

Greenberg N (1982) A forebrain atlas and stereotaxic technique for the lizard, *Anolis carolinensis*. J Morphol 174(2):217–236.

Greenwood MP, Mecawi AS, Hoe SZ, Mustafa MR, Johnson KR, Al-Mahmoud GA, *et al*. (2015) A comparison of physiological and transcriptome responses to water deprivation and salt loading in the rat supraoptic nucleus. Am J Physiol Regul Integr Comp Physiol 308:R559–R568. DOI 10.1152/ajpregu.00444.2014.

Groseclose MR, Andersson M, Hardesty WM, Caprioli RM (2007) Identification of proteins directly from tissue: *in situ* tryptic digestions coupled with imaging mass spectrometry. J Mass Spectrom 42:254–262. DOI 10.1002/jms.1177.

Guest PC, Urday S, Ma D, Stelzhammer V, Harris LW, Amess B, *et al*. (2012) Proteomic analysis of the maternal protein restriction rat model for schizophrenia: Identification of translational changes in hormonal signaling pathways and glutamate neurotransmission. Proteomics 12:3580-3589. DOI 10.1002/pmic.201200376.

Habib N, Avraham-Davidi I, Basu A, Burks T, Shekhar K, Hofree M, *et al*. (2017) Massively parallel single-nucleus RNA-seq with DroNc-seq. Nat Meth 14:955–958. DOI 10.1038/nmeth.4407.

Haendel MA, Balhoff JP, Bastian FB, Blackburn DC, Blake JA, Bradford Y, *et al*. (2014) Unification of multi-species vertebrate anatomy ontologies for comparative biology in Uberon. J Biomed Semant 5, 21. DOI 10.1186/2041-1480-5-21.

Hahn JD (2010) Comparison of melanin-concentrating hormone and hypocretin/orexin peptide expression patterns in a current parceling scheme of the lateral hypothalamic zone. Neurosci Lett 468:12–17. DOI 10.1016/j.neulet.2009.10.047.

Hahn JD, Swanson LW (2010) Distinct patterns of neuronal inputs and outputs of the juxtaparaventricular and suprafornical regions of the lateral hypothalamic area in the male rat. Brain Res Rev 64(1):14–103. DOI 10.1016/j.brainresrev.2010.02.002.

Hahn TM, Breininger JF, Baskin DG, Schwartz MW (1998) Coexpression of Agrp and NPY in fasting-activated hypothalamic neurons. Nat Neurosci 1:271–272. DOI 10.1038/1082.

Harthoorn LF, Sañé A, Nethe M, Van Heerikhuize JJ (2005) Multi-transcriptional profiling of melanin-concentrating hormone and orexin-containing neurons. Cell Mol Neurobiol 25:1209–1223. DOI 10.1007/s10571-005-8184-8.

Hatcher NG, Atkins N Jr, Annangudi SP, Forbes AJ, Kelleher NL, Gillette MU, *et al*., (2008) Mass spectrometry-based discovery of circadian peptides. Proc Natl Acad Sci USA 105:12527–12532. DOI 10.1073/pnas.0804340105.

Hatton GI, JI Johnson, CZ Malatesta (1972) Supraoptic nuclei of rodents adapted for mesic and xeric environments: Numbers of cells, multiple nucleoli, and their distributions. J Comp Neurol 145(1):43–59. DOI 10.1002/cne.901450104.

Häusser M (2000) The Hodgkin-Huxley theory of the action potential. Nat Neurosci 3 (Suppl) 1165.

Hazell GJG, Hindmarch CC, Pope GR, Roper JA, Lightman SL, Murphy D, *et al*. (2012) G protein-coupled receptors in the hypothalamic paraventricular and supraoptic nuclei – Serpentine gateways to neuroendocrine homeostasis. Front Neuroendocrinol 33:45–66. DOI 10.1016/j.yfrne.2011.07.002.

Heijs B, Carreira RJ, Tolner EA, de Ru AH, van den Maagdenberg AMJM, van Veelen PA, McDonnell LA (2015) Comprehensive analysis of the mouse brain proteome sampled in mass spectrometry imaging. Anal Chem 87:1867–1875. DOI 10.1021/ac503952q.

Heiman M, Schaefer A, Gong S, Peterson JD, Day M, Ramsey KE, *et al*., (2008) A translational profiling approach for the molecular characterization of CNS cell types. Cell 135(4):738–748. DOI 10.1016/j.cell.2008.10.028.

Heisler LK, Pronchuk N, Nonogaki K, Zhou L, Raber J, Tung L, *et al*. (2007) Serotonin activates the hypothalamic-pituitary-adrenal axis via serotonin 2C receptor stimulation. J Neurosci 27(26):6956–6964. DOI 10.1523/JNEUROSCI.2584-06.2007.

Helmholtz H (1850) Messungen über den zeitlichen Verlauf der Zuckung animalischer Muskeln und die Fortpflanzungsgeschwindigkeit der Reizung in den Nerven. Archiv für Anatomie, Physiologie und Wissenschaftliche Medicin, 276–364. Veit et Comp, Berlin.

Henry FE, Sugino K, Tozer A, Branco T, Sternson SM (2015) Cell type-specific transcriptomics of hypothalamic energy-sensing neuron responses to weight-loss. eLife 4:e09800. DOI 10.7554/eLife.09800.

Hernandez AE, Khan AM (2016) Migration, spatial alignment, and registration of multi-scale neuroscientific datasets related to the control of motivated behaviors within canonically defined maps of the lateral hypothalamic area. Program No. 453.12. 2016 Society for Neuroscience Meeting Planner. San Diego, CA. Society for Neuroscience. Online.

Heydorn WE, Creed GJ, Goldman D, Kanter D, Merrill CR, Jacobowitz DM (1983) Mapping and quantitation of proteins from discrete nuclei and other areas of the rat brain by two-dimensional gel electrophoresis. J Neurosci 3(12):2597–2606. DOI 10.1523/JNEUROSCI.03-12-02597.1983.

Heydorn WE, Creed GJ, Patel J, Jacobowitz DM (1986) Distribution of proteins in different subcellular fractions of rat brain studied by two-dimensional gel electrophoresis. Neurochem Int 9(3):357–370. DOI 10.1016/0197-0186(86)90077-X.

Higgins SE, Ellestad LE, Trakooljul N, McCarthy F, Saliba J, Cogburn LA, Porter TE (2010) Transcriptional and pathway analysis in the hypothalamus of newly hatched chicks during fasting and delayed feeding. BMC Genomics 11:162. DOI 10.1186/1471-2164-11-162.

Hill AV (1932) Chemical wave transmission in nerve. The Macmillan Company, New York.

Hindmarch C, Yao S, Beighton G, Paton J, Murphy D (2006) A comprehensive description of the transcriptome of the hypothalamoneurohypophyseal system in euhydrated and dehydrated rats. Proc Natl Acad Sci USA 103(5):1609–1614. DOI 10.1073/pnas.0507450103.

Hindmarch C, Yao S, Hesketh S, Jessop D, Harbuz M, *et al*. (2007) The transcriptome of the rat hypothalamic-neurohypophyseal system is highly strain-dependent. J Neuroendocrinol 19:1009–1012. DOI 10.1111/j.1365-2826.2007.01612.x.

Hindmarch CCT, Franses P, Goodwin B, Murphy D (2013) Whole transcriptome organisation in the dehydrated supraoptic nucleus. Braz J Med Biol Res 46:1000–1006. DOI 10.1590/1414-431X20133328.

Hirst BH (2004) Secretin and the exposition of hormonal control. J Physiol (London) 560:339. DOI 10.1113/jphysiol.2004.073056.

Hitzemann R, Darakjian P, Walter N, Iancu OD, Searles R, McWeeney S (2014) Introduction to sequencing the brain transcriptome. Int Rev Neurobiol 116:1–19. DOI 10.1016/B978-0-12-801105-8.00001-1.

Hodgkin AL, Huxley AF (1939) Action potentials recorded from inside a nerve fibre. Nature 144:710–711. DOI 10.1038/144710a0.

Hodgkin AL, Huxley AF (1945) Resting and action potentials in single nerve fibers. J Physiol (Lond) 104:176–195.

Hodgkin AL, Huxley AF (1952a) Propagation of electrical signals along giant nerve fibres. Proc R Soc Lond B Biol Sci 140:177–183.

Hodgkin AL, Huxley AF (1952b) Currents carried by sodium and potassium ions through the membrane of the giant axon of *Loligo*. J Physiol (Lond) 116:449–472.

Hodgkin AL, Huxley AF (1952c) The components of membrane conductance in the giant axon of *Loligo*. J Physiol 116:473–496.

Hodgkin AL, Huxley AF (1952d) The dual effect of membrane potential on sodium conductance in the giant axon of *Loligo*. J Physiol (Lond) 116:497–506.

Hodgkin AL, Huxley AF (1952e) A quantitative description of membrane current and its application to conduction and excitation in nerve. J Physiol (Lond) 117:500–544.

Hodgkin AL, Huxley AF (1952f) Movement of sodium and potassium ions during nervous activity. Cold Spr Harb Symp 17:43–52.

Hodgkin AL, Huxley AF, Katz B (1952) Measurement of current-voltage relations in the membrane of the giant axon of *Loligo*. J Physiol (Lond) 116:424–448.

Hoffmann A (1973) Stereotaxic atlas of the toad's brain. Acta Anat (Basel) 84(3):416–451.

Holland PM, Abramson RD, Watson R, Gelfand DH (1991) Detection of specific polymerase chain reaction product by utilizing the 5'-3' exonuclease activity of *Thermus aquaticus* DNA polymerase. Proc Natl Acad Sci USA 88:7276–7280.

Honda M, Eriksson KS, Zhang S, Tanaka S, Lin L, Salehi A, *et al*., (2009) IGFBP3 colocalizes with and regulates hypocretin (orexin). PLoS One 4(1):e4254. DOI 10.1371/journal.pone.0004254.

Hu SP, Yang JS, Wu MY, Shen ZY, Zhang KH, Liu JW, *et al*. (2005) Effect of one-step 100% ethanol fixation and modified manual microdissection on high-quality RNA recovery from esophageal carcinoma specimen. Dis Esophag 18:190–198. DOI 0.1111/j.1442-2050.2005.00475.x.

Humerick M, Hanson J, Rodriguez-Canales J, Lubelski D, Rashid OM, Salinas YD, *et al*. (2013) Analysis of transcription factor mRNAs in identified oxytocin and vasopressin magnocellular neurons isolated by laser capture microdissection. PLoS One 8(7):e69407. DOI: 10.1371/journal.pone.0069407.

Huxley AF (2002) Hodgkin and the action potential. J Physiol (London) 538:2. DOI 10.1013/jphysiol.2001.014118.

Hydén H (1959) Quantitative assay of compounds in isolated fresh nerve cells and glial cells from control and stimulated animals. Nature 184(4684):433–435.

Hydén H (1967) Dynamic aspects on the neuron-glia relationship. A study with micro-chemical methods. In: The Neuron (H. Hydén, ed.), pp. 179–219. Elsevier, Amsterdam.

Ihnatko R, Post C, Blomqvist A (2013) Proteomic profiling of the hypothalamus in a mouse model of cancer-induced anorexia-cachexia. Br J Cancer 109:1867–1875. DOI 10.1038/bjc.2013.525.

Iqbal J, Li W, Ullah K, Hasan M, Linna G, Awan U, *et al*. (2013) Study of rat hypothalamic proteome by HPLC/ESI ion trap and HPLC/ESI-Q-TOF MS. Proteomics 13:2455–2468. DOI 10.1002/pmic.201300073.

Iqbal J, Li W, Hasan M, Li YJ, Ullah K, Yun W, *et al*. (2014a) Distortion of homeostatic signaling proteins by simulated microgravity in rat hypothalamus: A $^{16}O/^{18}O$-labeled comparative integrated proteomic approach. Proteomics 14:262–273. DOI 10.1002/pmic.201300337.

Iqbal J, Li W, Hasan M, Liu K, Awan U, Saeed Y, *et al*. (2014b) Differential expression of specific cellular defense proteins in rat hypothalamus under simulated microgravity induced conditions: Comparative proteomics. Proteomics 14:1424–1433. DOI 10.1002/pmic.201400019.

Jacobowitz DM (1974) Removal of discrete fresh regions of the rat brain. Brain Res 80:111–115. DOI: 10.1016/0006-8993(74)90726-4.
Jacobowitz DM (2006) The birth of neurochemical maps. Neurochem Res 31(2):125–126. DOI: 10.1007/s11064-005-9002-x.

Jacobowitz DM, Palkovits M (1974) Topographic atlas of catecholamine and acetylcholinesterase-containing neurons in the rat brain. I. Forebrain (Telencephalon, Diencephalon). J Comp Neurol 157:13–28. DOI: 10.1002/cne.901570103.

Jékely G (2013) Global view of the evolution and diversity of metazoan neuropeptide signaling. Proc Natl Acad Sci USA 110(21):8702–8707. DOI 10.1073/pnas.1221833110.

Jeong JH, Woo YJ, Chua S Jr, Jo YH (2016) Single-cell gene expression analysis of cholinergic neurons in the arcuate nucleus of the hypothalamus. PLoS One 11:e0162839. DOI 10.1371/journal.pone.0162839.

Jin S, Sun D, Xi Q, Dong X, Song D, Fu H, *et al.*, (2016) Identification of genes in the hypothalamus-pituitary-gonad axis in the brain of Amur sturgeons (*Acipenser schrenckii*) by comparative transcriptome analysis in relation to kisspeptin treatment. Gene 595:53–61. DOI 10.1016/j/.gene.2016.09.026.

Jing X, Ratty AK, Murphy D (1998) Ontogeny of the vasopressin and oxytocin mRNAs in the mouse hypothalamus. Neurosci Res 30:343–349. DOI 10.1016/S0168-0102(98)00017-0.

Jockusch H, Voigt S, Eberhard D (2003) Localization of GFP I frozen sections from unfixed mouse tissues: immobilization of a highly soluble marker protein by formaldehyde vapor. J Histochem Cytochem 51:401–404. DOI 10.1177/002215540305100315.

Johnson KR, Hindmarch CCT, Salinas YD, Shi Y, Greenwood M, Hoe SZ, *et al.* (2015) A RNA-Seq analysis of the rat supraoptic nucleus transcriptome: Effects of salt loading on gene expression. PLoS One 10(4):e0124523. DOI 10.1371/journal.pone.0124523.

Johnston PV, Roots BI (1966) The presence of phosphatidylcholine in neurons isolated from the lateral vestibular nucleus of ox brain. Biochem J 98:157–158.

Johnston PV, Roots BI (1970) Neuronal and glial perikarya preparations: An appraisal of present methods. Int Rev Cytol 29:265–280.

Jovanovic Z, Tung YCL, Lam BYH, O'Rahilly S, Yeo GSH (2010) Identification of the global transcriptomic response of the hypothalamic arcuate nucleus to fasting and leptin. J Neuroendocrinol 22(8):915–925. DOI 10.1111/j.1365-2826.2010.02026.x.

Kabra DG, Pfuhlmann K, García-Cáceres C, Schriever SC, García VC, Kebede AF, *et al*. (2016) Hypothalamic leptin action is mediated by histone deacetylase 5. Nat Commun 7:10782. DOI: 10.1038/ncomms10782.

Karas M, Bachmann D, Bahr U, Hillenkamp F (1987) Matrix-assisted ultraviolet laser desorption of non-volatile compounds. Int J Mass Spectr Ion Proc 78:53–68.

Kefaloyianni E, Lyssand JS, Moreno C, Delaroche D, Hong M, Fenyö D, *et al*. (2013) Comparative proteomic analysis of the ATP-sensitive K+ channel complex in different tissue types. Proteomics 13:368–378. DOI 10.1002/pmic.201200324.

Kernan IA, Buck BJ, Evans SJ, Akil H, Watson SJ (2006) Combining laser capture microdissection with quantitative real-time PCR: Effects of tissue manipulation on RNA quality and gene expression. J Neurosci Meth 153:71–85. DOI 10.1016/j.jneumeth.2005.10.010.

Khan AM (2009) [2 parts] Nerve, muscle, blood, toil, tears, and sweat: England's pioneering biophysicist, soldier, and statesman. J Hist Neurosci 18:80–81; 98–105. DOI: 10.1080/09647040802105854, and DOI 10.1080/09647040802349817.

Khan AM (2013) Controlling feeding behavior by chemical or gene-directed targeting in the brain: What's so spatial about our methods? Front Neurosci 7 (Article 182):1–49. DOI 10.3389/fnins.2013.00182.

Khan AM, Hahn JD, Cheng W-C, Watts AG, Burns GAPC (2006) NeuroScholar's electronic laboratory notebook and its application to neuroendocrinology. Neuroinformatics 4(2):139–161. DOI 10.1385/NI:4:2:139.

Khan AM, Perez J, Wells CE, Fuentes O (2018) Computer vision evidence supporting craniometric alignment of rat brain atlases to streamline expert-guided, first-order migration of hypothalamic spatial datasets related to behavioral control. Front Syst Neurosci 12 (Article 7):1–29. DOI 10.3389/fnsys.2018.00007.

Khan AM, Ponzio TA, Sanchez-Watts G, Stanley BG, Hatton GI, Watts AG (2007) Catecholaminergic control of mitogen-activated protein kinase signaling in paraventricular neuroendocrine neurons *in vivo* and *in vitro*: A proposed role during glycemic challenges. J Neurosci 27(27):7344–7360. DOI 10.1523/JNEUROSCI.0873-07.2007.

Khan AM, Walker EM, Watts AG (2017) Tracking the coupling of external signals to intracellular programs controlling peptide synthesis and release in hypothalamic neuroendocrine neurons. In: Fink G (ed) Stress: Neuroendocrinology and Neurobiology, Elsevier, Amsterdam, pp 67–81. DOI 10.1016/B978-0-12-802175-0.00007-3.

Khodosevich K, Inta D, Seeburg PH, Monyer H (2007) Gene expression analysis of *in vivo* fluorescent cells. PLoS One 2: e1151. DOI journal.pone.0001151.

Kim H-J, Park HJ, Hong MS, Song JY, Park H-K, Jo DJ, *et al*. (2010) Effect by acupuncture on hypothalamic expression of maternally separated rats: Proteomic approach. Neurol Res 32 (Suppl 1):69–73. DOI 10.1179/016164109X12537002794129.

Kim J-H, Kim J-H, Cho Y-E, Baek M-C, Jung J-Y, Lee M-G, *et al*. (2014) Chronic sleep deprivation-induced proteome changes in astrocytes of the rat hypothalamus. J Prot Res 13:4047–4061. DOI 10.1021/pr500431j.

Kleinzeller A (1999) Charles Ernest Overton's concept of a cell membrane, In: Deamer DW, Kleinzeller A, Fambrough DM (eds) Membrane Permeability: 100 Years Since Ernest Overton. Academic Press, San Diego, pp 1–22.

Klimov LO, Ershov NI, Efimov VM, Markel AL, Redina OE (2016) Genome-wide transcriptome analysis of hypothalamus in rats with inherited stress-induced arterial hypertension. BMC Genet 17(Suppl 1):13. DOI 10.1186/s12863-015-0307-8.

Knight ZA, Tan K, Birsoy K, Schmidt S, Garrison JL, Wysocki RW, *et al*. (2012) Molecular profiling of activated neurons by phosphorylated ribosome capture. Cell 151(5):1126–1137. DOI 10.1016/j.cell.2012.10.039.

Koelle GB, Friedenwald JS (1949) A histochemical method for localizing cholinesterase activity. Proc Soc Exp Biol Med 70:617–622.

Konig JFR, Klippel RA (1963) *The Rat Brain: A Stereotaxic Atlas of the Forebrain and Lower Parts of the Brain Stem*. Baltimore: The Williams and Wilkins Co.

Korner J, Savontaus E, Chua SC Jr, Leibel RL, Wardlaw SL (2001) Leptin regulation of *Agrp* and *Npy* mRNA in the rat hypothalamus. J Neuroendocrinol 13:959–966. DOI 10.1046/j.1365-2826.2001.00716.x.

Kuenzel WJ, Beck MM, Teruyama R (1999) Neural sites and pathways regulating food intake in birds: A comparative analysis to mammalian systems. J Exp Zool 283:348–364. DOI 10.1002/(SICI)1097-010X(19990301/01)283:4/5<348::AID-JEZ5>3.0.CO;2-5.

Kuhla B, Kuhla S, Rudolph PE, Albrecht D, Metges CC (2007) Proteomics analysis of hypothalamic response to energy restriction in dairy cows. Proteomics 7:3602–3617. DOI 10.1002/pmic.200700248.

Kuo Y-M, Shiue Y-L, Chen C-F, Tang P-C, Lee Y-P (2005) Proteomic analysis of hypothalamic proteins of high and low egg production strains of chickens. Theriogenol 64:1490–1502. DOI 10.1016/j/theriogenology.2005.03.20.

Kurrasch DM, Cheung CC, Lee FY, Tran PV, Hata K, Ingraham HA (2007) The neonatal ventromedial hypothalamus transcriptome reveals novel markers with spatially distinct patterning. J Neurosci 27(50):13624–13634. DOI 10.1523/JNEUROSCI.2858-07.2007.

Lachuer J, Ouyang L, Legras C, Rio JD, Barlow C (2005) Gene expression profiling reveals an inflammatory process in the *anx*/*anx* mutant mice. Mol Brain Res 139:372–376. DOI 10.1016/j.molbrainres.2005.06.003.

Lake BB, Ai R, Kaeser GE, Salathia NS, Yung YC, Liu R, *et al*. (2016) Neuronal subtypes and diversity revealed by single-nucleus RNA sequencing of the human brain. Science 352:1586–1590. DOI 10.1126/science.aaf1204.

Lam BYH, Cimino I, Polex-Wolf J, Kohnke SN, Rimmington D, *et al*. (2017) Heterogeneity of hypothalamic pro-opiomelanocortin-expressing neurons revealed by single-cell RNA sequencing. Mol Metab 6:383–392. DOI 10.1016/j.molmet.2017.02.007.

Landmann EM, Schellong K, Melchior K, Rodekamp E, Ziska T, Harder T, Plagemann A (2012) Short-term regulation of the hypothalamic melanocortinergic system under fasting and defined glucose-refeeding conditions in rats: A lasercapture microdissection (LMD)-based study. Neurosci Lett 515(1):87–91. DOI 10.1016/j.neulet.2012.03.025.

Lee JH, Atkins N, Hatcher NG, Zamdborg L, Gillette MU, Sweedler JV, *et al.*, (2010) Endogenous peptide discovery of the rat circadian clock: a focused study of the suprachiasmatic nucleus by ultrahigh performance tandem mass spectrometry. Mol Cell Proteomics 9:285–297. DOI 10.1074/mcp.M900362-MCP200.

Lee JE, Zamdborg L, Southey BR, Atkins N Jr, Mitchell JW, Li M, *et al*. (2013) Quantitative peptidomics for discovery of circadian-related peptides from the suprachiasmatic nucleus. J Proteome Res 12:585–593. DOI 10.1021/pr300605p.

Lee JH, Daugharthy ER, Scheiman J, Kalhor R, Ferrante TC, Terry R, *et al*. (2015) Fluorescent *in situ* sequencing (FISSEQ) of RNA for gene expression profiling in intact cells and tissues. Nat Protoc 10:442–458. DOI 10.1038/nprot.2014.191.

Lee JH, Daugharthy ER, Scheiman J, Kalhor R, Yang JL, Ferrante TC, *et al*. (2014) Highly multiplexed subcellular RNA sequencing *in situ*. Science 343:1360–1363. DOI 10.1126/science.1250.21.

Lee S, Bookout AL, Lee CE, Gautron L, Harper MJ, Elias CF, *et al*., (2012) Laser-capture microdissection and transcriptional profiling of the dorsomedial nucleus of the hypothalamus. J Comp Neurol 520(16):3617–3632. DOI 10.1002/cne.23116.

Lehrer GM, Maker HS (1972) Quantitative histochemical approaches to energy metabolism in nervous tissue. In: Balázs R, Cremer JE (eds) Metabolic compartmentation in the brain. John Wiley & Sons, New York, pp 235–244.

Lenoir T, Giannella E (2006) The emergence and diffusion of DNA microarray technology. J Biomed Discov Collab 1:11. DOI 10.1186/1747-5333-1-11.

Levey AI, Wainer BH, Rye DB, Mufson EJ, Mesulam M-M (1983) Choline acetyltransferase-immunoreactive neurons intrinsic to rodent cortex and distinction from acetylcholinesterase-positive neurons. Neurosci 13:341–353.

Li J-Y, Kuick R, Thompson RC, Misek DE, Lai Y-M, Liu Y-Q, *et al*. (2005) Arcuate nucleus transcriptome profiling identifies ankyrin repeat and suppressor of cytokine signaling box-containing protein 4 as a gene regulated by fasting in central nervous system feeding circuits. J Neuroendocrinol 17:394–404. DOI 10.1111/j.1365-2826.2005.01317.x.

Li J-Y, Lescure PA, Misek DE, Lai Y-M, Chai B-X, Kuick R, *et al*. (2002) Food deprivation-induced expression of minoxidil sulfotransferase in the hypothalamus uncovered by microarray analysis. J Biol Chem 277(11):9069–9076. DOI 10.1074/jbc.M110467200.

Li X, Qu F, Xie W, Wang F, Liu H, Song S, *et al*. (2014) Transcriptomic analyses of neurotoxic effects in mouse brain after intermittent neonatal administration of thimerosal. Toxicol Sci 139(2):452–465. DOI 10.1093/toxsci/kfu049.

Liberini CG, Boyle CN, Cifani C, Venniro M, Hope BT, Lutz TA (2016) Amylin receptor components and the leptin receptor are co-expressed in single rat area postrema neurons. Eur J Neurosci 43:653–661, 2016. DOI 10.1111/ejn.13163.

Lisser H (1927) Hypophysis versus hypothalamus. Calif Western Med 26(4):490–492.

Liu X, Zeng J, Zhou A, Theodorsson E, Fahrenkrug J, Reinscheid RK (2011) Molecular fingerprint of neuropeptide S-producing neurons in the mouse brain. J Comp Neurol 519: 1847–1866. DOI 10.1002/cne.22603.

Loewi O (1921) Über humorale Übertragbarkeit der Herznervenwirkung. I. Mitteilung. Pfluger's Archiv 189(1):239–242.

Lowry OH (1953) The quantitative histochemistry of the brain. Histological sampling. J Histochem Cytochem 1(6):420–428. DOI 10.1177/1.6.420.

Luan X, Cao Z, Li R, Liu M, Hu J (2014) Differential expression profiling of hypothalamus genes in laying period and ceased period Huoyan geese. Mol Biol Rep 41:3401–3411. DOI 10.1007/s11033-014-3202-x.

Macosko EZ, Basu A, Satija R, Nemesh J, Shekhar K, Goldman M, *et al*. (2015) Highly parallel genome-wide expression profiling of individual cells using nanoliter droplets. Cell 161:1202–1214. DOI: 10.1016/j.cell.2015.05.002.

Manciu FS, Lee KH, Durrer WG, Bennet KE (2013) Detection and monitoring of neurotransmitters – A spectroscopic analysis. Neuromodulation 16:192–199. DOI 10.1111/j.1525-1403.2012.00502.x.

Manousopoulou A, Koutmani Y, Karaliota S, Woelk CH, Manolakos ES, Karalis K, *et al*., (2016) Hypothalamus proteomics from mouse models with obesity and anorexia reveals therapeutic targets of appetite regulation. Nutrition & Diabetes 6, e204. DOI 10.1038/nutd.2016.10.

Martinez A, Pinales BE, Khan AM (2015) Connections of the rostral portion of the hypothalamic arcuate nucleus: A combined anterograde and retrograde study in the adult male rat. Program No. 616.10. 2015 Neuroscience Meeting Planner. Chicago, IL. Society for Neuroscience, 2015. Online.

Martinez A, Pinales BE, Khan AM (2016) Further elaboration of arcuate hypothalamic nucleus circuitry based on retrograde studies in the adult male rat. Program No. 453.11. 2016 Neuroscience Meeting Planner. San Diego, CA. Society for Neuroscience, 2016. Online.

Martyniuk CJ, Doperalski NJ, Kroll KJ, Barber DS, Denslow ND (2013) Sexually dimorphic transcriptomic responses in the teleostean hypothalamus: A case study with the organochlorine pesticide dieldrin. Neurotoxicol 34:105–117. DOI 10.1016/j.neuro.2012.09.012.

Martyniuk CJ, Feswick A, Spade DJ, Kroll KJ, Barber DS, Denslow ND (2010a) Effects of acute dieldrin exposure on neurotransmitters and global gene transcription in largemouth bass (*Micropterus salmoides*) hypothalamus. Neurotoxicol 31:356–366. DOI 10.1016/j.neuro.2010.04.008.

Martyniuk CJ, Kroll KJ, Doperalski NJ, Barber DS, Denslow ND (2010b) Genomic and proteomic responses to environmentally relevant exposures to dieldrin: Indicators of neurodegeneration? Toxicol Sci 117(1):190–199. DOI 10.1093/toxsci/kfq192.

McIlwain H (1959) Biochemistry and the central nervous system, 2nd edition. J & A Churchill, Ltd., London

Mennigen JA, Martyniuk CJ, Crump K, Xiong H, Zhao E, Popesku J, *et al*. (2008) Effects of fluoxetine on the reproductive axis of female goldfish (*Carassius auratus*). Physiol Genomics 35:273–282. DOI 10.1152/physiolgenomics.90263.2008.

Mercader JM, Lozano JJ, Sumoy L, Dierssen M, Visa J, Gratacòs M, *et al*., (2008) Hypothalamus transcriptome profile suggests an anorexia-cachexia syndrome in the *anx*/*anx* mouse model. Physiol Genomics 35:341–350. DOI 10.1152/physiolgenbomics.90255.2008.

Mickelsen LE, Kolling IV FW, Chimileski B, Norris CE, Nelson CE, Jackson AC. (2017) Neurochemical heterogeneity among lateral hypothalamic hypocretin/orexin and melanin-concentrating hormone neurons identified through single cell gene expression analysis. eNeuro. 4(5) e0013-17.2017 1–24. DOI 10.1523/ENEURO.0013-17.2017.

Middleton FA, Ramos EJB, Xu Y, Diab H, Zhao X, Das UN, *et al*., (2004) Application of genomic

technologies: DNA microarrays and metabolic profiling of obesity in the hypothalamus and in subcutaneous fat. Nutrition 20:14–25. DOI 10.1016/j.nut.2003.10.002.

Miller JA, Ding S-L, Sunkin SM, Smith KA, Ng L, Szafer A, *et al*. (2014) Transcriptional landscape of the prenatal human brain. Nature 508:199–206. DOI 10.1038/nature13185.

Mirabeau O, Joly J-S (2013) Molecular evolution of peptidergic signaling systems in bilaterians. Proc Natl Acad Sci USA 110(22):E2028–E2037. DOI 10.1073/pnas.1219956110.

Mishra A, Cheng C-H, Lee W-C, Tsai L-L (2009) Proteomic changes in the hypothalamus and retroperitoneal fat from male F344 rats subjected to repeated light-dark shifts. Proteomics 9:4017–4028. DOI 10.1002/pmc.200800813.

Mitchell JW, Atkins NA Jr, Sweedler JV, Gillette MU (2011) Direct cellular peptidomics of hypothalamic neurons. Front Neuroendocrinol 32(4):377–386. DOI 10.1016/j.yfrne.2011.02.005.

Mizuno TM, Mobbs CV (1999) Hypothalamic agouti-related protein messenger ribonucleic acid is inhibited by leptin and stimulated by fasting. Endocrinol 140:814–817. DOI 10.1210/endo.140.2.6491.

Mo B, Callegari, Telefont M, Renner KJ (2006) Proteomic analysis of the ventromedial nucleus of the hypothalamus (*pars lateralis*) in the female rat. Proteomics 6:6066–6074. DOI 10.1002/pmic.200600072.

Moore RY, Speh JC, Leak RK (2002) Suprachiasmatic nucleus organization. Cell Tiss Res 309:89–98. DOI 10.1007/s00441-002-0575-2.

Moulédous L, Hunt S, Harcourt R, Harry J, Williams KL, Gutstein HB (2002) Lack of compatibility of histological staining methods with proteomic analysis of laser-captured microdissected brain samples. J Biomol Tech 13:258–264.

Moulédous L, Hunt S, Harcourt R, Harry J, Williams KL, Gutstein HB (2003) Navigated laser capture microdissection as an alternative to direct histological staining for proteomic analysis of brain samples. Proteomics 3:610–615. DOI 10.1002/pmic.200300398.

Mountjoy KG, Mortrud MT, Low MJ, Simerly RB, Cone RD (1994) Localization of the melanocortin-4 receptor (MC4-R) in neuroendocrine and autonomic control circuits in the brain. Mol Endocrinol 8:1298–1308.

Mungall CJ, McMury JA, Köhler S, Balhoff JP, Borromeo C, Brush M, *et al.* (2017) The Monarch Initiative: An integrative data and analytics platform connecting phenotypes to genotypes across species. Nucleic Acids Res 45:D712–D722. DOI 10.1093/nar/gkw1128.

Mutsuga N, Gainer H (2006) Molecular analysis of the magnocellular neuroendocrine phenotype: From the micropunch to laser microdissection. Neurochem Res 31:189–199. DOI 10.1007/s11064-005-9008-4.

Mutsuga N, Shahar T, Verbalis JG, Brownstein MJ, Xiang CC, Bonner RF, *et al*., (2004) Selective gene expression in magnocellular neurons in rat supraoptic nucleus. J Neurosci 24(32):7174–7185. DOI 10.1523/JNEUROSCI.2022-04.2004.

Nadler JJ, Zou F, Huang H, Moy SS, Lauder J, Crawley JN, *et al*. (2006) Large-scale gene expression differences across brain regions and inbred strains correlate with a behavioral phenotype. Genetics 174:1229–1236. DOI 10.1534/genetics.106.061481.

Navarro JF, Sjöstrand J, Salmén F, Lundeberg J, Ståhl PL (2017) ST pipeline: An automated pipeline for spatial mapping of unique transcripts. Bioinformatics 33:2591–2593. DOI 10.1093/bioinformatics/btx211.

Nectow AR, Ekstrand MI, Friedman JM (2015) Molecular characterization of neuronal cell types based on patterns of projection with Retro-TRAP. Nat Protoc 10(9):1319–1327. DOI 10.1038/nprot.2015.087.

Nectow AR, Moya MV, Ekstrand MI, Mousa A, McGuire KL, Sferrazza CE, *et al*. (2017) Rapid molecular profiling of defined cell types using viral TRAP. Cell Rep 19(3):655–667. DOI 10.1016/j.celrep.2017.03.048.

Nedungadi TP, Carreño FR, Walch JD, Bathina CS, Cunningham JT (2011) Region-specific changes in transient receptor potential vanilloid channel expression in the vasopressin magnocellular system in hepatic cirrhosis-induced hyponatraemia. J Neuroendocrinol 24:642–652. DOI 10.1111/j.1365-2826.2011.02273.x.

Nedungadi TP, Cunningham JT (2014) Differential regulation of TRPC4 in the vasopressin magnocellular system by water deprivation and hepatic cirrhosis in the rat. Am J Physiol Regul Integr Comp Physiol 306(5):R304–R314. DOI 10.1152/ajpregu.00388.2013.

Nedungadi TP, Dutta M, Bathina CS, Caterina MJ, Cunningham JT (2012) Expression and distribution of TRPV2 in rat brain. Exp Neurol 237(1):223–237. DOI 10.1016/j.expneurol.2012.06.017.

Nernst W (1888) Zur Kinetik der in Lösung befindlichen Körper. I. Theorie der Diffusion. Zeitschrift für physikalische Chemie 2:613–637.

Nichols N, Perlmutter A, Mejino JLV Jr, Brinkley JF (2010) Representing neural connectivity in the foundational model of anatomy ontology. Proc. Annu. Symp. Am. Med. Inform. Assoc., Washington DC.

Nilaweera KN, Archer ZA, Campbell G, Mayer C-D, Balik A, Ross AW, *et al*. (2009) Photoperiod regulates genes encoding melanocortin 3 and serotonin receptors and secretogranins in the dorsomedial posterior arcuate of the Siberian hamster. J Neuroendocrinol 21:123–131. DOI 10.1111/j.1365-2826.2008.01810.x.

Nilsson A, Stroth N, Zhang X, Qi H, Fälth M, *et al*. (2012) Neuropeptidomics of mouse hypothalamus after imipramine treatment reveal somatostatin as a potential mediator of antidepressant effects. Neuropharmacol 62:347–357. DOI 10.1016/j.neuropharm.2011.08.004.

O'Farrell PH (1975) High resolution two-dimensional electrophoresis of proteins. J Biol Chem 250:4007–4021.

Okaty BW, Sugino K, Nelson SB (2011) A quantitative comparison of cell-type-specific microarray gene expression profiling methods in the mouse brain. PLoS One 6:e16493. DOI 10.1371/journal.pone.0016493.

Olszewski PK, Cedernaes J, Olsson F, Levine AS, Schiöth H (2008) Analysis of the network of feeding neuroregulators using the Allen Brain Atlas. Neurosci Biobehav Rev 32:945–956. DOI 10.1016/j.neubiorev.2008.01.007.

Orozco-Solís R, Matos RJB, Guzmán-Quevedo O, Lopes de Souza S, Bihouée A, Houlgatte R, *et al*. (2010) Nutritional programming in the rat is linked to long-lasting changes in nutrient sensing and energy homeostasis in the hypothalamus. PLoS One 5(10):e13537. DOI 10.1371/journal.pone.0013537.

Osborne NN (1974) Microchemical analysis of nervous tissue. Pergamon, Oxford.

Osumi-Sutherland D, Reeve S, Mungall CJ, Neuhaus F, Ruttenberg A, Jefferis GSXE, *et al.*, (2012) A strategy for building neuroanatomy ontologies. Bioinformatics 28:1262–1269. DOI 10.1093/bioinformatics/bts113.

Overton E (1902a) Beiträge zur allgemeinen Muskel- und Nervenphysiologie. I. Ueber die osmotischen Eigenschaften der Muskeln. Pflüger Arch 92:115–280.

Overton E (1902b) ——. II. Mittheilung. Ueber die Unentbehrlichkeit von Natrium- (oder Lithium-)Ionen für den Contractionsact des Muskels. Pflüger Arch 92:346–386.

Palkovits M (1973) Isolated removal of hypothalamic or other brain nuclei of the rat brain. Brain Res 59:449–450. DOI 10.1016/0006-8993(73)90290-4.

Palkovits M (1975) Isolated removal of hypothalamic nuclei for neuroendocrinological and neurochemical studies. In: Stumpf WE, Grant LD (eds) Anatomical Neuroendocrinology. Basel, Karger, pp 72–80.

Palkovits M (1986) Microdissection of individual brain nuclei and areas. Neuromethods 1:1–17. DOI: 10.1385/0-89603-075-x:1.

Palkovits M (1989) Microdissection in combination with biochemical microassays as a tool in tract tracing. In: Heimer L, Zaborszky L (eds) Neuroanatomical Tract-Tracing Methods 2. New York, Springer US, pp 299–310.

Palkovits M, Jacobowitz DM (1974) Topographic atlas of catecholamine and acetylcholinesterase-containing neurons in the rat brain. II. Hindbrain (Mesencephalon, Rhombencephalon). J Comp Neurol 157(1):29–42. DOI: 10.1002/cne.901570104.

Pan H, Che F-Y, Peng B, Steiner DF, Pintar JE, Fricker LD (2006) The role of prohormone convertase-2 in hypothalamic neuropeptide processing: A quantitative neuropeptidomic study. J Neurochem 98:1763–1777. DOI 10.1111/j.1471-4159.2006.04067.x.

Panda S, Antoch MP, Miller BH, Su AI, Schook AB, Straume M, *et al.* (2002) Coordinated transcription of key pathways in the mouse by the circadian clock. Cell 109:307–320. DOI 10.1016/S0092-8674(02)00722-5.

Park J, Zhu H, O'Sullivan S, Ogunnaike BA, Weaver DR, Schwaber JS, *et al*., (2016) Single-cell transcriptional analysis reveals novel neuronal phenotypes and interaction networks involved in the central circadian clock. Front Neurosci 10:481. DOI 10.3389/fnins.2016.00481.

Paternain L, Batlle MA, De La Garza AL, Milagro FI, Martínez JA, Campión J (2012) Transcriptomic and epigenetic changes in the hypothalamus are involved in an increased susceptibility to a high-fat-sucrose diet in prenatally stressed female rats. Neuroendocrinol 96:249–260. DOI 10.1159/000341684.

Paulsen SJ, Larsen LK, Jelsing J, Janßen U, Gerstmayer B, Vrang N (2009) Gene expression profiling of individual hypothalamic nuclei from single animals using laser capture microdissection and microarrays. J Neurosci Meth 177(1):87–93. DOI 10.1016/j.jneumeth.2008.09.024.

Pavlidis P, Noble WS (2001) Analysis of strain and regional variation in gene expression in mouse brain. Genome Biol 2(10):research0042.1–research0042.15.

Paxinos G, Franklin K (2012) The Mouse Brain in Stereotaxic Coordinates, 4th edition. San Diego, Academic Press.

Paxinos G, Watson C (2007) The Rat Brain in Stereotaxic Coordinates, 6th edition. Academic Press, Burlington.

Pederson T (2011) The Nucleolus. Cold Spring Harb Perspect Biol 3:a000638, DOI 10.1101/cshperspect.a000638.

Pedroso AP, Souza AP, Dornellas APS, Oyma LM, Nascimento CMO, Santos GMS, *et al*. (2017) Intrauterine growth restriction programs the hypothalamus of adult male rats: Integrated analysis of proteomic and metabolomics data. J Proteome Res 16:1515–1525. DOI 10.1021/acs.jproteome.6b00923.

Pedroso AP, Watanabe RLH, Albuquerque KT, Telles MM, Andrade MCC, Perez JD, *et al*. (2012) Proteomic profiling of the rat hypothalamus. Proteome Sci 10:26. DOI 10.1186/1477-5956-10-26.

Pembroke WG, Babbs A, Davies KE, Ponting CP, Oliver PL (2015) Temporal transcriptomics suggest that twin-peaking genes reset the clock. eLife 4:e10518. DOI 10.7554/eLife.10518.

Perez J, Fuentes O, Khan AM (2017) Towards automatic registration of histological data to canonical brain atlases. Program No. 604.05. 2017 Neuroscience Meeting Planner. Washington, DC: Society for Neuroscience, 2017. Online.

Perkel JM (2008) Neuropeptidomics study profiles hypothalamic "nucleus", individual cells. J Proteome Res 7:4610. DOI 10.1021/pr800672a.

Petyuk VA, Qian W-J, Chin MH, Wang H, Livesay EA, Monroe ME, *et al*. (2007) Spatial mapping of protein abundances in the mouse brain by voxelation integrated with high-throughput liquid chromatography-mass spectrometry. Genome Res 17:328–336. DOI 10.1101/gr.5799207.

Phillipps HR, Ladyman SR, Grattan DR (2013) Maintained expression of genes associated with metabolism in the ventromedial hypothalamic nucleus despite development of leptin resistance during pregnancy in the rat. Physiol Rep 1(6):e00162. DOI: 10.1002/phy2.162.

Pilgrim C (1974) Histochemical differentiation of hypothalamic areas. Prog Brain Res 41:97–110. DOI 10.1016/S0079-6123(08)61901-9.

Pomeranz LE, Ekstrand MI, Latcha KN, Smith GA, Enquist LW, Friedman JM (2017) Gene expression profiling with Cre-conditional pseudorabies virus reveals a subset of midbrain neurons that participate in reward circuitry. J Neurosci 37(15):4128-4144. DOI 10.1523/JNEUROSCI.3193-16.2017.

Popesku JT, Martyniuk CJ, Denslow ND, Trudeau VL (2010) Rapid dopaminergic modulation of the fish hypothalamic transcriptome and proteome. PLoS One 5(8):e12338. DOI 10.1371/journal.pone.0012338.

Poplawski MM, Mastaitis JW, Yang X-J, Mobbs CV (2010) Hypothalamic responses to fasting indicate metabolic reprogramming away from glycolysis toward lipid oxidation. Endocrinol 151(11):5206–5217. DOI 10.1210/en.2010-0702.

Porterfield VM, Mintz EM (2009) Temporal patterns of light-induced immediate-early gene expression in the suprachiasmatic nucleus. Neurosci Lett 463:70–73. DOI 10.1016/j.neulet.2009.07.066.

Porterfield VM, Piontkivska H, Mintz EM (2007) Identification of novel light-induced genes in the suprachiasmatic nucleus. BMC Neurosci 8:98. DOI 10.1186/1471-2202-8-98.

Poulin J-F, Tasic B, Hjerling-Leffler J, Trimarchi JM, Awatramani R (2016) Disentangling neural cell diversity using single-cell transcriptomics. Nat Neurosci 19(9):1131–1141. DOI 10.1038/nn.4366.

Qiu J, Hindmarch CCT, Yao ST, Tasker JG, Murphy D (2011) Transcriptomic analysis of the osmotic and reproductive remodeling of the female rat supraoptic nucleus. Endocrinol 152:3483–3491. DOI 10.1210/en.2011-1044.

Qiu F, Qu M, Zhang X, Wang H, Ding S (2018) Hypothalamus and pituitary transcriptome profiling of male and female Hong Kong grouper (*Epinephelus akaara*). Gene 656:73–79. DOI 10.1016/j.gene.2018.02.057.

Qiu J, Keineidam A, Gouraud S, Yao ST, Greenwood M, Hoe SZ, *et al*. (2014) The use of protein-DNA, chromatin immunoprecipitation, and transcriptome arrays to describe transcriptional circuits in the dehydrated male rat hypothalamus. Endocrinol 155:4380–4390. DOI 10.1210/en.2014-1448.

Rabaglino MB, Chang EI, Richards EM, James MO, Keller-Wood M, Wood CE (2016) Genomic effect of triclosan on the fetal hypothalamus: Evidence for altered neuropeptide regulation. Endocrinol 157:2686–2697. DOI 10.1210/en.2016-1080.

Replogle K, Arnold AP, Ball GF, Band M, Bensch S, Brenowitz EA, *et al*. (2008) The songbird neurogenomics (SoNG) initiative: community-based tools and strategies for study of brain gene function and evolution. BMC Genomics 9:131. DOI 10.1186/1471-2164-9-131.

Rabaglino MB, Richards E, Denslow N, Keller-Wood M, Wood CE (2012) Genomics of estradiol-3-sulfate action in the ovine fetal hypothalamus. Physiol Genomics 44:669–677. DOI 10.1152/physiolgenomics.00127.2011.

Richter CA, Martyniuk CJ, Annis ML, Brumbaugh WG, Chasar LC, Denslow ND, *et al.*, (2014) Methylmercury-induced changes in gene transcription associated with neuroendocrine disruption in largemouth bass (*Micropterus salmoides*). Gen Comp Endocrinol 201:215–224. DOI 10.1016/j.ygcen.2014.03.029.

Richter D (ed) (1957) Metabolism of the nervous system. Pergamon Press, New York.

Roberts E, Baxter CF (1963) Neurochemistry. Annu Rev Biochem 32:513–552. DOI 10.1146/annurev.bi.32.070163.002501.

Roberts S, Keller MR (1953) Respiration and glycolysis in the hypophysis and hypothalamus of the rat. Arch Biochem Biophys 44(1):9–14. DOI 10.1016/0003-9861(53)90003-4.

Roberts S, Keller MR (1955) Influence of epinephrine and cortisone on the metabolism of the hypophysis and hypothalamus of the rat. Endocrinol 57(1):64–69. DOI 10.1210/endo-57-1-64.

Romanov RA, Alpár A, Zhang M-D, Zeisel A, Calas A, Landry M, *et al.* (2014) A secretagogin locus of the mammalian hypothalamus controls stress hormone release. EMBO J e201488977. DOI 10.15252/embj.201488977.

Romanov RA, Zeisel A, Bakker J, Girach F, Hellysaz A, Tomer R, *et al*. (2017) Molecular interrogation of hypothalamic organization reveals distinct dopamine neuronal subtypes. Nat Neurosci 20(2):176–188. DOI 10.1038/nn.4462.

Romanova EV, Sweedler JV (2015) Peptidomics for the discovery and characterization of neuropeptides and hormones. Trends Pharmacol Sci 36(9):579–586. DOI 10.1016/j.tips.2015.05.009.

Römpp A, Guenther S, Schober Y, Schulz O, Takats Z, Kummer W, *et al.*, (2010) Histology by mass spectrometry: Label-free tissue characterization obtained from high-accuracy bioanalytical imaging. Angew Chem Int Ed 49:3834–3838. DOI 10.1002/anie.20095559.

Roots BI, Johnston PV (1965) Lipids of isolated neurons. Biochem J 94:61–63.

Ropp SA, Grunwald WC Jr, Morris M, Cool DR (2008) Pyridostigmine crosses the blood-brain barrier to induce cholinergic and non-cholinergic changes in mouse hypothalamus. J Med CBR Def 6.

Rose SPR (1999) Holger Hyden and the biochemistry of memory. Brain Res Bull 50(5/6):443. DOI 10.1016/S0361-9230(99)00125-2.

Rossner MJ, Hirrlinger J, Wichert SP, Boehm C, Newrzella D, Hiemisch H, *et al*. (2006) Global transcriptome analysis of genetically identified neurons in the adult cortex. J Neurosci 26:9956–9966. DOI 10.1523/JNEUROSCI.0468-06.2006.

Roth CL, McCormack AL, Lomniczi A, Mungenast AE, Ojeda SR (2006) Quantitative proteomics identifies a change in glial glutamate metabolism at the time of puberty. Mol Cell Endocrinol 254–255: 51–59. DOI 10.1016/j.mce.2006.04.017.

Roy M, Kim N, Kim K, Chung W-H, Achawanantakun R, Sun Y, *et al.*, (2013) Analysis of the canine brain transcriptome with an emphasis on the hypothalamus and cerebral cortex. Mamm Genome 24:484–499. DOI 10.1007/s00335-013-9480-0.

Russ T, Ramakrishnan C, Hovy E, Bota M, Burns G (2011) Knowledge engineering tools for reasoning with scientific observations and interpretations: A neural connectivity use case. BMC Bioinformatics 12, 351. DOI 10.1186/1471-2105-12-351.

Sakakibara M, Uenoyama Y, Minabe S, Watanabe Y, Deura C, Nakamura S, *et al.*, (2013) Microarray analysis of perinatal-estrogen-induced changes in gene expression related to brain sexual differentiation in mice. PLoS One 8(11):e79437. DOI 10.1371/journal.pone.0079437.

Sandberg R, Yasuda R, Pankratz DG, Carter TA, Del Rio JA, Wodicka L, *et al*. (2000) Regional and strain-specific gene expression mapping in the adult mouse brain. Proc Natl Acad Sci USA 97(20):11038–11043. DOI 10.1073/pnas.97.20.11038.

Sanna PP, King AR, van der Stap LD, Repunte-Canoningo V (2005) Gene profiling of laser-microdissected brain regions and sub-regions. Brain Res Protoc 15:66–74. DOI 10.1016/j.brainresprot.2005.04.002.

Sarkar P, Sarkar S, Ramesh V, Kim H, Barnes S, Kulkarni A, *et al*. (2008) Proteomic analysis of mouse hypothalamus under simulated microgravity. Neurochem Res 33:2335–2341. DOI 10.1007/s11064-008-9738-1.

Sawyer CH, Everett JW, Green JD (1954) The rabbit diencephalon in stereotaxic coordinates. J Comp Neurol 101(3):801–824.

Schmidlin T, Boender AJ, Frese CK, Heck AJR, Adan RAH, Altelaar AFM (2015) Diet-induced neuropeptide expression: Feasibility of quantifying extended and highly charged endogenous peptide sequences by selected reaction monitoring. Anal Chem 87:9966–9973. DOI 10.1021/acs.analchem.5b03334.

Schrader M, Schulz-Knappe P, Fricker LD (2014) Historical perspective of peptidomics. EuPA Open Proteomics 3:171–182. DOI 10.1016/j.euprot.2014.02.014.

Schwartz S, Reyzer ML, Caprioli RM (2003) Direct tissue analysis using matrix-assisted laser desorption/ionization mass spectrometry: Practical aspects of sample preparation. J Mass Spectrom 38:699–708. DOI 10.1002/jms.505.

Schwiening CJ (2012) A brief historical perspective: Hodgkin and Huxley. J Physiol (Lond) 590:2571–2575.

Secher A, Kelstrup CD, Conde-Frieboes KW, Pyke C, Raun K, Wulff BS, *et al.*, (2016) Analytic framework for peptidomics applied to large-scale neuropeptide identification. Nat Commun 7:11436. DOI 10.1038/ncomms11436.

Segal JP, Stallings NR, Lee CE, Zhao L, Socci N, Viale A, *et al*. (2005) Use of laser-capture microdissection for the identification of marker genes for the ventromedial hypothalamic nucleus. J Neurosci 25(16):4181–4188. DOI 10.1523/JNEUROSCI.0158-05.2005.

Shariatgorji M, Nilsson A, Goodwin RJA, Källback P, Schintu N, Zhang X, *et al*. (2014a) Direct targeted quantitative molecular imaging of neurotransmitters in brain tissue sections. Neuron 84:697–707. DOI 10.1016/j.neuron.2014.10.011.

Shariatgorji M, Svenningsson P, Andrén P (2014b) Mass spectrometry imaging, an emerging technology in neuropsychopharmacology. Neuropsychopharmacol Rev 39:34–49. DOI 10.1038/npp.2013.215.

Sharma K, Schmitt S, Bergner CG, Tyanova S, Kannaiyan N, Manrique-Hoyos N, *et al*. (2015) Cell type- and brain region-resolved mouse brain proteome. Nat Neurosci 18:1819–1831. DOI 10.1038/nn.4160.

Simmons DM, Swanson LW. (2009) Comparing histological data from different brains: Sources of error and strategies for minimizing them. Brain Res Rev 60(2):349–367. DOI 10.1016/j.brainresrev.2009.02.002.

Sköld K, Svensson M, Kaplan A, Björkesten L, Åström J, Andren PE (2002) A neuroproteomic approach to targeting neuropeptides in the brain. Proteomics 2:447–454. DOI 10.1002/1615-9861(200204)2:4<447::AID-PROT447>3.0.CO;2-A.

Sköld K, Svensson M, Norrman M, Sjögren B, Svenningsson P, Andrén PE (2007) The significance of biochemical and molecular sample integrity in brain proteomics and peptidomics: Stathmin 2-2- and peptides as sample quality indicators. Proteomics 7:4445–4456. DOI 10.1002/pmic.200700142.

Skynner HA, Amos DP, Murray F, Salim K, Knowles MR, *et al*. (2006) Proteomic analysis identifies alterations in cellular morphology and cell death pathways in mouse brain after chronic corticosterone treatment. Brain Res 1102:12–26. DOI 10.1016/j.brainres.2006.04.112.

Smithies O, Poulik MD (1956) Two-dimensional electrophoresis of serum proteins. Nature 177(4518):1033. DOI: 10.1038/1771033a0.

Soga T, Dalpatadu SL, Wong DW, Parhar IS (2012) Neonatal dexamethasone exposure down-regulates GnRH expression through the GnIH pathway in female mice. Neurosci 218:56–64. DOI 10.1016/j.neuroscience.2012.05.023.

Sotelo C, Palay SL (1968) The fine structure of the lateral vestibular nucleus in the rat. I. Neurons and neuroglial cells. J Cell Biol 36:151–179. DOI 10.1083/jcb.36.1.151.

Soukup J, Krskova L, Hilska I, Kodet R (2003) Ethanol fixation of lymphoma samples as an alternative approach for preservation of the nucleic acids. Neoplasma 50: 300–304.

Southey BR, Lee JE, Zamdborg L, Atkins N Jr, Mitchell JW, Li M, *et al*. (2013) Comparing label-free quantitative peptidomics approaches to characterize diurnal variation of peptides in the rat suprachiasmatic nucleus. Anal Chem 86:443–452. DOI 10.1021/ac40233781.

Spengler B, Hubert M, Kaufmann R (1994) MALDI ion imaging and biological ion imaging with a new scanning UV-laser microprobe. 42nd Annual Conference on Mass Spectrometry and Allied Topics, ASMS 1994, May 29–Jun 3, Chicago, Illinois.

Spraggins JM, Rizzo DG, Moore JL, Noto MJ, Skaar EP, Caprioli RM (2016) Next-generation technologies for spatial proteomics: Integrating ultra-high speed MALDI-TOF and high mass resolution MALDI FTICR imaging mass spectrometry for protein analysis. Proteomics 16(11–12):1678–1689. DOI 10.1002/pmic.201600003.

Ståhl PL, Salmén F, Vickovic S, Lundmark A, Navarro JF, Magnusson J, *et al*. (2016) Visualization and analysis of gene expression in tissue sections by spatial transcriptomics. Science 353:78–82. DOI 10.1126/science.aaf2403.

St.-Amand J, Yoshioka M, Tanaka K, Nishida Y (2012) Transcriptome-wide identification of preferentially expressed genes in the hypothalamus and pituitary gland. Front Endocrinol 2: Article 111. DOI 10.3389/fendo.2011.00111.

Stelzhammer V, Amess B, Martins-de-Souza D, Levin Y, Ozanne SE, Martin-Gronert MS, *et al*. (2012) Analysis of the rat hypothalamus proteome by data-independent label-free LC-MS/MS. Proteomics 12:3386–3392. DOI 10.1002/pmic.201100642.

Stewart L, Hindmarch CCT, Qiu J, Tung Y-C L, Yeo GSH, Murphy D (2011) Hypothalamic transcriptome plasticity in two rodent species reveals divergent differential gene expression but conserved pathways. J Neuroendocrinol 23:177–185. DOI 10.1111/j.1365-2826.2010.02093.x.

Stocker CJ, Wargent ET, Martin-Gronert MS, Cripps RL, O'Dowd JF, Zaibi MS, *et al*. (2012) Leanness in postnatally nutritionally programmed rats is associated with increased sensitivity to leptin and a melanocortin receptor agonist and decreased sensitivity to neuropeptide Y. Int J Obes (Lond) 36(8):1040–1046. DOI 10.1038/ijo.2011.226.

Su JM, Perlaky L, Li XN, Leung HC, Antalffy B, Armstrong D, *et al.*, (2004) Comparison of ethanol versus formalin fixation on preservation of histology and RNA in laser capture microdissected brain tissues. Brain Pathol 14:175–182. DOI 10.1111/j.1750-3639.2004.tb00050.x.

Sun H, Jiang R, Xu S, Zhang Z, Xu G, *et al*. (2015) Transcriptome responses to heat stress in hypothalamus of a meat-type chicken. J Anim Sci Biotechnol 6:6. DOI 10.1186/s40104-015-0003-6.

Sun W, Lee S, Zhabotynsky V, Zou F, Wright FA, Crowley JJ, *et al*. (2012) Transcriptome atlases of mouse brain reveals differential expression across brain regions and genetic backgrounds. Genes, Genomes, Genetics 2:203–211. DOI 10.1534/g3.111.001602.

Sunkin SM, Ng L, Lau C, Dolbeare T, Gilbert TL, Thompson CL, *et al.*, (2013) Allen Brain Atlas: An integrated spatio-temporal portal for exploring the central nervous system. Nucleic Acids Res 41:D996–D1008. DOI 10.1093/nar/gks1042.

Sutcliffe JG, de Lecea L (2002) The hypocretins: Setting the arousal threshold. Nat Rev Neurosci 3:339–349. DOI 10.1038/nrn808.

Svensson M, Sköld K, Svenningsson P, Andren PE (2003) Peptidomics-based discovery of novel neuropeptides. J Proteome Res 2:213–219. DOI 10.1021/pr020010u.

Swanson LW (2004) Brain Maps: Structure of the Rat Brain, 3rd edition. Amsterdam, Elsevier.

Swanson LW (2007) Quest for the basic plan of nervous system circuitry. Brain Res Rev 55(2):356–372. DOI 10.1016/j.brainresrev.2006.12.006.

Swanson LW (2018) Brain Maps 4.0 – Structure of the Rat Brain: An open access atlas with global nervous system nomenclature ontology and flatmaps. J Comp Neurol 526(6):935–943. DOI: 10.1002/cne.24381.

Swanson LW, Sanchez-Watts G, Watts AG (2005) Comparison of melanin-concentrating hormone and hypocretin/orexin mRNA expression patterns in a new parceling scheme of the lateral hypothalamic zone. Neurosci Lett 387(2):80–84. DOI 10.1016/j.neulet.2005.06.066.

Swart I, Jahng JW, Overton JM, Houpt TA (2002) Hypothalamic NPY, AGRP, and POMC mRNA responses to leptin and refeeding in mice. Am J Physiol Regul Integr Comp Physiol 283:R1020–R1026. DOI 10.1152/ajpregu.00501.2001.

Tallis M, Thompson R, Russ TA, Burns GAPC (2011) Knowledge synthesis with maps of neural connectivity. Front Neuroinform 5, 24. DOI 10.3389/fninf.2011.00024.

Taouis M (2016) MicroRNAs in the hypothalamus. Best Pract Res Clin Endocrinol Metab 30:641–651. DOI 10.1016/j.beem.2016.11.006.

Taraslia VK, Kouskoukis A, Anagnostopoulos AK, Stravopodis DJ, Margaritis LH, Tsangaris G Th (2013) Proteomic analysis of normal murine brain parts. Cancer Genom Proteom 10:125–154.

Tatemoto K, Carlquist M, Mutt V (1982) Neuropeptide Y – a novel brain peptide with structural similarities to peptide YY and pancreatic polypeptide. Nature 296:659–660. DOI 10.1038/296659a0.

Tatemoto K, Mutt V (1980) Isolation of two novel candidate hormones using a chemical method for finding naturally occurring polypeptides. Nature 285:417–418. DOI 10.1038/285417a0.

Tatemoto K, Rökaeus Å, Jörnvall H, McDonald TJ, Mutt V (1983) Galanin – a novel biologically active peptide from porcine intestine. FEBS Lett 164:124–128. DOI 10.1016/0014-5793(83)80033-7.

Ten Donkelaar HJ, Nicholson C (1998) Appendix – (Stereotaxic) Atlases. A bibliography of (stereotaxic) brain atlases arranged by chapter, In: Nieuwenhuys R, Ten Donkelaar HJ, Nicholson C (eds) The Central Nervous System of Vertebrates, Volume 1. Springer, Berlin, pp. 354–355.

Thudicum JLW (1884) A treatise on the chemical constitution of the brain. Baillière, Tindall, and Cox, London.

Tindal JS (1965) The forebrain of the guinea pig in stereotaxic coordinates. J Comp Neurol 124(2):259–266.

Trivedi C, Shan X, Tung YC, Kabra D, Holland J, Amburgy S, *et al*. (2015) Tachykinin-1 in the central nervous system regulates adiposity in rodents. Endocrinol 156(5):1714–1723. DOI 10.1210/en.2014-1781.

Tu W-L, Cheng C-Y, Wang S-H, Tang P-C, Chen C-F, Chen H-H, *et al.*, (2016) Profiling of differential gene expression in the hypothalamus of broiler-type Taiwan country chickens in response to acute heat stress. Theriogenol 85:483–494. DOI 10.1016/j.theriogenology.2015.09.028.

Tung YC, Ma M, Piper S, Coll A, O'Rahilly S, Yeo GS (2008) Novel leptin-regulated genes revealed by transcriptional profiling of the hypothalamic paraventricular nucleus. J Neurosci 28: 12419–12426. DOI 10.1523/JNEUROSCI.3412-08.2008.

Uz T, Arslan AD, Kurtuncu M, Imbesi M, Akhisaroglu M, Dwivedi Y, *et al*. (2005) The regional and cellular expression profile of the melatonin receptor MT1 in the central dopaminergic system. Mol Brain Res 136:45–53. DOI 10.1016/j.molbrainres.2005.01.002.

van de Plas R, Yang J, Spraggins J, Caprioli RM (2015) Image fusion of mass spectrometry and microscopy: A multimodality paradigm for molecular tissue mapping. Nat Meth 12:366–374. DOI 10.1038/nmeth.3296.

van Tienhoven A, Juhász LP (1962) The chicken telencephalon, diencephalon and mesencephalon in stereotaxic coordinates. J Comp Neurol 118(2):185–197. DOI 10.1002/cne.901180205.

Vasilache AM, Anderson J, Nilsberth C (2007) Expression of PGE_2 EP_3 receptor subtypes in the mouse preoptic region. Neurosci Lett 423:179–183. DOI 10.1016/j.neulet.2007.06.048.

Vasilache AM, Kugelberg U, Blomqvist A, Nilsberth C (2013) Minor changes in gene expression in the mouse preoptic hypothalamic region by inflammation-induced prostaglandin E_2. J Neuroendocrinol 25:635–643. DOI 10.1111/jne.12044.

Volgin DV, Swan J, Kubin L (2004) Single-cell RT-PCR gene expression profiling of acutely dissociated and immunocytochemically identified central neurons. J Neurosci Meth 136:229–236. DOI 10.1016/j.jneumeth.2004.01.013.

Wada M, Urano A, Gorbman A (1980) A stereotaxic atlas for diencephalic nuclei of the frog, *Rana pipiens*. Arch Histol Jpn 43(2):157–173.

Walch JD, Nedungadi TP, Cunningham JT (2014) ANG II receptor subtype 1a gene knockdown in the subfornical organ prevents increased drinking behavior in bile duct-ligated rats. Am J Physiol Regul Integr Comp Physiol 307:R597–R607. DOI 10.1152/ajpregu.00163.2014.

Waller R, Woodroofe MN, Francese S, Heath PR, Wharton SB, Ince PG, *et al*. (2012) Isolation of enriched glial populations from post-mortem human CNS material by immuno-laser capture microdissection. J Neurosci Meth 208:108–113. DOI 10.1016/j.jneumeth.2012.04.014.

Wang S-S, Kamphius W, Huitinga I, Zhou J-N, Swaab DF (2008) Gene expression analysis in the human hypothalamus in depression by laser microdissection and real-time PCR: the presence of multiple receptor imbalances. Mol Psychiatr 13:786–799. DOI 10.1038/mp.2008.38.

Wang Q-m, Yang H, Tian D-r, Cai Y, Wei Z-n, *et al*., (2011) Proteomic analysis of rat hypothalamus revealed the role of ubiquitin-proteasome system in the genesis of DR or DIO. Neurochem Res 36:939–946. DOI 10.1007/s11064-011-0423-4.

Warburg O, Negelein E, Posener K. (1924) Versuche an Überlebendem carcinomgewebe. Klinische Wochenschrift 3(24):1062–1064.

Wells CE, Khan AM (2013) Data transformations between rat brain atlases: Mapping central microinjection sites on stereotaxically aligned and anisotropically scaled digital atlas plates in Paxinos & Watson and Swanson reference spaces. Program No. 198.06. 2013 Neuroscience Meeting Planner. San Diego, CA: Society for Neuroscience, 2013. Online.

Williams DL, Schwartz MW, Bastian LS, Blevins JE, Baskin DG (2008) Immunocytochemistry and laser capture microdissection for real-time quantitative PCR identify hindbrain neurons activated by interaction between leptin and cholecystokinin. J Histochem Cytochem 56(3):285–293. DOI 10.1369/jhc.7A7331.2007.

Williams KW, Margatho LO, Lee CE, Choi M, Lee S, Scott MM, *et al*., (2010). Segregation of acute leptin and insulin effects in distinct populations of arcuate proopiomelanocortin neurons. J Neurosci 30(7):2472–2479. DOI 10.1523/JNEUROSCI.3118-09.2010.

Winden KD, Oldham MC, Mirnics K, Ebert PJ, Swan CH, Levitt P, *et al*. (2009) The organization of the transcriptional network in specific neuronal classes. Mol Syst Biol 5:291. DOI 10.1038/msb.2009.46.

Winrow CJ, Tanis KQ, Rigby AM, Taylor RR, Serikawa K, Tokiwa GY, *et al*. (2009) Refined anatomical isolation of functional sleep circuits exhibits distinctive regional and circadian gene transcriptional profiles. Brain Res 1271:1–17. DOI 10.1016/j.brainres.2009.02.083.

Wiśniewski JR, Zougman A, Nagaraj N, Mann M (2009) Universal sample preparation method for proteome analysis. Nat Methods 6(5):359–362. DOI 10.1038/nmeth.1322.

Wolf L, Goldberg C, Manor N, Sharan R, Ruppin E (2011) Gene expression in the rodent brain is associated with its regional connectivity. PLoS Comput Biol 7(5):e1002040. DOI 10.1371/journal.pcbi.1002040.

Wong MH, Saam JR, Stappenbeck TS, Rexer CH, Gordon JI (2000) Genetic mosaic analysis based on Cre recombinase and navigated laser capture microdissection. Proc Natl Acad Sci USA 97(23):12601–12606. DOI 10.1073/pnas.230237997.

Wood CE, Rabaglino MB, Chang EI, Denslow N, Keller-Wood M, Richards E (2013) Genomics of the fetal hypothalamic cellular response to transient hypoxia: Endocrine, immune, and metabolic responses. Physiol Genomics 45:521–527. DOI 10.1152/physiolgenomics.00005.2013.

Xi D, Kusano K, Gainer H (1999) Quantitative analysis of oxytocin and vasopressin messenger ribonucleic acids in single magnocellular neurons isolated from supraoptic nucleus of rat hypothalamus. Endocrinol 140:4677–4682. DOI 10.1210/endo.140.10.7054.

Xu J, Huang W, Zhong C, Luo D, Li S, Zhu Z, *et al.*, (2011) Defining global gene expression changes of the hypothalamic-pituitary-gonadal axis in female sGnRH-antisense transgenic common carp (*Cyprinus carpio*). PLoS One 6(6):e21057. DOI 10.1371/journal.pone.0021057.

Xu R-y, Wan Y-p, Tang Q-y, Wu J, Cai W (2008) The effects of high fat on central appetite genes in Wistar rats: A microarray analysis. Clin Chim Acta 397:96–100. DOI 10.1016/j.cca.2008.07.027.

Xu C, Houck JR, Fan W, Wang P, Chen Y, Upton M, *et al*. (2008) Simultaneous isolation of DNA and RNA from the same cell population obtained by laser capture microdissection for genome and transcriptome profiling. J Mol Diag 10:129–134. DOI 10.2353/jmoldx.2008.070131.

Yamashita M, Glasgow E, Zhang BJ, Kusano K, Gainer H (2002) Identification of cell-specific messenger ribonucleic acids in oxytocinergic and vasopressinergic magnocellular neurons in rat supraoptic nucleus by single-cell differential hybridization. Endocrinol 143:4464–4476. DOI 10.1210/en.2002-220516.

Yao I, Sugiura Y, Matsumoto M, Setou M (2008) *In situ* proteomics with imaging mass spectrometry and principal component analysis in the *Scrapper*-knockout mouse brain. Proteomics 8:3692–3701. DOI 10.1002/pmic.200701121.

Yao ST, Gouraud S, Paton JF, Murphy D (2005) Water deprivation increases the expression of neuronal nitric oxide synthase (nNOS) but not orexin-A in the lateral hypothalamic area of the rat. J Comp Neurol 490:180–193. DOI 10.1002/cne.20662.

Yasuda M, Lepkovsky S (1969) The chicken diencephalon in stereotaxic coordinates. Jap J Zootech Sci 40(10):417–431.

Yelin-Bekerman L, Elbaz I, Diber A, Dahary D, Gibbs-Bar L, Alon S *et al*. (2015) Hypocretin neuron-specific transcriptome profiling identifies the sleep modulator Kcnh4a. Elife 4:e08638. DOI 10.7554/eLife.08638.

Yonehara K, Suzuki M, Nishihara M (2002) Sex-related differences in gene expression in neonatal rat hypothalamus assessed by cDNA microarray analysis. Endocr J 49(2):131–137. DOI 10.1507/endocrj.49.131.

Yue C, Mutsuga N, Verbalis J, Gainer H (2006) Microarray analysis of gene expression in the supraoptic nucleus of normoosmotic and hypoosmotic rats. Cell Mol Neurobiol 26(4–6):959–978. DOI 10.1007/s10571-006-9017-0.

Zapala MA, Hovatta I, Ellison JA, Wodicka L, Del Rio JA, Tennant R, *et al*. (2005) Adult mouse brain gene expression patterns bear an embryologic imprint. Proc Natl Acad Sci USA 102(29):10357–10362. DOI 10.1073/pnas.0503357102.

Zettergren A, Karlsson S, Studer E, Sarvimäki A, Kettunen P, Thorsell A, *et al*. (2017) Proteomic analyses of limbic regions in neonatal male, female and androgen receptor knockout mice. BMC Neurosci 18:9. DOI 10.1186/s12868-016-0332-1.

Zhang D, Xiong H, Mennigen JA, Popesku JT, Marlatt VL, Martyniuk CJ, *et al*. (2009) Defining global neuroendocrine gene expression patterns associated with reproductive seasonality in fish. PLoS ONE 4(6):e5816. DOI 10.1371/journal.pone.005816.

Zhang L, Cai Z, Wei S, Zhou H, Zhou H, Jiang X, *et al*., (2013) MicroRNA expression profiling of the porcine developing hypothalamus and pituitary tissue. Int J Mol Sci 14(10):20326–20339. DOI 10.3390/ijms141020326.

Zhang X, Petruzziello F, Zani F, Fouillen L, Andren PE, Solinas G, *et al.*, (2012) High identification rates of endogenous neuropeptides from mouse brain. J Proteome Res 11:2819–2827. DOI 10.1021/pr3001699.

Zhong L, Zhou J, Wang D, Zou X, Lou Y, Liu D, *et al*. (2015) Proteomics and bioinformatics analysis of mouse hypothalamic neurogenesis with or without EPHX2 gene deletion. Int J Clin Exp Pathol 8:12634–12645. PMCID: PMC4680398.

Zhu H, Vadigepalli R, Rafferty R, Gonye GE, Weaver DR, Schwaber JS (2012) Integrative gene regulatory network analysis reveals light-induced regional gene expression phase shift programs in the mouse suprachiasmatic nucleus. PLoS One 7(5):e37833. DOI:10.1371/journal.pone.0037833.

Zmora N, Stubblefield J, Zulperi Z, Biran J, Levavi-Sivan B, Muñoz-Cueto JA, *et al.*, (2012) Differential and gonad stage-dependent roles of kisspeptin1 and kisspeptin2 in reproduction in the modern teleosts, *Morone* species. Biol Reprod 86(6):177. DOI 10.1095/biolreprod.111.097667.

Zséli G, Vida B, Martinez A, Lechan RM, Khan AM, Fekete C (2016) Elucidation of the anatomy of a satiety network: Focus on connectivity of the parabrachial nucleus in the adult rat. J Comp Neurol 524(14):2803–2827. DOI 10.1002/cne.23992.

Table 1. Transcriptomic studies in whole hypothalamus and by hypothalamic sub-region

Study	Animal	Extraction	Target(s) *a priori*?	Screen [S], Validation [V]	Map or Schematic	Major findings
Whole hypothalamus						
Gautvik et al., 1996	Rt	dissection	N	subtractive hybridization [S]; Southern and Northern blots; ISH [V]	N	Pioneering transcriptomic study of the hypothalamus; identified 53 hypothalamus-specific mRNAs
Akhtar et al., 2002	Ms	dissection	N	µ-array [S] ISH [V]	N	Liver possesses cycling transcripts that are also in SCH but which do not cycle rhythmically there; Liver cycling dependent on intact SCH
Li et al., 2002	Rt	dissection	N	µ-array [S] Northern [V]	N	Fasting induced 96 mRNAs, and down-regulated 73 mRNAs
Yonehara et al., 2002	Rt	dissection	N	µ-array [S] RT-PCR [V]	N	12 genes display 2-fold greater increase in male vs. female neonates; 20 genes w 2-fold increase in female vs. male neonates
Mutsuga et al., 2004	Rt	dissection	N	µ-array [S] ISH [V]	N	Found 1,385 genes expressed in SO at levels two times greater than in the hypothalamus as a whole
Lachuer et al., 2005	Ms	dissection	N	µ-array [S] qRT-PCR [V]	N	Found NPY mRNA and AgRP mRNA to be downregulated in *anx*/*anx* mice relative to wild-type mice
Shiue et al., 2006	Ck	dissection	N	qRT-PCR	N	16 mRNAs in high egg-yielding strain
Chen L-R et al., 2007	Ck	dissection	N	qRT-PCR	N	25 egg production-related mRNAs
Conti et al., 2007	Rt	dissection	N	µ-array	schematic	294/269 mRNAs up/down-reg to fluoxetine treatment
Kurrasch, Cheung, et al. 2007	Ms, Fs	dissection	N	µ-array [S] ISH, qPCR [V]	Ms: N, but photos; Fs: schematic , photos	Identified 200 genes enriched in neonatal VMH tissue; knockdown of some in zebrafish impairs development
Mennigen et al., 2008	Fs	NS	N	µ-array	N	17 mRNAs induced, 70 mRNAs down-regulated by fluoxetine
Mercader et al., 2008	Ms	dissection	N	µ-array	N	In *anx*/*anx* mice, 141 mRNAs induced, 14 down-reg, relative to wild-type
Xu et al., 2008	Rt	dissection	N	µ-array	N	27 mRNAs affected by high-fat diet: 14 induced, 13 down-regulated
Zhang et al., 2009	Fs	NS	N	µ-array	N	873 genes differentially expressed among May, Aug, Dec
Byerly et al., 2010	Ck	dissection	N	µ-array [S] qRT-PCR [V]	N	Found differential expression of six genes in fat vs lean chickens involved in body fat control, and nine genes involved in glucose metabolism and glucose sensing
Ding et al., 2010	Ms	dissection	N	µ-array	N	Several genes differentially expressed after neonatal deprivation relative to adults
Higgins et al., 2010	Ck	dissection	N	µ-array	N	119 genes differentially expressed after fasting

Martyniuk et al., 2010a	Fs	dissection	N	μ-array	N	227 mRNAs differentially expressed after acute dieldrin exposure
Martyniuk et al., 2010b	Fs	dissection	N	μ-array	N	3,135 mRNAs differentially expressed after chronic dieldrin exposure
Orozco-Solís et al., 2010	Rt	NS	N	μ-array	N	997 genes associated with nutritional deficiency during development
Popesku et al., 2010	Fs	dissection	N	μ-array	N	3,088 ESTs were differentially regulated by dopamine receptor agonists
Poplawski et al., 2010	Ms	NS	N	qRT-PCR	N	48-h fast shifts metabolism from glucose to lipid metabolism
Xu et al., 2011	Fs	dissection	N	μ-array	N	Nine genes differentially expressed
Zmora et al., 2012	Fs	LCM	Y	qRT-PCR	N	Identified two kisspeptin systems
Chadwick et al., 2012	Rt	dissection	N	μ-array	N	GIT2 as aging-related molecule
Gonzáles et al., 2012	Rt	dissection	N	qRT-PCR	N	Neuropeptide S and NPS-R both modulated by hyperthyroidism
Knight et al., 2012	Ms	dissection	Y	qRT-PCR, RNA-Seq, μ-array, IHC	N	Found various actively translating mRNAs in rats to be upregulated, under various stimuli conditions
Paternain et al., 2012	Rt	dissection	N	qRT-PCR	N	A high fat/sucrose diet decreased expression of *Slc6a3*, *Npy*, and insulin receptor, and increased *Pomc* expression
Rabaglino et al., 2012	Sh	dissection	N	μ-array [S] qRT-PCR [V]	N	Estradiol-3-sulfate exposure altered fetal hypothalamic transcripts (Npy, AgRP, especially)
St. Amand et al., 2012	Ms	dissection	N	SAGE [S] qRT-PCR [V]		Found six unclassified and three novel transcripts enriched in hypothalamus
Farajzadeh et al., 2013	Pg	dissection	N	RNA-Seq	N	Transcriptional start site analysis revealed a proportionally greater number of sites for the hypothalamus relative to other regions sampled
Martyniuk et al., 2013	Fs	dissection	N	μ-array	N	Sexually dimorphic response to dieldrin
Roy et al., 2013	Dg	dissection	N	RNA-Seq	N	Found significant differences in alternatively spliced genes in hypothalamus as compared to cerebral cortex
Sakakibara et al., 2013	Ms	dissection	N	μ-array [S] RT-PCR [V]	N	Found >100 genes downregulated by estradiol benzoate treatment underwent biphasic elevations in expression; validated a small subset of these genes by RT-PCR, including *Hcrt* and *Ptgds* (which encodes prostaglandin D2)
Wood et al., 2013	Sh	dissection	N	μ-array [S] qRT-PCR [V]	N	Fetal hypoxia triggered changes in gene expression associated with reduced metabolism, mobilization of the immune and neuroendocrine response.
Zhang et al., 2013	Pg	NS	N	μ-array [S] qRT-PCR [V]	N	Found 175 unique micro RNAs including 39 novel ones, in the hypothalamus

Balakrishnan et al., 2014	Sp	NS	N	RNA-Seq [S] CZE [V]	N	Found transcripts with BLAST hits to 16,646 genes (93% of Ensembl annotated genes)
Fang et al., 2014	Ck	dissection	N	μ-array	N	Fasting up-regulated NPY and AgRP transcripts and those associated with fatty acid oxidation; and downregulated POMC, GHRH and other transcripts associated with fatty acid synthesis/transport
Luan et al, 2014	Gs	dissection	N	subtractive hybridization [S]; qRT-PCR [V]	N	Found 46 up-regulated and 49 down-regulated expressed sequence tags showing homology to known genes; identified GnRH-related regulatory genes to be expressed differentially during and after egg laying
Richter et al., 2014	Fs	dissection	N	μ-array	N	Methylmercury exposure triggers large-scale gene expression
Fortes et al., 2015	Cw	dissection	N	RNA-Seq	N	Identified 978 genes expressed in hypothalamus
Gao et al., 2015	Gs	NS	N	Illumina MiSeq [S] RT-PCR [V]	N	Found 48 hypothalamic transcripts up-regulated in the pre-egg laying period and 180 upregulated during the laying period; fund a few transcripts differentially expressed between the two periods
Sun et al., 2015	Ck	dissection	N	μ-array [S] qRT-PCR [V]	N	Found heat shock proteins significantly altered in expression in response to thermal stress; identified 11 genes by qRT-PCR that were consistently expressed across samples, and 38 differentially expressing genes encoding growth-related functions and enzymatic activities.
Yelin-Bekerman et al., 2015	Fs	dissection/ digestion	Y	FACS, Illumina TruSeq [S]; RT-PCR, ISH [V]	N	Identified dozens of H/O-specific neuronal transcripts, and confirmed their expression and localization using imaging; identified Kcnh4a, which encodes a voltage-gated K+ channel, in Hcrt neurons; CRISPR-based silencing of this gene reduced sleep time in zebrafish
Fortes et al., 2016	Cw	dissection	N	μ-array	N	Identified five transcription factors with potential regulatory functions in hypothalamus that were expressed differentially pre- and post-pubertally
Klimov et al., 2016	Rt	NS	N	RNA-Seq [S] qRT-PCR [V]	N	Found multiple differentially expressed genes in a hypertensive rat model
Rabaglino et al., 2016	Sh	dissection	N	μ-array [S] qRT-PCR [V]	N	Fetal hypothalamic transcripts for cell cycle, reproduction, and feeding were upregulated after acute exposure to triclosan, whereas transcripts for steroid metabolism, lipoproteins, fatty acids and glucose were downregulated after exposure.

Tu et al., 2016	Ck	NS	N	µ-array [S] qRT-PCR [V]	N	Found differentially expressed genes in hypothalamic samples as a result of heat stress, including genes encoding neuropeptides and heat shock proteins.
Chen et al., 2017	Ms	dissection	N	Drop-Seq [S] ISH, IHC [V]	N	Identified 11 non-neuronal and 34 neuronal cell types, and the restricted expression of genes such as *Crabp1* and *Pax6*.
Nectow et al., 2017	Ms	dissection	Y	vTRAP [S] ISH database, IHC, RNA-Seq [V]	N	Isolated translating mRNAs in MCH neurons using viral TRAP following injection of eGFP-L10a constructs into lateral hypothalamus; note that tissue isolation was at the level of the whole hypothalamus
Qiu et al., 2018	Fs	dissection	N	RNA-Seq [S] qRT-PCR [V]	N	Found >30K unigenes mapping to known genes, 275 of which were expressed differentially in immature male and female adults, and 561 between mature male and female adults.
Diencephalon						
Dalal et al., 2013	Ms	dissection	Y	TRAP [S]; µ-array/ISH [V]	N	Homogenized diencephalon to run TRAP assays from transgenic mice expressing eGFP-L10a fusion protein; confirmed identification of 15 transcripts expressed in H/O neurons
Medial hypothalamus (various sub-regions)						
Romanov et al., 2017	Ms	dissection, manual dissociation	N	Single cell RNA-Seq [S]; Drop-Seq, IHC [V]	N	Sampled a large portion of the medial hypothalamus which included portions of the Preoptic nucleus, PVH, AHN, SCH, DMH and ARH; identified single phenotypes (62 in total) on the basis of clustering analysis, including novel subtypes of GABA, glutamate, and dopamine-containing neurons
AHA: Anterior hypothalamic area						
Sanna et al., 2005	Rt	LCM	N	µ-array	Y	Established a working protocol for microarray analysis of LCM samples
ARH: Arcuate hypothalamic nucleus						
Li et al., 2005	Rt	µ-punch	N	µ-array	N	118 mRNAs up-regulated and 203 mRNAs down-regulated after fasting
Segal et al., 2005	Ms	LCM	N	µ-array [S] ISH [V]	N	Found genes for VMH enriched as compared to ARH
Nilaweera et al., 2009	Hm	LCM	N	µ-array	N	Found a number of genes in dorsomedial ARH that are regulated by photoperiod
Paulsen et al., 2009	Rt	LCM	N	µ-array [S] qRT-PCR [V]	N	Fasting-induced changes in NPY and POMC expression; 3480 other genes
Arai et al., 2010	Ms	LCM	N	qRT-PCR	N	Increased NPY mRNA/peptide in neurogenin3 null mutants
Jovanovic et al., 2010	Ms	LCM	N	µ-array	N	Fasting induces 639 genes and down-regulates 452 genes

Adler et al., 2012	Rt	LCM	Y	multiplex, nested PCR	Y	Sex differences in WAT projection neuron neurochemistry
Amar et al., 2012	Rt	µ-punch	N	RNA-Seq	schematic only	Found moderate to high expression for 20 miRNAs among 210 miRNA genes examined
Landmann et al., 2012	Rt	LCM	Y	qRT-PCR	No, but atlas levels specified	Fasting induces AgRP but not POMC
Stocker et al., 2012	Rt	LCM	N	qRT-PCR	N	Pups cross-fostered to dams fed low protein diet increase leptin and melanocortin-3 receptor expression
Zmora et al., 2012	Fs	LCM	Y	qRT-PCR, ISH	N	Detected expression of kisspeptin genes and genes for their receptors in males and females
Henry et al., 2015	Ms	manual sorting	Y	RNA-Seq	N	selective changes in AgRP neurons after food deprivation
Doubi-Kadmiri et al., 2016	Rt	dissection	Y	qRT-PCR	N	Analyzed >300 miRNAs from ARH/ME samples, and >30% of these underwent maternal diet-induced expression changes in progeny
Jeong et al., 2016	Ms	dissection; aspiration	Y	Single-cell qRT-PCR	N	Characterized transcripts in single cells captured in ARH that had a cholinergic phenotype; found that the cells diverged in the types of transcripts each expressed
Kabra et al., 2016	Ms	LCM	N	qRT-PCR	N	HDAC5 is an important component of leptin signaling and food intake control
Campbell et al., 2017	Ms	dissection	N	Drop-Seq, single-cell RNA-Seq [S]; ISH database; IHC [V]		Catalogued and identified 34 distinct neuronal populations and 36 non-neuronal populations in ARH-ME (arcuate hypothalamus-median eminence) samples from >20K individual profiles of ARH cells.
DMH: Dorsomedial hypothalamic nucleus						
Segal et al., 2005	Ms	LCM	N	µ-array [S] ISH [V]	N	Found genes for VMH enriched as compared to DMH
Lee et al., 2012	Ms	LCM	N	µ-array	camera lucida	Highly expressed DMH genes: *Gpr50*, *Pcsk5*, *Sulf1*, *Rorb*, others
GnRH: GnRH motor neuron pool of the preoptic area						
Vasilache et al., 2007	Ms	LCM	Y	qRT-PCR	N	Distinct EP3 receptor isoform profiles
Soga et al., 2012	Ms	LCM	Y	qRT-PCR	Y	Neonatal dexamethasone exposure upregulates GnIH-GnRH pathway
Vasilache et al., 2013	Ms	LCM	N	µ-array	N	Prostaglandin E synthase 1 KO and inflammation induce some gene expression changes
Eberwine & Bartfai, 2011	Ms	patch pipette	Y	µ-array	N	Unique receptor on warm-sensitive neurons
LHA: Lateral hypothalamic area						
Volgin et al., 2004	Rt	acute dissociation	Y	ICC [S], RT-PCR [V]	N	Demonstrated single-cell isolation, immunocytochemical identification, and mRNA recovery for Hcrt and MCH peptidergic neurons of the LHA

Ahmed et al., 2005	Rt	dissection	N	μ-array	N	75–100 mRNAs up/down-regulated with cocaine escalation
Harthoorn et al., 2005	Rt	LCM	Y	ICC [S], RT-PCR [V]	N	Identified mRNAs for MCH, Hcrt, CART, dynorphin, various receptors, and GABA/Glu markers in Hcrt and MCH neurons
Sanna et al., 2005	Rt	LCM	N	μ-array	Y	Established a working protocol for microarray analysis of LCM samples
Honda et al., 2009	Hu, Ms	dissection	N	μ-array [S], RT-PCR, IHC, ISH [V]	N	Compared transcriptomes of control and narcoleptic post mortem human brains, and control vs. transgenic mice lacking H/O neurons; found insulin-like growth factor binding protein (IGFBP3) downregulated in both transgenic mouse and narcoleptic human brains
Chen et al., 2013	Ms	NS	Y	μ-array	N	Syndecan-3 mRNA was up-regulated in LHA after cocaine self-administration
Mickelsen et al., 2017	Ms	dissection, FACS	Y	single-cell qPCR [S]; dual FISH, IHC [V]	Y	Found H/O and MCH neurons express 48 key genes encoding multiple neuropeptides and markers for fast neurotransmission; found, strikingly, that virtually all MCH neurons, and about half of the H/O neurons express markers for glutamate release, GABA synthesis, but not GABA release
PVH: Paraventricular hypothalamic nucleus						
Bonaventure et al., 2002	Rt	LCM	N	μ-array	N	Found gene-relatedness based correlations in brain sub-regions in PVH
Sanna et al., 2005	Rt	LCM	N	μ-array	Y	Established a working protocol for microarray analysis of LCM samples
Hindmarch et al., 2006	Rt	dissection	N	μ-array	N	Found mRNAs regulated by dehydration, enriched in PVH and SO
Heisler et al., 2007	Ms	LCM	N	μ-array	Fos map	Found 5-HT2CR & 5-HT1DR mRNAs
Hindmarch et al., 2007	Rt	NS	N	μ-array	N	mRNA expression differences between strains for the neurohypophysial system
Tung et al., 2008	Ms	LCM	N	μ-array [S] qRT-PCR [V]	Y	Profiled transcripts from ad lib-fed vs 48 h-fasted mice with or without leptin treatment. Found 527 transcripts with altered expression by fasting that could at least be partially reversed by leptin
Blevins et al., 2009	Rt	LCM	Y	qRT-PCR	injections	Found MC4R mRNAs in NTS-projecting PVH neurons
Atkins et al., 2011	Ms	dissection	N	RNA-Seq	N	Established protocol
Amar et al., 2012	Rt	μ-punch	N	RNA-Seq	schematic only	Found moderate to high expression for 20 miRNAs among 210 miRNA genes examined
Romanov et al., 2014	Ms	dissection, dissociation	Y	RNA-Seq	Y	Phenotyped 151 neurons from the mouse PVH, including neuropeptide phenotypes in cells with excess of 100 mRNA copy numbers per cell: somatostatin, galanin, cholecystokinin, neurotensin S, and CART
SCH: Suprachiasmatic hypothalamic nucleus						

Panda et al., 2002	Ms	dissection	N	μ-array [S]; RT-PCR, ISH [V]	N	Found approx. 650 cycling transcripts in the SCH
Winrow et al., 2009	Rt	LCM	N	μ-array	N	Differential profiles across circadian cycle
Porterfield & Mintz, 2009	Ms	LCM	N	qRT-PCR	N	Induction of genes in early dark phase to light pulse
Boone et al., 2012	Rt	LCM	N	qRT-PCR	LCM image	TBI model shows altered circadian gene expression patterns
Zhu et al., 2012	Ms	LCM	N	qRT-PCR	N	Transcript differences in core and shell at time points in and out of phase of light reset
Boone et al., 2013	Rt	LCM	Y	qRT-PCR, μ-array	LCM image	TBI model shows altered gene expression patterns in SCH and hippocampus
Pembroke et al., 2015	Ms	LCM	N	RNA-Seq [S]; ISH [V]	N	Identified 146 genes highly enriched in the SCH; four of these were confirmed using ISH; also identified twin-peaking genes in the SCH and novel transcripts with circadian profiles
Park et al., 2016	Ms	LCM	Y	qRT-PCR	N	Identified transcriptional changes in dark-adapted mice and those dark-adapted and then exposed to a brief light pulse; identified distinct expression profiles across groups, but no specific spatial organization of expression patterns
SFO: Subfornical organ						
Walch et al., 2014	Rt	LCM	N	qRT-PCR	N	Detected AT1aR expression in SFO that was markedly reduced by virally mediated RNA interference
SO: Supraoptic hypothalamic nucleus						
Mutsuga et al., 2004	Rt	LCM	N	μ-array [S] ISH [V]	N	Found 1,385 genes expressed in SO at levels two times greater than in the hypothalamus as a whole
Hindmarch et al., 2006	Rt	dissection	N	μ-array	N	Found mRNAs regulated by dehydration, enriched in PVH and SO
Yue et al., 2006	Rt	LCM	Y	μ-array	N	40 mRNAs greater in hypo-osmotic vs. normo-osmotic conditions
Goraud et al., 2007	Rt	dissection	N	μ-array [S]; RT-PCR [V]	N	Confirmed up-regulation of 14-3-3 family of proteins in dehydrated SO and also identified a novel 14-3-3 binding partner protein
Hindmarch et al., 2007	Rt	NS	N	μ-array	N	mRNA expression differences between strains for the neurohypophysial system
Qiu et al., 2011	Rt	dissection	N	μ-array [S] ISH [V]	N	Found 567 genes commonly regulated by dehydration in the male and by lactation and euhydration in the female.
Stewart et al., 2011	Ms	LCM	N	μ-array [S] ISH [V]	N	Identified 69 genes that have altered gene expression under conditions of dehydration in mice (and in rats compared from a previous data set); four of these genes were validated by

						ISH and were found to be up-regulated as a result of dehydration
Nedungadi et al., 2012	Rt	LCM	Y	qRT-PCR	N	TRPV2 mRNA detected
Humerick et al., 2013	Rt	LCM	Y	qRT-PCR	N	Transcription factors differentially expressed in OT and VP neurons
Qiu et al., 2014	Rt	dissection	N	µ-array [S] EMSA, ELISA, qPCR [V]	N	Found changes in binding for 26 consensus elements in dehydrated relative to control rats
Greenwood et al., 2015	Rt	µ-punch	N	µ-array [S] qPCR [V]	N	Compared salt loading vs water deprivation on transcript expression in SO; identified and validated five new genes and confirmed nine others
Johnson et al., 2015	Rt	LCM	N	RNA-Seq, µ-array [S]; IHC, qPCR [V]	N	Detected 9,709 genes by RNA-Seq, 552 of which altered their expression in SO as a result of salt-loading
VMH: Ventromedial hypothalamic nucleus						
Segal et al., 2005	Ms	LCM	N	qRT-PCR	N	Four of twelve mRNAs reduced in steroidogenic factor 1 knockouts
Kurrasch et al., 2007	Ms	dissection	N	µ-array [S]; qRT-PCR, ISH [V]	N	Identified approx. 200 mRNAs enriched in neonatal VMH, including several transcriptional regulators

* Abbreviations: µ-array, microarray; µ-punch, micropunch; Ck, chicken; Cw, cow; CZE, capillary zone electrophoresis; Dg, dog; ELISA, enzyme-linked immunosorbent assay; EMSA, electrophoretic mobility shift assay; Fs, fish; Gs, goose; Hm, hamster; Hu, human; ICC, immunocytochemistry; IHC, immunohistochemistry; ISH, *in situ* hybridization; LCM, laser capture microdissection; Ms, mouse; NS, not stated; Pg, pig; qRT-PCR, quantitative real-time polymerase chain reaction; RNA-Seq, next-generation RNA sequencing; Rt, rat; SAGE, serial analysis of gene expression; Sh, sheep; Sp, sparrow; WB, Western blotting

Table 2. Proteomic studies in whole hypothalamus and by hypothalamic sub-region

Study	Animal	Extraction	Target(s) *a priori*?	Screen [S], Validation [V]	Map or Schematic	Major findings
Whole hypothalamus						
Sung et al., 2004	Rt	dissection	N	MALDI TOF MS	N	36 proteins expressed in a neuropathic pain model relative to controls
Kuo et al., 2005	Ck	dissection	N	2D-GE [S] LC-MS/MS, qRT-PCR [V]	N	6 proteins associated with high egg production
Roth et al., 2006	Rt	dissection	N	2DLC-MS/MS & clCAT	N	Found differential expression of five proteins involved in glutamate metabolism in juvenile versus peri-pubertal females
Skynner et al., 2006	Ms	dissection	N	MALDI-TOF MS	N	Chronic corticosterone altered markers of glycolysis, gluconeogenesis and nitrogen metabolism
Kuhla et al., 2007	Cw	dissection	N	MALDI-TOF MS [S]	N	Found nine proteins differentially expressed in ad lib fed vs. energy restricted cows
Ropp et al., 2008	Ms	dissection	N	SELDI-TOF	N	Distinct protein profiles following sub-acute pyridostigmine treatment
Sarkar et al., 2008	Ms	dissection	N	2D-GE, WB, MALDI-TOF-MS	N	Found seven proteins that were significantly different in hypothalamus in control versus microgravity-treated animals
Mishra et al., 2009	Rt	dissection	N	2D-GE, LC-MS/MS [S]; WB [V]	N	Light-dark shifts in circadian cycle resulted in increased food intake, body weight gain, retroperitoneal fat mass, and expression levels of 4 of 5 hypothalamic 2D-GE spots; these were identified by MS and included glycolytic and citric acid cycle enzymes.
Kim et al., 2010	Rt	dissection	N	2D-GE, MALDI-TOF MS	N	Maternal separation was associated with down-regulation of 14 proteins from hypothalamus; maternal separation with acupuncture was associated with five down- and nine up-regulated proteins relative to maternal separation alone.
Popesku et al., 2010	Fs	dissection	N	iTRAQ labeling & MS	N	42 proteins differentially regulated by treatment with DA receptor agonists
Argüelles et al., 2011	Rt	NS	N	MALDI-TOF/TOF-MS	N	Oxidative stress could be involved in the alterations of eEF-2 and several other proteins
Wang et al., 2011	Rt	dissection	N	MALDI-TOF/TOF-MS	N	Ubiquitin was significantly decreased in diet-resistant rats but not changed in diet-induced obese rats
Alexandre-Gouabau et al., 2012	Rt	dissection	N	LC-MS/MS	N	Protein restriction *in utero* alters numerous pathways
Gasperini et al., 2012	Rt	dissection	N	2D-GE, MALDI-TOF MS/MS	N	Found 26 of 28 protein spots on 2D gels for hypothalamus show significant expression after i.c.v. PACAP; including cytoskeletal, signaling and synaptic proteins
Guest et al., 2012	Rt	dissection	N	LC-MS	N	Identified hypothalamic proteins that differ in expression in rats subjected to

						a low-protein diet as compared to wild-type controls
Pedroso et al., 2012	Rt	dissection	N	MALDI-TOF MS [S]; 2D-GE, WB [V]	N	Identified 86 hypothalamic proteins in Wistar rats
Stelzhammer et al., 2012	Rt	dissection	N	LC-MS/MS [S]	N	Found 21,455 peptides that corresponded to 622 unique proteins
Zhang X et al., 2012	Ms	dissection	N	LC-FT-MS/MS, SIEVE analysis, spectral analysis	N	Identified 367 peptides from neuropeptide precursors
Ihnatko et al., 2013	Ms	dissection	N	LC-MS/MS	N	Differential up- and down-regulation of proteins in tumor-bearing mice and caloric-restricted pair fed mice
Kefaloyianni et al., 2013	Rt	dissection	N	LC-MS^{E} and LC-MS/MS	N	KATP channels in different tissues assemble with proteins having common functions
Taraslia et al., 2013	Ms	dissection	N	2D-GE, MALDI-TOF MS [S]	N	515 different single-gene products were identified, eight of which were unique to hypothalamus
Iqbal et al., 2014a	Rt	dissection	N	HPLC/ESI-TOF & HPLC-Q-TOF	N	35 and 97 significantly differentially expressed proteins by two analyses in simulated microgravity model
Iqbal et al., 2014b	Rt	dissection	N	HPLC/ESI-TOF & HPLC-Q-TOF	N	Differential expression of 17 specific cellular defense proteins in simulated microgravity model
Kim et al., 2014	Rt	dissection	N	LC-ESI-MS/MS [S]; WB, IHC [V]	N	Following chronic partial sleep deprivation in rats for 7 d, 89 and 50 proteins were up- and down-regulated, respectively
Chao et al., 2015	Rt	dissection	N	2D-GE, LC-MS/MS [S]; WB [V]	N	Found a few proteins induced by heatstroke that had their levels normalized by cooling
Zhong et al., 2015	Ms	dissection	N	ESI-LC-MS/MS	N	Found 31 overexpressed proteins in wild-type group compared to *EPHX2* KO group
Manousopoulou et al., 2016	Ms	dissection	N	ESI-LC-MS/MS [S]; qPCR [V]	N	Quantitative profiling yielded 9,249 protein groups, with 7,718 groups profiled with a minimum of two unique peptides each; high-fat diet or lipopolysaccharide challenge produced unique proteomic profiles
Pedroso et al., 2017	Rt	dissection	N	Q-TOF MS [S]; 2D-GE [V]	N	1,356 proteins were identified and 348 were quantified, along with 127 metabolites. Intrauterine growth restriction resulted in down-regulation of 36 proteins and 5 metabolites, and up-regulation of 21 proteins and 9 metabolites in the hypothalamus.
Zettergren et al., 2017	Ms	dissection	N	MS and MS/MS; iTRAQ [S]; PRM [V]	N	Identified 2,998 proteins in hypothalamus and amygdala of neonatal male, female and androgen receptor knockout male mice; of which 173 proteins were expressed differentially in males and females. Verified expression of seven genes using targeted proteomics.

ARH: Arcuate hypothalamic nucleus

Amigó-Correig et al., 2012	Ms	dissection	N	MALDI-TOF/TOF	N	Adult lean and high fat diet-induced obese mice orally treated with sodium tungstate had modified levels of proteins involved in cell morphology, axonal growth and tissue remodeling
PVH: Paraventricular hypothalamic nucleus						
Romanov et al., 2014	Rt	dissection	Y	Illumina HiSeq2000 sequencer, MALDI-TOF	Y	Profiled secretagogin neurons as a distinct CRH-releasing neuron population
SCH: Suprachiasmatic hypothalamic nucleus						
Deery et al., 2009	Ms	NS	N	2D-DIGE & MS	N	13% of soluble proteins were found to be subject to circadian regulation
SO: Supraoptic hypothalamic nucleus						
Goraud et al., 2007	Rt	dissection	N	2D-GE, MALDI-TOF MS [S]; WB, IHC [V]	N	Identified 14-3-3 proteins that are up-regulated as a consequence of chronic dehydration
VLPO: Ventrolateral preoptic nucleus						
Dooley et al., 2010	Rt	dissection	N	MALDI-TOF/TOF MS	N	Identified diaminochlorotriazine (DACT) protein adducts formed in Atrazine-exposed rats
VMH: Ventromedial hypothalamic nucleus						
Mo et al., 2008	Rt	µ-punch	N	RPLC-nanoESI-MS/MS	N	Up-regulation of 29 identified proteins with estradiol treatment

* Abbreviations: 2D-DIGE, 2-D Difference Gel Electrophoresis; 2D-GE, two-dimensional gel electrophoresis; µ-punch, micropunch; Ck, chicken; Cw, cow; ESI, Electrospray Ionization; Fs, fish; FT, Fourier transformation; FTICR, Fourier-transform Ion Cyclotron Resonance; HCD and ETD-based MS/MS, High-energy Collisional Dissociation and Electron-transfer Dissociation-based tandem mass spectrometry; IHC, immunohistochemistry; iTRAQ, isobaric tag for relative and absolute quantitation; LC, liquid chromatography; LC-MS^E , liquid chromatography – label-free mass spectrometry; LTQ, Linear Trap Quadrupole; MALDI-TOF, Matrix-Assisted Laser Desorption/Ionization-Time of Flight; Ms, mouse; MS/MS, tandem mass spectrometry; MSPD, Matrix Solid-Phase Dispersion; nanoESI, nano-electrospray ionization; NS, not stated; qRT-PCR, quantitative real-time polymerase chain reaction; Q-TOF, Quad Time of Flight; RPLC, reversed-phase liquid chromatography; SELDI-TOF, Surface-Enhanced Laser Desorption/Ionization-Time of Flight; SRM, Selected Reaction Monitoring; Triple Quad MS, triple quadrupole mass spectrometry; Rt, rat; WB, Western blotting

Table 3. Peptidomic studies in whole hypothalamus and by hypothalamic sub-region*

Study	Animal	Extraction	Target(s) *a priori*?	Screen [S], Validation [V]	Map or Schematic	Major findings
Whole hypothalamus						
Bures et al., 2001	Ms	dissection	N	LC-MS [S]; LC-MS/MS [S]	N	Identified 27 peptides derived from known neuropeptides as well as 25 additional peptides not known to be in the neuropeptide processing pathway; all upregulated in carboxypeptidase E mutant mice
Svensson et al., 2003	Rt, Ms	dissection	N	nanoLC-ESI-Q-TOF-MS	N	Detected 550 endogenous peptides
Che et al., 2005	Ms	dissection	N	LC-MS/MS	N	Knockdown of carboxypeptidase E activity in two paradigms for decreasing body mass show different peptide profiles
Pan et al., 2006	Ms	dissection	N	Isotopic labeling & LC-ESI-MS	N	Approx. one-third of the peptides found in wild-type mice were not found in prohormone convertase KO mice
Che et al., 2007	Ms	dissection	N	Nano-LC MS/MS	N	Identified 95 peptides from samples, 64 of which were neuropeptides or other peptides derived from proteins in the secretory pathway; found oxytocin to be preferentially abundant in hot-acid extracts over hot-water extracts
Sköld et al., 2007	Ms	dissection	N	Nano-LC MS [S]; Q-TOF LTQ MS/MS [V]	N	Identified 23 neuropeptides, hormones and potentially biologically active peptides; all were primarily upregulated in control mouse brain relative to brains processed with longer post mortem times
Cai et al., 2011	Pg	dissection	N	MSPD & Nano-LC MS/MS	N	14 potential endogenous peptides were identified using MSPD extracts versus to peptides using acid extracts
Colgrave et al., 2011	Cw	dissection	N	LC-MS/MS	N	Used thermal stabilization methods to refine the yield of neuropeptides isolated from hypothalamus
Nilsson et al., 2012	Ms	dissection	N	nano-LC-ESI-LTQ MS/MS or nano-LC-ESI-LTQ-FTICR-MS/MS	N	14 peptides were significantly regulated by imipramine treatment
Zhang et al., 2012	Ms	dissection	N	LC-FT-MS/MS	N	Identified 367 peptides from neuropeptide precursors from hypothalamic samples.
Fouillen et al., 2013	Sw	dissection	N	LC-FT-MS/MS, SIEVE analysis,	N	12 hypothalamic peptides were up-regulated following prolonged general anesthesia
Frese et al., 2013	Rt	dissection	N	HCD and ETD-based MS/MS [S]; LC-MS [V]	N	Identified 1,292 unique peptides from hypothalamus in rats fed on a regular diet, high-fat and high sucrose (HFHS) diet, restricted chow diet, or chocolate diet. HFHS diet produced the greatest

						increases in peptides as determined by label-free quantification.
Gao et al., 2013	Rt	dissection	N	2D-GE, MALDI-TOF MS [S]; qRT-PCR, WB [V]	N	Identified 17 hypothalamic proteins with twofold or greater expression after electroacupuncture intervention of sciatic pain
Schmidlin et al., 2015	Rt	dissection	N	LC-MS/MS [S]; SRM/Triple-Quad MS [V]	N	Demonstrated the feasibility of using selective reaction monitoring (SRM) to evaluate *a priori* selected transitions of key neuropeptide fragments from the hypothalamus
Secher et al., 2016	Rt	dissection	N	LC-MS/MS [S]	N	Identified 14,416 peptides in 786 protein families; sorted these by longest peptide variants (LPVs) to isolate 2,835 peptides derived from 356 prohormone precursors; of these, 105 LPVs were not previously described
SCH: Suprachiasmatic hypothalamic nucleus						
Hatcher et al., 2008	Rt	acute tissue slice prep; μ-punch	N	HPLC, LC, SPE beads [S]; MALDI-TOF MS/MS ; LTQ FTMS [V]	N	Identified peptides released from acute slice preparations containing SCH, including after electrical stimulation of the retinohypothalamic input to the SCH; found peptide content in releasates to be stimulation-specific
Lee et al., 2010	Rt	μ-punch	N	LC-FTMS/MS	N	list of 102 endogenous peptides, including 33 that were previously unidentified; also identified novel post-translational modifications
Lee et al., 2013	Rt	μ-punch	N	LC-FTMS/MS, SIEVE analysis	N	list of 190 endogenous peptides from 310 identified
Chiang et al., 2014	Ms	dissection	N	fractionation, LC MS/MS [S]; RT-PCR, WB, IHC [V]	N	quantified 2112 proteins, 20% of which exhibited a time-of-day-dependent profile; found 48 proteins exhibiting circadian rhythms of expression from this time-of-day proteome
Southey et al., 2014	Rt	μ-punch	N	Spectral count, spectra index, SIEVE analysis	N	differential peptide abundances between day and night conditions
SO: Supraoptic hypothalamic nucleus						
Bora et al., 2008 [also see: Perkel, 2008]	Rt	μ-punch	Y	LC/MS & tandem mass spectrometry	N	20 unique peptides identified

* Abbreviations: 2D-GE, two-dimensional gel electrophoresis; μ-punch, micropunch; Cw, cow; ESI, Electrospray Ionization; Fs, fish; FT, Fourier transformation; FTICR, Fourier-transform Ion Cyclotron Resonance; HCD and ETD-based MS/MS, High-energy Collisional Dissociation and Electron-transfer Dissociation-based tandem mass spectrometry; Hu, human; LC, liquid chromatography; LTQ, Linear Trap Quadrupole; MALDI-TOF, Matrix-Assisted Laser Desorption/Ionization-Time of Flight; Ms, mouse; MS/MS, tandem mass spectrometry; MSPD, Matrix Solid-Phase Dispersion; Pg, pig; qRT-PCR, quantitative real-time polymerase chain reaction; Q-TOF, Quad Time of Flight; SRM, Selected Reaction Monitoring; Triple Quad MS, triple quadrupole mass spectrometry; Rt, rat; SPE beads, solid-phase extraction beads; Sw, shrew